Understanding the biogenesis of telomerase RNA (Tlc1) in *Saccharomyces cerevisiae*

Dissertation

Zur Erlangung des Grades

Doktor der Naturwissenschaften

Am Fachbereich Biologie

Der Johannes Gutenberg-Universität Mainz

Abinaya Manivannan

geb. am 16.10.1993, India

Mainz, 2023

Tag der mündlichen Prüfung: 28-11-2023

Table of Contents

1. Zusammenfassung

Telomere sind konservierte Nukleoproteinstrukturen an den Enden der eukaryontischen Chromosomen, die die Integrität des Genoms und die zelluläre Vermehrungsfähigkeit fördern. Die meisten Eukaryoten setzen Telomerase ein, einen spezialisierten Ribonukleoprotein-Komplex, um dem fortschreitenden Verlust terminaler chromosomaler DNA bei jeder Zellteilung entgegenzuwirken. Die Telomerase, eine reverse Transkriptase, verwendet ein bestimmtes Segment ihrer RNA-Komponente als Vorlage, um die telomeren Wiederholungen an den Enden des Chromosoms zu wiederholen. Eine Störung der Telomerregulation führt zu genomischer Instabilität mit schädlichen Folgen wie vorzeitigem Zelltod oder Umwandlung in unsterbliche Krebszellen. Diese nachteiligen Auswirkungen zeigen, dass es dringend notwendig ist, die Biogenese und Regulation der Telomerase zu entschlüsseln. Die RNA-Untereinheit der Telomerase von Saccharomyces cerevisiae (Tlc1) wird zunächst als längerer Vorläufer transkribiert und anschließend an ihrem 3'-Ende zu der reifen Form gekürzt, die in der funktionellen Telomerase zu finden ist. Tlc1 verfügt über zwei einzigartige Transkriptionsterminationssignale: Das durch Nrd1-Nab3-Sen1 (NNS) vermittelte Terminierungssignal und das Polyadenylierungs-Terminierungssignal. Die Bedeutung der beiden Transkriptionsterminationswege und des 3'-Prozessierungsmechanismus, die zu stabilem und funktionsfähigem reifem Tlc1 führen, war bisher unklar.

In dieser Studie konnten wir zeigen, dass der NNS-Transkriptionsterminationsweg für die Aufrechterhaltung eines stabilen Niveaus von reifem Tlc1 nicht wesentlich ist. In Abwesenheit von NNS-Terminationssignalen wird der über den alternativen Polyadenylierungs-Terminationsweg produzierte Poly(A+)-Precursor erfolgreich am 3'-Ende prozessiert und trägt so zur Bildung einer stabilen reifen Form bei. Zusätzlich zu den beiden bekannten Vorläuferformen, die über den NNS- und den Polyadenylierungsweg entstehen, haben wir eine dritte stabile Form identifiziert. Darüber hinaus haben wir ein Ribozym eingesetzt, um die normale 3'-Prozessierung durch schnelle Spaltung von Tlc1 an vorgewählten Stellen zu umgehen. Wir stellten fest, dass Tlc1-Moleküle, die auf diese Weise prozessiert werden, sehr instabil sind. Wir erörtern hier die Rolle von Prozessierungsfaktoren, die Beladung mit Telomerase-Komponenten und die Kinetik der 3'-Prozessierung bei der Bestimmung der Stabilität von Tlc1.

2. Abstract

Telomeres are conserved nucleoprotein structures present at the eukaryotic chromosome extremities that facilitates genome integrity and cellular proliferative capacity. Most eukaryotes employ telomerase, a specialized ribonucleoprotein complex, to counteract the progressive loss of terminal chromosomal DNA with every round of cell division. Telomerase, a reverse transcriptase, uses a specific segment of its RNA component as a template to reiteratively add the telomeric repeats at the ends of the chromosome. Abnormality in telomere regulation causes genomic instability with deleterious end results such as premature cell death or transformation into immortal cancer cells. These detrimental implications indicate the pressing need to decipher the biogenesis and regulation of telomerase. The RNA subunit of *Saccharomyces cerevisiae* telomerase (Tlc1) is initially transcribed as a longer precursor and is subsequently trimmed at its 3' end to the mature form found in functional telomerase. Tlc1 harbors two unique transcriptional termination signals: Nrd1-Nab3-Sen1 (NNS) mediated termination signal and polyadenylation termination signal. The relevance of two transcriptional termination pathways and the 3' processing mechanism that give rise to stable and functional mature Tlc1 has remained unclear.

In this study, we demonstrate that NNS transcriptional termination pathway is not essential to maintain steady-state levels of mature Tlc1. In the absence of NNS termination signals, the poly(A+) precursor produced via the alternative polyadenylation termination pathway is successfully processed at the 3' end and thereby contributes to the formation of stable mature form. In addition to the two known precursor forms resulting from NNS and polyadenylation pathways, we identified a third stable form. Furthermore, we made use of a ribozyme to bypass normal 3' processing events by rapid cleavage of the Tlc1 at preselected sites. We observed that Tlc1 molecules processed in such a manner are highly unstable. Here, we discuss the role of processing factors, the loading of telomerase components and 3' processing kinetics on determining the stability of Tlc1.

3. Introduction

3.1. Introduction to telomeres

One of the remarkable attributes of eukaryotes is the arrangement of their genetic information as linear chromosomes. Majorly eukaryotes have linear chromosomes whereas, the presence of such a genome organization is rather sporadic in prokaryotes [1]. Prokaryotes predominantly have circular chromosomes which are incompatible with meiosis unlike the linear DNA [2, 3]. The Meiosis event is crucial for shuffling of genetic information between parent chromosomes, contributing to genetic diversity during sexual reproduction. The genetic diversity arising from the recombination event is advantageous for species, as it allows better survival chances in the constantly changing environment [4]. However, such an evolutionarily advantageous linear genome arrangement posed two major shortcomings, namely: the end protection problem and the end replication problem. Evolution of linear chromosomes was possible, despite the shortcomings posed by such a genome organization, mainly because of the acquisition of protective-DNA repeat-cap structures called telomeres at the ends of the chromosomes.

3.1.1. The end protection problem

The linear configuration of chromosomes makes their ends exposed. Such open DNA ends are prone to exonucleolytic degradation, posing a threat to the faithful maintenance of genetic information. Additionally, linear chromosome ends have the potential to be mistaken for double stranded breaks, thereby attracting DNA repair machineries. Recognition and action by the DNA repair machinery will subsequently lead to chromosome end to end fusions. The end-to-end fusions can either be inter or intra chromosomal fusions thereby disturbing the genetic stability. But we know that cells can maintain genetic stability with linear chromosome conformation. Telomeres bound by a six membered protein complex called Shelterin, protects the mammalian linear chromosome ends, thereby serving as a solution for the end protection problem [5].

In 1930's Hermann Muller using *Drosophila melanogaster* and Barbara McClintock using *Zea mays*, individually converged at the same conclusion that natural chromosome ends are distinct from the ends generated by accidental or experimental chromosomal breaks. McClintock documented that the broken ends exhibited the property of "stickiness", i.e., tendency to fuse, while natural termini lacked this feature [6]. H. Muller used x-rays to fragment chromosomes and

observed that the broken chromosome ends underwent rearrangement and fusion events. Whereas the natural chromosome termini exhibited no such instability, and he named the natural protective ends “telomeres” [7]. These research works framed the foundation for telomere biology.

3.1.2. The end replication problem

Yet another problem of linear DNA configuration surfaced upon the discovery of DNA polymerase and DNA synthesis mechanism by Arthur Kornberg [8]. DNA replication is semiconservative i.e., the newly generated double stranded DNA has one template/parent strand and one nascent/daughter strand [9]. Since DNA polymerase requires a 3’-hydroxyl (3’-OH) group for the addition of nucleotide, the DNA synthesis can only happen in 5’—3’ direction. The directionality of the daughter strand synthesized is opposite to the directionality of the template strand. Hence during linear DNA replication, the leading strand synthesis (5’—3’ direction) using 3’—5’ template DNA strand happens continuously until the very end, thereby generating a complete end. The lagging strand synthesis uses the 5’—3’ template. Since the DNA polymerase cannot synthesize in 3’—5’ direction, it synthesizes short fragments in 5’—3’ direction each initiating with an RNA primer. These short fragments are called Okazaki fragments [10]. The RNA primers are removed, and the gap is filled by the extension of the adjacent Okazaki fragment. However, the gap obtained from the RNA primer removed from the very 5’ end of the lagging strand cannot be filled. DNA polymerase also uses an RNA primer to initiate the leading strand synthesis, hence a gap is generated upon removal of this primer too. This means that there will be gradual loss of genetic information with every successive round of DNA replication [11]. The inability of the DNA polymerase to copy the very 3’ end of the linear template strand is referred to as the end replication problem [Fig 1].

Viruses having linear chromosomes demonstrated few solutions for the end replication problem. Lamda phage and phage M13 viruses temporarily shift to circular genome architecture to circumvent the end replication problem. T7 virus forms concatemers of viral genomes, thereby facilitating priming from the adjacent viral DNA strand. Mammalian adenoviruses and phage ø29 employ a protein, covalently attached to the 5’ nascent strand, to substitute for the DNA polymerase’s requirement of 3’OH group to prime synthesis.

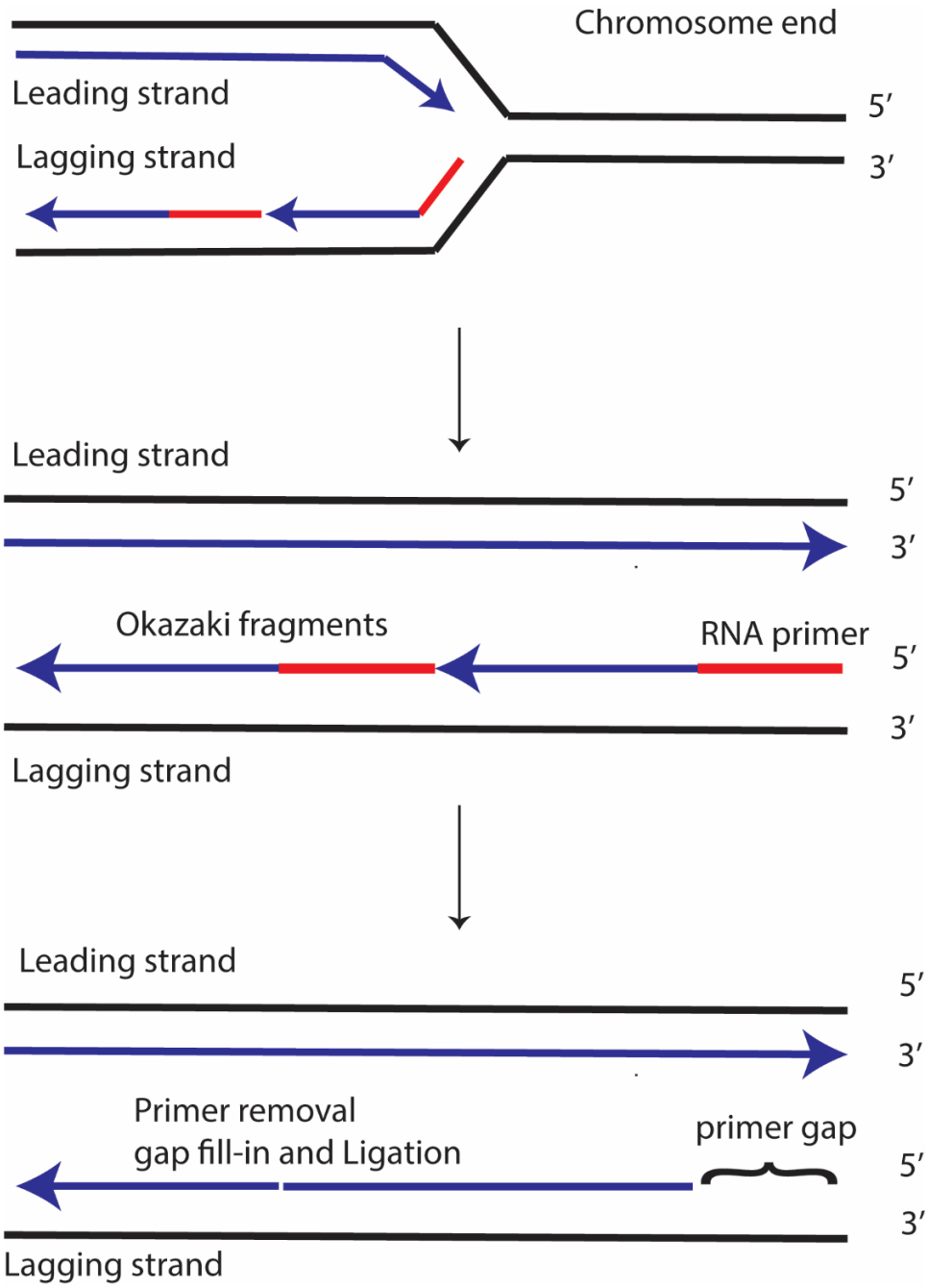

Figure 1: The end replication problem. During DNA replication, the leading strand synthesis happens continuously in 5'-3' direction. However, the lagging strand is synthesized as multiple short fragments, called Okazaki fragments, using RNA primers. Upon the RNA primer removal, the gap thus generated is filled by the extension of the adjacent Okazaki fragment. However, the gap obtained at the very 5' end of the lagging strand cannot be filled due to the absence of an adjacent Okazaki fragment. This inability of DNA polymerase to copy the very 3' end of the linear template strand is referred to as the end replication problem.

Cavalier-Smith proposed a model as a solution, that the ends of the linear chromosomes have palindromic sequences, allowing the 3' tail to fold back and pair with itself and form a loop.

According to the stated model, the 3'OH is now provided by the fold back loop which can be utilized by DNA polymerase to fill the gap. The closed loop was proposed to be finally unfolded by a sequence specific endonuclease nick. This led to an idea that the palindromic end sequences of all species are conserved so that only one specific endonuclease is employed.

Eukaryotes have telomeric repeat sequences at the chromosome ends. The majority of eukaryotes use Telomerase- a reverse transcriptase, to reiteratively add the telomeric repeats at the ends of the chromosome, to maintain genome stability and cellular proliferative capacity.

3.1.3. Telomeric DNA

Telomeric DNA was first identified by Elizabeth Blackburn in *Tetrahymena thermophila* by sequencing the ends of ribosomal DNA (rDNA) minichromosomes [12]. She reported that *T. thermophila* rDNA ends had tandem repeats of hexanucleotide units 3'CCCCAA5'/5'TTGGGG3'. The number of tandem repeats were quite heterogenous ranging from 20 ~ 70 repeat units per end. E. Blackburn found that additional telomeric repeats were being added to the already existing telomere repeats in rDNA minichromosomes [13]. Observing this Elizabeth proposed that the telomere sequences could be either transposoned/recombined onto chromosome ends, or the repeat sequences were added *de novo* at the DNA termini by a synthetic machinery.

It was established that linearized plasmid ends are highly reactive in yeast [14]. If the ends of linearized plasmid had homology to genome, it was immediately recombined and integrated into the genome. In the absence of homologous regions, the linear plasmid was either degraded, ligated, or rearranged. Surprisingly, linear plasmid vector ligated with the identified ciliate termini repeat DNA to its ends were stably maintained in yeast, whereas the linear vector by itself was not [15]. Furthermore, yeast specific heterogeneous TG_{1-3} telomeric repeats were added to the ciliate telomere capped linear plasmid upon introduction into *S. cerevisiae*. Telomeric ends from distantly related organism- *Tetrahymena* can be recognized and used by yeast. This showcased that the telomere replication mechanism must be highly conserved in evolution.

Despite the variation in the exact oligonucleotide repeat sequence, telomere DNA in most eukaryotes consists of a double stranded short tandem repeats and terminated with a G-rich 3' overhang (G-tail)[16]. The telomere DNA length was also quite variable across species. Protozoans and fungi have short telomeres (Eg. 20-30 bp in *Oxytricha* and *Euplotes*; 300 ± 75 bp

in *S. cerevisiae*)[17]. Contrastingly, vertebrates show longer telomeres with human telomere typically ranging 5-15 kb and *Mus musculus* up to 150 kb [18-20]. Drosophila chromosomal termini is an exception: instead of short tandem repeats they possess non-long terminal repeat retrotransposons [21].

3.1.4. Telomere positioning effect

Telomere near regions on chromosome are gene poor. The transcription of telomere proximal genes is repressed due to the heterochromatin conformation, and this transcriptional regulation is referred to as the telomere positioning effect [22].

3.1.5. Telomere binding proteins and telomere associated proteins

Mammalian telomere is bound by the shelterin complex: a six membered specialized protein complex comprising of Trf1, Trf2, Rap1, Tin2, Tpp1 and Pot1, where Trf1 and Trf2 exist as homodimers [5].

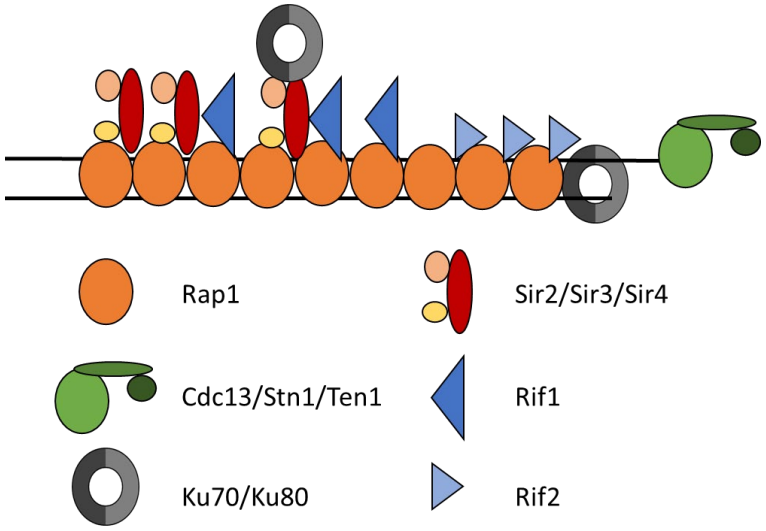

Figure 2: Telomere associated proteins in budding yeast *S. cerevisiae*. Telomeres are coated with Rap1 which serves as a docking site for Sir-family proteins and Rif-family proteins. G-rich 3' overhang is bound by Cdc13, which recruits Stn1 and Ten1, forming the CST complex. Ku70/80 is recruited to telomeres by its ability to associate with Sir4.

S. cerevisiae does not have the shelterin complex, instead Rap1 is the major telomere binding protein and serves as a docking site for the telomere associated proteins namely Sir-family proteins and Rif-family proteins [23] [Fig 2]. The G-rich 3' overhang is bound by Cdc13, which recruits Stn1 and Ten1, forming the CST complex [24]. CST complex resembles the replication

protein A complex (RPA) and is essential for chromosome end protection and telomere replication [24].

3.2. Telomere maintenance

In 1960, Leonard Hayflick documented that human diploid fibroblasts had finite limit of cultivation, which is referred to as the 'Hayflick limit' [25]. He proposed the cellular theory of aging upon the observation that human diploid cells derived from adult lungs exhibited significantly lower cell doubling potential relative to the fetal cells [26]. Alexei Olovnikov linked the limited cell division potential of fibroblasts to the end replication problem and predicted that cellular senescence is due to the gradual shortening of telomeres with each cell division [27].

The self-renewal capacity of embryonic stem cells (ESCs) and the ability of most cancer cells to overcome the limit to cell division can be attributed to efficient telomere maintenance. Unicellular fungi and protozoa exhibit indefinite proliferative capacity; hence they must possess a mechanism of continuous replenishment of telomeres.

3.2.1. Telomerase mediated telomere maintenance

Telomerase was first discovered by Carol Greider and E. Blackburn in *Tetrahymena*. Progressive bands of six base periodicity were observed on a sequencing gel when synthetic DNA oligonucleotide $(TTGGGG)_4$ was incubated with *Tetrahymena* cell extract along with radiolabeled dGTP [28]. The same experiment when done with a synthetic oligonucleotide with yeast telomeric repeat sequence terminating with TGGG at its 3'end, showed one base shift in the band pattern, indicating a terminal G was added before the progressive 6 base repeat addition. This experiment confirmed that the telomere repeats were added by a specific enzyme that has a terminal transferase activity and was named 'telomerase'[28, 29]. Furthermore, treating the cell extract with RNase abolished telomerase activity, hinting that the enzyme uses an RNA template to specify the telomeric sequences. Fishing for an RNA with the telomeric template sequence, Carol successfully cloned the *Tetrahymena* telomerase RNA [30]. The identified telomerase RNA copurified with telomerase, and blocking the template region on the RNA abolished the telomerase activity. She formulated the model for mode of telomere elongation by telomerase. E. Blackburn's lab further confirmed the reverse transcriptase activity of telomerase *in vivo*, by introducing mutations on the RNA template region and validating the incorporation of the altered sequence at telomeres [31].

3.2.1.1. Discovery of *S. cerevisiae* telomerase

Parallel to the discovery of *Tetrahymena* telomerase, Lundblad identified an interesting yeast mutant with a phenotype of gradual loss of telomere DNA and named the gene *EST1* for 'ever shorter telomeres' [32]. Singer and Gottschling discovered the RNA component (*TLC1*) of yeast telomerase by making use of the telomere positioning effect [33]. *TLC1* was identified from a screen for genes that when overexpressed showed repression of telomere silencing. Est1 was later found to be one of the components of telomerase RNP but not the catalytic subunit, and three additional *EST* genes were subsequently identified (*EST2; EST3; EST4 alias CDC13*) [34-36]. Joachim Lingner and Tom Cech successfully identified the yeast telomerase subunits and discovered that Est2 was the telomerase catalytic subunit exhibiting reverse transcriptase activity [37].

3.2.2. Recombination mediated telomere maintenance

Telomerase is not the only activity that is capable of telomere maintenance. Recombination event serves as an alternative mechanism. The alternative recombination mediated telomere maintenance was first discovered in *S. cerevisiae* [38]. A small subset of cells with est1Δ escaped senescence and formed viable colonies. However, such survivors were absent when cells had est1Δ rad52Δ background. This phenomenon demonstrated the importance of recombination for survival in telomerase deficient cells, as Rad52 is crucial for homologous recombination [38-40].

When telomeres reach a critically short length in telomerase deficient cells, growth arrest is triggered. A single chromosome terminus lacking telomere is sufficient to activate growth arrest [41-43]. Even in the presence of functional telomerase, an occasional short telomere generated during DNA replication can trigger growth arrest [44, 45]. Survivors from such arrested cultures emerge and continue to grow. The survivors however exhibit slower growth rate and may undergo multiple rounds of growth arrests.

Survivors are classified as type I and type II owing to their different telomeric DNA arrangements [38, 46]. Rad52 and replication protein Pol32 are required for the generation of both survivor classes [38, 47]. Type I survivors are more frequent than type II [48]. However, due to the lack of stability of type I survivors, they switch to type II. Thus, these two survivor groups are not mutually exclusive.

Adjacent to the telomeric repeat DNA, telomere associated sequences (TAS) are present and *S. cerevisiae* has two classes of TAS: X and Y'[49]. X is present in all telomeres and is quite heterogeneous in size [50, 51]. Whereas Y' is found only in nearly half of the telomeres and exist in two sizes: Y' long (6.7 kb) and Y' short (5.2 kb) [49].

Type I survivors have abnormally long arrays of Y' repeats, generated by recombination from extrachromosomal circular Y' elements [38, 52]. The very ends of telomere in these survivors are still critically short double stranded telomere with normal 3' overhang.

Type II survivors, in contrast, have minor amplification of TAS and possess a very long telomeric repeat DNA [46, 48]. Rolling circle replication event initiates type II survivor telomeric DNA arrangement, and telomeric DNA circles are spotted in this survivor class [52, 53].

3.3. Components of telomerase holoenzyme in *S. cerevisiae*

3.3.1. Est1

Est1 is a 699-amino acid (aa) long protein and binds to TG_{1-3} DNA with a 3'OH *in vitro* [32, 54]. Est1 binds to the RNA component-Tlc1 at the IVc stem loop [55]. Even though yeast cells lacking Est1 (est1Δ) showed telomerase-deficient phenotype, Est1 was dispensable for *in vitro* primer extension assay [34]. This experiment was important to understand that Est1 was not the catalytic subunit of telomerase. However, Est1 immunoprecipitates with Tlc1 and exhibited telomerase activity suggesting it being a part of the telomerase holoenzyme [56, 57]. Est1 directly binds to the stem-bulge of Tlc1, and disruption of this interaction exhibited telomerase-negative phenotype [55]. Est1-Tlc1 interaction is important for recruiting Est2 (reverse transcriptase subunit) to telomeres. Est1's role of recruiting telomerase to telomeres is orchestrated by its interaction with the telomeric G-overhang bound protein-Cdc13 [58]. Moreover, est1Δ phenotype was rescued upon expression of fusion protein: Est2 and DNA binding domain (DBD) of Cdc13 [59]. Est1, unlike the other subunits of telomerase, is cell-cycle regulated, showing 2~3 fold increase in both transcript and protein levels in early S-phase [60]. Est1 has also been proposed to play a role in telomerase regulation by associating and activating telomerase at specific cell cycle stages, apart from simply acting as a bridge between Cdc13 and telomerase [61].

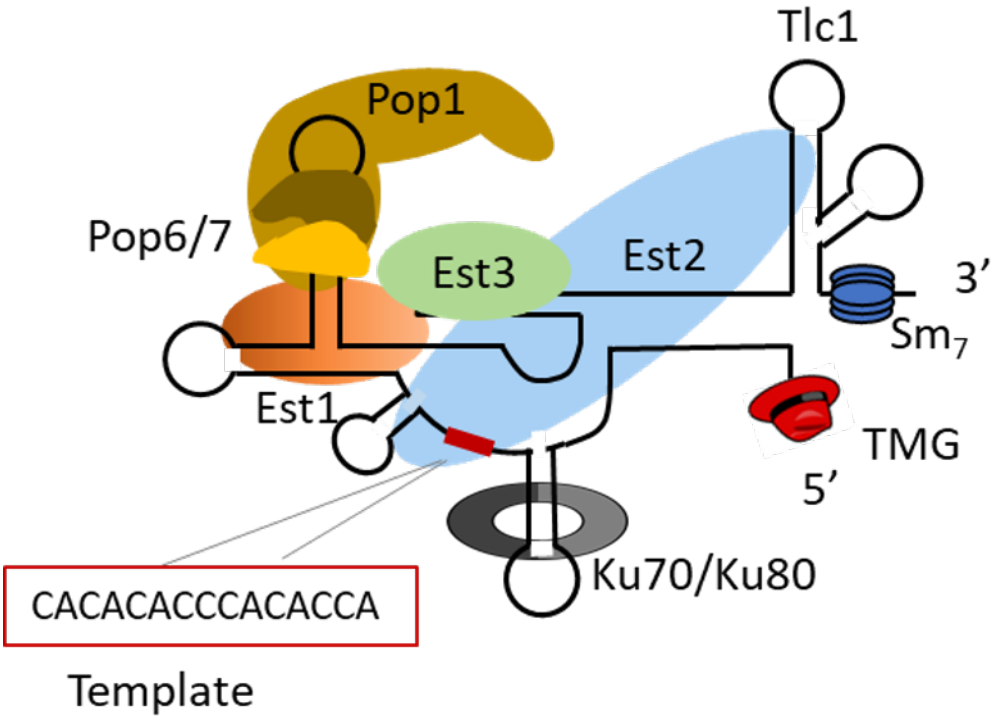

Figure 3: Telomerase holoenzyme of *S. cerevisiae*. Est1 and Est2 bind to Tlc1. Est3 does not bind directly to Tlc1, rather it acts as linker protein for Est1 and Est2. Pop1, Pop6 and Pop7 bind to the P3 domain of Tlc1. Ku70/80 heterodimer binds to Tlc1. Tlc1 is bound by Sm_7 complex at its 3' end and harbors a 2,2,7-trimethyl guanosine (TMG) cap at the 5' end. Template region of Tlc1 used in reverse transcription is denoted in the red box.

3.3.2. Est2

Est2 is an 884-aa protein, comprising of motifs resembling those present in known reverse transcriptases [35, 37]. It possesses the highly conserved three invariant aspartate residues which are essential for the reverse transcriptase activity [37]. Mutation of one of the three aspartate residues of Est2 led to telomerase-negative phenotype *in vivo* and loss of telomerase activity *in vitro* [37]. Thus, confirming that Est2 is indeed the catalytic reverse transcriptase subunit of telomerase. Est2 has a long N-terminal domain (TEN) which facilitates its interaction with several components of the telomerase holoenzyme, and the TEN domain is an essential region for telomerase activity *in vitro* as well as *in vivo* [62]. Est2 binds to the Tlc1, at the proximal center where the three stems meet forming a pseudoknot [63].

3.3.3. Est3

Est3 is a 181-aa protein and is synthesized by a programmed translation frameshift [64]. Like Est1, Est3 too is essential for telomere maintenance *in vivo*, but is dispensable for *in vitro* telomerase activity [35, 65]. Immunoprecipitation assays revealed Est3 is a part of the telomerase holoenzyme [66]. Est3 does not bind to Tlc1, however it directly interacts with Est1 and with the TEN domain of Est2 [67-70]. Est3 acts as a linker for Est1 and Est2 and these interactions mediate its recruitment to telomerase RNP [67-70]. Despite the similarities, Est1 and Est3 are not functionally redundant. DBD Cdc13-Est3 fusion protein rescues est3Δ cells but not est1Δ cells [66].

3.3.4. Pop1, Pop6 and Pop7 complex

The Pop1, Pop6 and Pop7 proteins are associated with the P3 stem loop of the Rpr1 and Nme1 RNA subunits of evolutionarily conserved RNase P/MRP complex [71]. It has been shown that P3 domain is important for RNase P/MRP stability and enzymatic activity. All individual components of RNase P/MRP complex are essential for cell viability [71].

Tlc1 contains an essential domain- IVc stem loop which is structurally and functionally equivalent to the RNase P/MRP P3 domain [72]. Experimental evidence showed that Tlc1, Rpr1 and Nme1 P3 domains are functionally interchangeable. Pop1, Pop6 and Pop7 proteins bind to the P3-like stem on Tlc1 (IVc stem loop), in close proximity to the Est1 binding [55, 72]. Deletion or mutation of the Tlc1-P3 stem loop caused complete loss of telomerase activity *in vivo* [73]. Tlc1-P3 stem loop deletion led to the complete loss of Est1 binding and major loss of Est2 binding, explaining the observed telomerase deficient phenotype [72]. *pop* temperature sensitive alleles also exhibited unstable association of Est1 and Est2 to Tlc1 [74]. It has been shown that Pop1, Pop6 and Pop7 bound P3 stem loop, and not just the P3 domain RNA structure, is crucial for enabling Est1 and Est2 binding. For instance, Est1 absence does not affect *in vitro* telomerase activity, however P3 domain mutations showed a strong reduction in telomerase activity [35, 72, 75]. Moreover, Pop1, Pop6 and Pop7 proteins were detected in partially purified active telomerase RNP complex [72]. *pop1* and *pop6* temperature sensitive alleles exhibit short telomeres, Tlc1 abundance and cytoplasmic accumulation of Tlc1 [74]. In contrast, Rpr1 and Nme1 are less abundant in *pop1/6 ts* strains [74]. These results together suggested that Pop1-Pop6-Pop7 bound

P3 domain is an essential component of yeast telomerase RNP and is crucial for Est1 and Est2 recruitment.

3.3.5. Ku70/Ku80 complex

Ku heterodimer, comprised of Ku70 and Ku80, is known to bind double stranded DNA ends produced either by DNA damage or by recombination event and facilitate non-homologous end joining repair (NHEJ) [76, 77]. Knowing that Ku function in DNA repair, it was surprising when Ku complex was discovered to be bound at telomeric DNA ends, as the prime function of telomeres is to avoid recognition by DNA repair machineries that leads to end-to-end fusions [78]. Ku is recruited to telomeres by its ability to associate with the telomere binding protein Sir4 [79]. Sitting at the telomeres, it plays an important role in preventing C-strand degradation and promotes transcriptional silencing of telomere proximal genes [80].

Ku complex also directly binds to Tlc1 [81, 82]. However, the binding of Ku complex to telomeric DNA or to Tlc1 is mutually exclusive [83]. Since Est1 mediated telomerase recruitment to telomeres happens in late S phase, Ku facilitates telomerase recruitment to telomeres at the G1 phase [60, 84]. Even though telomerase mediated telomere elongation can happen in G1 phase, presence of Rif1 and Rif2 prevents such an event from occurring [85]. Tlc1 mutant harboring the kustemΔ, accumulated in the cytoplasm [85]. Thus, it is proposed that Ku is important for nuclear retention of telomerase. The mutants, Tlc1-kustemΔ as well as ku80-135 mutant, abolished Tlc1-Ku interaction without interfering with other functions of Ku, and exhibited shorter telomere length [81, 82]. However, Ku deficient cells exhibited a relatively more aggravated telomere shortening.

3.3.6. Sm_7 complex

Identification of 5'-2,2,7-trimethyl guanosine (TMG) cap on Tlc1 hinted that the telomerase RNA in budding yeast could have other hallmark features of snRNPs [86]. Sm_7 binding motif (AUUUUUGG) was present 8 bp upstream the 3' end of mature Tlc1- the RNA form that is associated with catalytically active telomerase [86]. Member proteins of Sm_7 complex co-immunoprecipitated Tlc1 [86]. SMD1 (component of Sm_7) conditional switch off destabilized Tlc1 [86]. Additionally, Tlc1 harboring mutations at Sm_7 binding site were highly unstable *in vivo* and exhibited severe telomere shortening [86]. These results indicated that the Sm_7 complex is crucial for Tlc1 stability and function.

The telomerase enzyme complex pulled down with Sm_7 exhibited functional telomerase activity which could be killed upon RNase treatment [86]. This confirmed that Sm_7 complex is indeed a part of the catalytically active RNP.

tlc1-sm- mutant (where the Sm_7 binding site completely unrelated sequence) was highly unstable. tlc1-sm- strain with rad52Δ background, showed a biphasic growth pattern i.e. a defective growth until 100-125 generations, and then the cells recovered and exhibited normal growth [86]. In the tlc1-sm- rad52Δ strain, the telomere length shortened initially and was subsequently maintained at a length shorter than the Wt, which correlated with the observed growth pattern [86]. This observed phenotype differed from that of the tlc1Δ rad52Δ strain, in which the telomere length continually shortened over time until the cells reached senescence (75-100 generations). The observation of tlc1-sm- rad52Δ strain surviving with a shorter telomere length even when almost no mature Tlc1 was detectable remains puzzling to date.

A long-standing model for telomerase RNP biogenesis in yeast proposes that Sm_7 complex binds to Tlc1 immediately after transcription or co-transcriptionally, thereby protecting Tlc1 from nuclear 3' degradation and stabilizing Tlc1 [87].

S. cerevisiae telomerase RNP biogenesis involves trafficking steps of export to cytoplasm and re-import to nucleus [87-89]. Vasianovich, using single molecule fluorescence *in situ* hybridization (smFISH) microscopy, showed that tlc1-sm- mutant transcripts are stably transcribed and exported to cytoplasm, but then degraded there [90]. Additionally. very few Sm_7 lacking Tlc1 molecules that managed to escape degradation were prevented from re-entering the nucleus [90]. This experimental evidence conveys that Sm_7 is essential for stabilizing Tlc1, once it reaches the cytoplasm and is important for the reimport of Tlc1 back to the nucleus. A new model for telomerase RNP biogenesis was proposed based on this observation that Sm_7 complex could bind to Tlc1 in the cytoplasm along with Est1, Est2 and Est3 subunits.

Whether the Sm_7 associates with Tlc1 co-transcriptionally or at the cytoplasmic phase remains elusive.

3.3.7. Tlc1: the RNA subunit

The telomerase RNA (Tlc1) in *S. cerevisiae* is transcribed by RNA polymerase II (RNA pol II), initially as longer transcript ~1.3 kb [91]. It undergoes processing at the 3' end and is trimmed to 1157/1158 nt. The trimmed Tlc1, referred to as the mature form, becomes a part of the catalytically active telomerase enzyme complex. Akin to all RNA pol II transcripts, Tlc1 too is assumed to get a 7-methyl guanosine cap at the 5' end in a co-transcriptional event. The 5' cap undergoes hypermethylation forming 2,2,7-trimethyl guanosine (TMG) [86, 92].

Tlc1 is present in less abundance, about 10~25 molecules per cell [93]. The predicted number of Tlc1 molecules per cell is less than the number of telomeres present, thus making the Tlc1 component the limiting factor for telomerase activity. Consistent with this, *TLC1* is a haplosufficient gene, where *TLC1/tlc1Δ* cells have shorter telomere relative to wild type (Wt) diploid cells [93]. Tlc1 transcription is cell cycle regulated, peaking at G1-S transition [94]. Moreover, Tlc1 transcript is highly stable, exhibiting a half-life of at least 60 min [95].

S. cerevisiae Tlc1 is relatively large in size compared to the human TER (451 nt) and ciliate TER (~150 nt) [30, 33, 96]. However, only 40% of Tlc1 was required for sufficient telomerase activity enabling sustained growth [63]. Essential regions of Tlc1 were determined by screening for *tlc1* deletion alleles that rescued *tlc1Δ rad52Δ* senescing cells It must be noted that the non-essential regions predicted from this experiment cannot be concluded as non-functional.

Tlc1 is reported to have a flexible scaffold to tether the protein subunits, with no specific RNP structure as a whole [97-99]. For instance, minimized Tlc1, where substantial portions of stems are deleted, can support telomerase activity *in vitro* and retain function *in vivo* [97]. Although, viable cells expressing mini-Tlc1 possess short telomeres and exhibit reduced fitness relative to Wt cells [97]. Additionally, Est1 binding site and Sm_7 binding site could be translocated to new positions on Tlc1 without loss of function [98, 100].

3.4. Diverse 3' processing mechanisms of telomerase RNA (TER) across eukaryotes

Despite the conserved motifs, TERs extensively vary in size, sequence, and biogenesis mechanism across species [101, 102].

3.4.1. Ciliate TER

The mature TER (159 nt) of the ciliate, *Tetrahymena thermophila*, retains the 3' uridine-rich transcriptional termination sequence, without undergoing further 3' end processing after being transcribed by RNA pol III [30]. This terminal poly(U) tract along with the stem I and IV serves as a binding site for p65, a La-family protein. p65 stabilizes TER, thereby facilitating efficient TERT assembly and catalytic activity [103, 104] [Fig 4].

3.4.2. Fungi TER

The TER in the budding yeast, *S. cerevisiae* (Tlc1), is bound by the proteins Nrd1 and Nab3 at their respective consensus binding sites at the 3' end [105, 106]. These proteins then recruit the helicase, Sen1, which facilitates transcriptional termination by unwinding the RNA-DNA hybrid at the active site of RNA pol II [105]. A short polyadenosine tail is added at the 3' end by the TRAMP complex and then the transcript is nucleolyticaly processed to the mature form (poly A- form) [105-108]. However, as a fail-safe mechanism, a longer adenylated form (poly A+) is produced by bypassing the Nrd1p/Nab3p termination, which could serve as a precursor and be processed giving rise to the mature Tlc1 [105].

A completely different TER maturation pathway exists in the fission yeast, *S. pombe*. Like *S. cerevisiae* both poly A+ and poly A- forms of TER is found in *S. pombe* [109]. However here the poly A+ acts as a precursor for the mature form. The precursor TER transcript includes an intron downstream the mature 3' end. The intron is removed by spliceosomal cleavage akin to the first transesterification reaction of splicing, and the 5' exon which is released serves as the functional mature TER [110]. Such a cleavage leaves the 3' end Sm_7 binding site compromised of the terminal G and hence destabilizes the Sm_7 complex binding [110]. Additional 3' end nucleotides are lost, leaving TER with a 3' terminal U-tract. Lsm2-8 complex binds to this U-tract and protects it from further exonucleolytic processing [111].

Spliceosomal cleavage mediated TER 3' end processing is widespread across fungi, which includes some fission yeast (*S. pombe*, *S. cryophilus*, *S. octosporus*), filamentous fungi (*Aspergilli*, *Neurospora*) and some budding yeast (*Candida*, *Hansenula*) [73, 110, 112-114]. Even though the role of spliceosomal cleavage in generating the 3' end of TER is conserved, the RNA elements and the underlying strategy which uncouples the two steps of splicing differs. We know at least

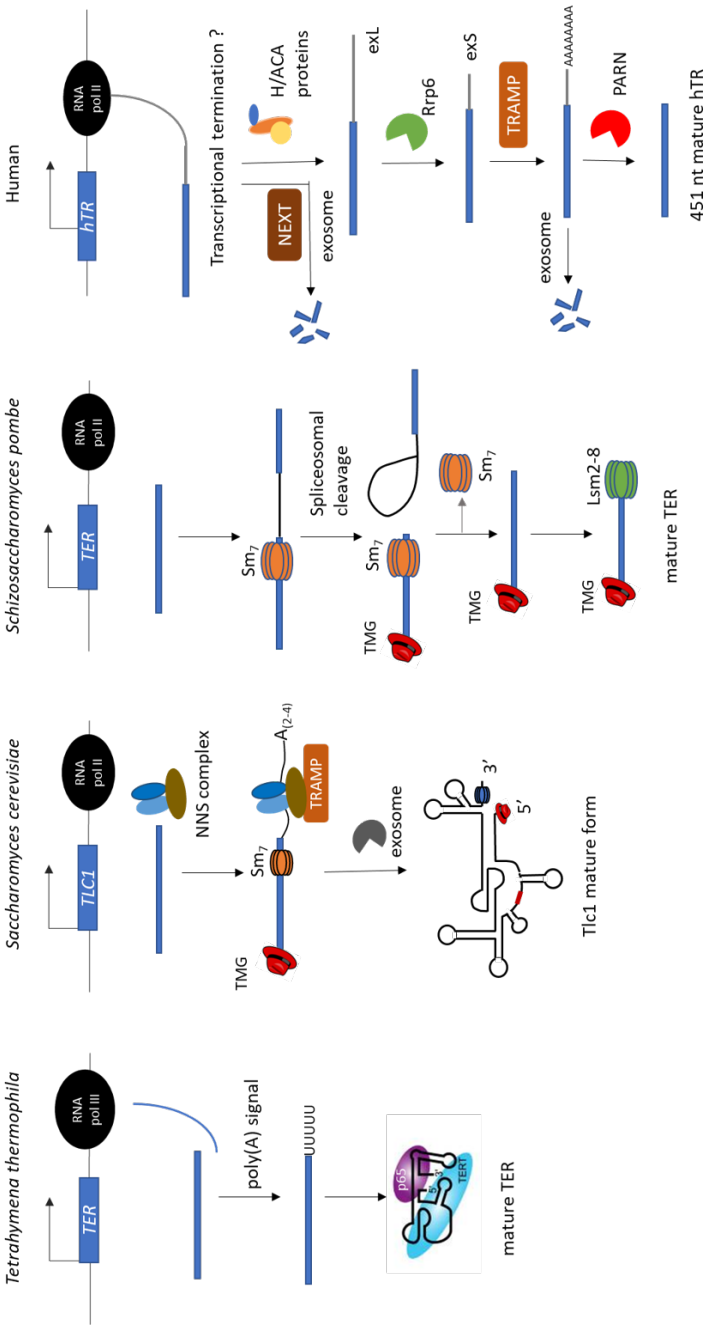

Figure 4: Diverse 3' processing mechanisms of telomerase RNA across eukaryotes. *Tetrahymena thermophila* TER undergoes no 3' trimming and the mature form retains the 3' terminal U-tract. In *S. cerevisiae*, Tlc1 undergoes Nrd1-Nab3-Sen1 mediated 3' processing. In *S. pombe*, spliceosomal cleavage produces mature TER. Human telomerase RNA undergoes multiple checkpoints, where during each step the decision to be degraded or further processed is made.

three different spliceosomal cleavage strategies used by different fungi [112, 114, 115]. In *S. pombe*, two attributes of the intron facilitate the release of splicing intermediate as a functional product by blocking the completion of the splicing event [114]. First, an unusually long distance (23 nt) between the branch point (BP) and 3' splice site (SS). Second, a branch site (BS) that is fully complementary to U2 snRNA binding site, causing extreme stability of U2-BS interaction. These attributes which impedes the transition from first to second step of splicing, triggers the Prp22 dependent 'discard pathway' and releases the products of the first transesterification reaction [114]. The discard pathway functions in recycling spliceosome complex from defective transcripts by rejecting the spliceosomal cleaved product, however in the case of TER processing it functions in the release of a functional product [116, 117].

In two other fission yeasts, *S. cryophilis* and *S. octosporus*, a polyadenylated TER precursor with an intron downstream the mature 3' end was identified to mature via spliceosomal cleavage [112, 115]. However, a close inspection of the intronic sequence revealed that a different attribute than what was observed previously with *S. pombe*, was owing to the observed efficient spliceosomal cleavage. An unusual 5' SS sequence (GUCAGU) was identified, which by hyperstabilizing the U6 snRNA and 5'SS interaction facilitated spliceosomal cleavage [115]. Yet another spliceosomal cleavage strategy was identified in filamentous fungi, *N. crassa* and *Aspergilli* species, where the adenine at the first position of the intron (AUA(A/C)GU) was crucial for blocking the second step of splicing [112, 115]. Bioinformatic analysis evidenced that this *N. crassa-Aspergilli*-type intronic sequence was conserved not only across the *Pezizomycotina* subphylum, but also in the early branching fission yeasts, *Saitoella complicate* and *Schizosaccharomyces japonicus*, which belongs to the subphylum *Taphrinomycotina* [112]. Such a widespread existence across the *Ascomycota* phylum makes the *N. crassa-Aspergilli*-type spliceosomal cleavage strategy appear to be ancestral than the two other observed fission yeast-strategies (*S. pombe* and *S. cryophilis*/*S. octosporus*) [112].

3.4.3. Human TER

The human telomerase RNA (hTR) maturation involves multiple check points, where there is a competition between degradation of the precursor and processing to mature form [118, 119]. Such a tight competition at multiple steps ensures a stringent regulation of physiological hTR levels and telomerase function. hTR is transcribed as a longer transcript by RNA pol II and is co-

transcriptionally bound by the H/ACA protein complex which plays a crucial role in conferring stability to hTR [120, 121]. The longer transcripts are either bound by CBC and NEXT complex and signalled to be degraded by exosome or trimmed by Rrp6 to a shorter hTR precursor (exS form) [119]. However, we cannot exclude the possibility that the shorter intermediates could also be transcribed independently as a primary transcript. The TRAMP complex is then recruited, which adds a poly(A) tail at the 3' end and thereby stimulates degradation by the exosome [118, 119]. The poly(A)-specific ribonuclease (PARN) antagonizes such a stimulated degradation by actively removing the terminal A-tail and thus facilitates processing of hTR to mature form [118, 119]. The transcriptional termination mechanism of hTR still remains elusive. A recent study demonstrated that the integrator complex is involved in the regulation of hTR transcriptional termination [122].

3.5. Tlc1 biogenesis in *S. cerevisiae*

3.5.1. RNA pol II transcriptional termination mechanisms in *S. cerevisiae*

The biological significance of transcription termination extends beyond marking the endpoint of transcription, as it is connected to the 3' processing, stability, and export of the transcripts, thereby determining the fate and function of the RNA [123].

In *S. cerevisiae*, two major pathways exist for termination of RNA pol II transcription [123-126]. One pathway relies on the cleavage and polyadenylation factor (CPF) and is essentially responsible for termination of mRNA transcripts [123, 127]. The CPF complex mediates transcription termination by coupling endonucleolytic cleavage to Pap1 mediated polyadenylation of the transcripts. As a result, these transcripts have a long poly(A)-tail, consisting of nearly ~70 adenosines. The acquired long A-tails of mRNA confer stability and aids in Nab2 mediated export to the cytoplasm. Nab2 functions with Mex67/Mtr2 dimer and supports THO/TREX complex during the export. Once the transcript reaches the cytoplasm, Nab2 is replaced by Pab1.

The other major transcriptional termination pathway employs Nrd1-Nab3-Sen1 complex (NNS) for the termination of small nuclear RNAs (snRNAs), small nucleolar RNAs (snoRNAs) and cryptic unstable transcripts (CUTs) [123]. Nrd1 and Nab3 bind to sequence specific motifs on the transcript, GUAA/G and UCUUG respectively [128, 129]. Nrd1 recognizes and interacts with the phosphorylated Serine (Ser5P) of RNA pol II C-terminal domain (CTD) and facilitates transcriptional termination [130]. The Nrd1-Nab3 heterodimer recruits Sen1, the DNA-RNA

helicase, which facilitates the unwinding of the nascent transcript from the template DNA [131]. A recent study shows that Sen1 also interacts with RNA pol II CTD and contributes to transcriptional termination [132]

The NNS dependent pathway involves TRAMP complex which constitutes: Trf4/5- poly(A) polymerase; Air1/2- a zinc knuckle RNA-binding protein; Mtr4- DExH-box RNA helicase [108, 133]. The Trf4/5 adds a short oligo(A) tail to the NNS dependent transcripts, making it a good substrate for the exosome complex [134, 135]. Exosome complex degrades the CUTs and trims the sn/snoRNAs via its 3' nuclease activity [136]. It has two catalytic subunits: 1) Dis3- possesses both 3'exonuclease and endonuclease activity and is essential for the cells; 2) Rrp6- harbors 3'exonuclease activity and is non-essential for the cells [137, 138]. Rrp6 also can additionally perform its function without being a part of the exosome complex [139]. The nine membered exosome complex functions with Dis3 in both nucleus and cytoplasm [140]. Whereas the function of exosome complex with Rrp6 is limited to the nucleus [140].

Nrd1 interacts with Trf4 with the same domain it uses to interact with RNA pol II [133]. NNS complex is thought to function in two forms: one through Nrd1 interaction with CTD of RNA pol II facilitating transcriptional termination; second through Nrd1 interaction with Trf4 facilitating exosome mediated degradation or processing [133].

The CTD of the RNA pol II undergoes dynamic phosphorylation throughout the transcription cycle [141]. The CPF complex recognizes phosphorylated serine at position 2 of CTD, which is prominent during middle and late elongation [142]. As a result, the poly(A) mediated transcription termination occurs >1 kb from transcription start site (TSS) [143]. Whereas the NNS dependent pathway recognizes Ser5 phosphorylation of CTD, which is an early elongation mark, thus transcription termination occurs <1 kb from TSS [130, 143].

Another major difference between the transcripts terminated by either of the pathways is their adenylation tail length. Transcripts from poly(A) mediated transcription termination, as the name suggests, possess a long poly(A) tail of ~70 adenosines [144]. Contrastingly NNS transcripts contain short oligo(A) tail of 4~5 adenosines [134, 135]. However, using direct RNA sequencing, a recent study shows that ncRNAs have poly(A) tails of 20-60 adenosines [145].

3.5.2. Evidence for polyadenylation mediated transcription termination of Tlc1

In 1997, Chapon made the initial efforts to map the 3'ends of Tlc1 in *S. cerevisiae* [91]. Total RNA extract was treated with poly(A) polymerase and subsequently reverse transcribed using oligo dT primer. PCR amplification with Tlc1 specific forward primer and oligo dT reverse primer, and subsequent sequencing of the amplicon enabled them to identify 5 different 3' ends of telomerase RNA (+1239, +1242, +1246, +1249, +1252) [Fig 5]. To their surprise *in vitro* A-tailing was not required to amplify Tlc1 using oligo dT primer. This suggested that Tlc1 possess an A-tail that is added post-transcriptionally. This result explained why Tlc1 was originally identified in a poly(dT) primed cDNA library.

Fractionation experiment using oligo(dT) column further confirmed that 2 different Tlc1 species existed, that not just varied in the 3' adenylation status but also in size [91]. A small fraction of a longer form (~1300 nt), which corresponded to 5-10% of total Tlc1, had a long A-tail. And a major fraction of Tlc1 was shorter, without the long A-tail. The shorter non-adenylated form is the one that is associated with the Est2 and is referred to as the mature form. The 3' end of the Est2 associated Tlc1 was mapped to +1158/+1157 [146]. The longer form with A-tail was referred to as the polyA+ form and the non-adenylated shorter form was called the polyA- form. Even though majority of the shorter form was in the flowthrough of the fractionation experiment, it must be noted that they did capture few molecules of the shorter A- species in the oligo(dT) column. This hinted that the short Tlc1 species could harbour short A-tracts that wasn't enabling them to be efficiently enriched in the oligo(dT) column.

In an approach to test whether the same mRNA poly(A) machinery is responsible for adenylating Tlc1, an interesting observation hinted that the polyA+ and polyA- forms have a precursor-product relationship. Pap1 is a poly(A) polymerase that is responsible for polyadenylation of mRNA in *S. cerevisiae*. *pap1-5 ts* (temperature sensitive) strain, upon shift to restrictive temperature, dramatically decreased the poly(A+) Tlc1 levels and was almost undetectable after 30 min of temperature shift [91]. Even though the polyA- levels were stable for the first 60 min at restrictive temperature, it showed a 2-fold reduction after 2 h [91]. The knowledge of Tlc1 being an extremely stable RNA with a predicted half-life of at least 60 min, explains the delayed reduction of polyA- form upon Pap1 disruption.

Apart from the observation of complete depletion of polyA+ Tlc1 upon Pap1 disruption, further evidence for poly(A) mediated transcriptional termination of Tlc1 was shown. In *S. cerevisiae*, three cis-acting elements contribute to mRNA polyadenylation mediated transcriptional termination: 1) a positioning element – which is an A-rich sequence that dictates the polyadenylation site and is situated 13~27 nt upstream the poly(A) site; 2) an efficiency element- which is an AU rich sequence present upstream the positioning element and enhances the function of the positioning element; 3) actual adenylation site- which is a pyridine followed by an adenosine [147]. Putative positioning and efficiency elements were identified at the 3' end of Tlc1 [91] [Fig 5]. Mutating the predicted Tlc1 efficiency element caused a drastic reduction of poly(A+) form and a 2-fold reduction of poly(A-) form relative to Wt [91]. Although the known poly(A+) form was depleted in the Tlc1 efficiency element mutant, a longer heterogenous RNA was detected [91]. This observation of a new longer precursor form can be due to the employment of cryptic polyadenylation sites, much downstream the actual polyadenylation site, for transcriptional termination [Fig 5].

The observation that poly(A-) levels is decreased when the poly(A+) form was drastically depleted, such as during Pap1 disruption and efficiency element mutation, exhibits the precursor-product relationship of the two Tlc1 forms [91]. Furthermore, overexpression of Tlc1 under a galactose inducible promoter led to a 100-fold increase in poly(A+) and a 10-fold increase in poly(A-) levels [91]. The steady-state proportion of poly(A+) and poly(A-) forms was not observed upon overexpression of Tlc1, as overwhelming levels of precursor Tlc1 could disturb the Tlc1 processing, transport and assembly factors required to produce the mature form. Additionally, in the same Tlc1 induction system, poly(A+) form levels were 90% of total Tlc1 after 5 min of induction, and gradually decreased with time reaching a plateau after 1 h and maintained thereafter at 60 % relative to total Tlc1 [91]. This result confirms that the poly(A+) is the initially transcribed Tlc1 species.

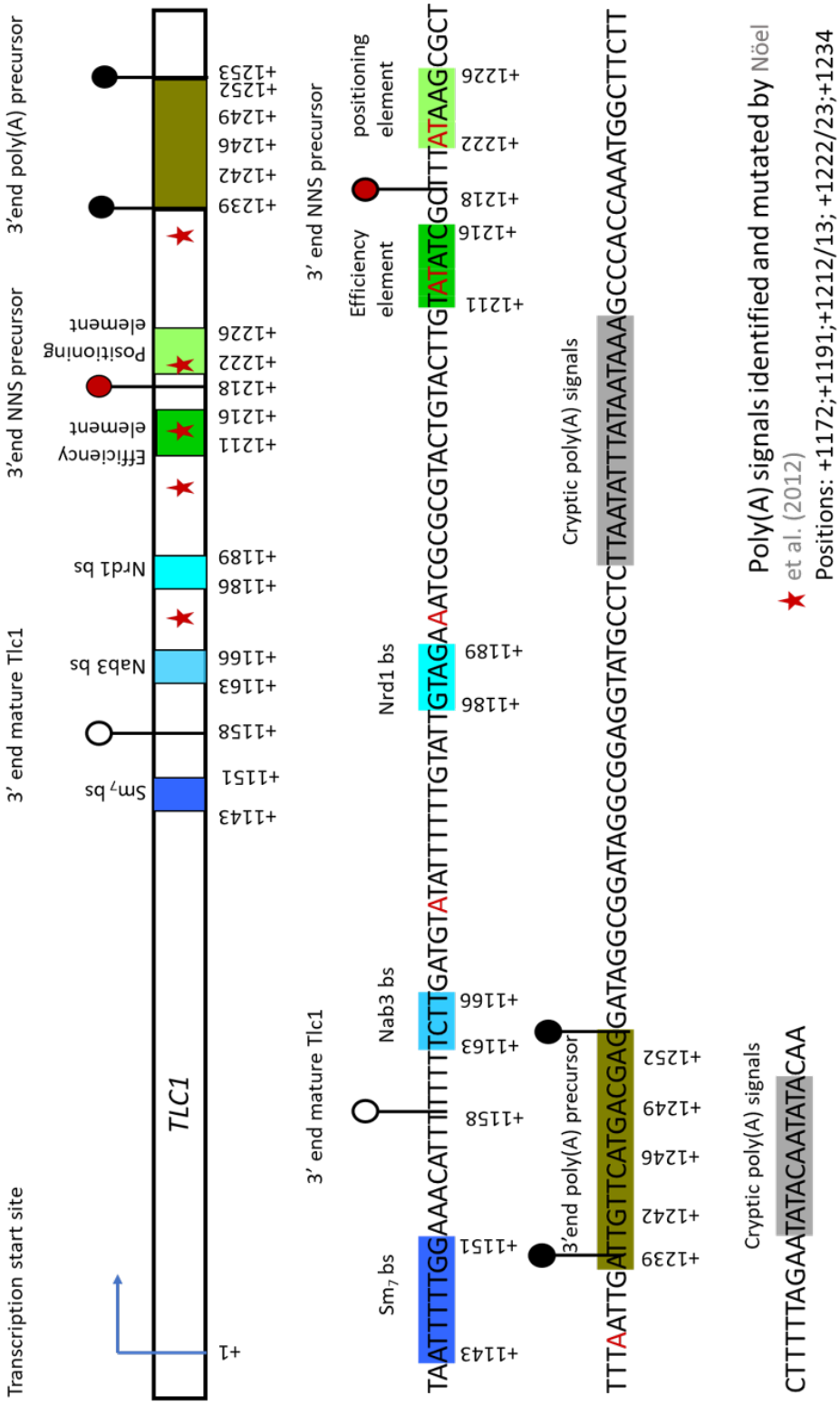

Figure 5: Schematic representation of the Tlc1 transcription unit with a focus on the 3' end. Important features of Tlc1 Nrd1-Nab3-Sen1 transcriptional termination and polyadenylation transcriptional termination are denoted. Nucleotide positions are in accordance with the transcription start site.

3.5.3. Evidence for Nrd1-Nab3-Sen1 (NNS) mediated transcription termination of Tlc1

With the above-mentioned evidence, it was convinced that Tlc1 undergoes transcriptional termination via polyadenylation mechanism, giving rise to a longer poly(A+) precursor which is then subsequently trimmed at 3' end to produce the mature form. However, in 2011, there was a change in this notion upon identifying Tlc1 in the transcriptome wide binding analysis of Nrd1 [106]. Nrd1 crosslinked to Tlc1 between +1188 ~ +1221 and these crosslinked Tlc1 molecules have non-genome encoded A-tails (≥3), hinting that Nrd1 could facilitate exosome mediated 3' processing of Tlc1.

Around the same time, Wellinger's lab using a different approach arrived at the same conclusion. Mutations on all probable and cryptic polyadenylation signals at 3' end of Tlc1, did not affect the mature Tlc1 levels, despite depleting the known poly(A+) form [105]. It must be noted that even though the known poly(A+) form was abolished due to the incorporated mutations, a new and a longer Tlc1 precursor was produced [105]. This observation mimics the visualization of long heterogenous transcript upon the efficiency element mutation observed by Chapon [91].

They employed an ACT1-*CUP1* fusion reporter construct to identify the Tlc1 sequence precisely required for transcription termination [105]. A construct with the first exon of actin, followed by intron of actin, is fused with *CUP1*. Cup1 is essential for growth in the presence of excess copper (Cu2+). Different 3' Tlc1 fragments were inserted at the actin intron. If the inserted sequence facilitates transcription termination, no Cup1 will be synthesized, hence no growth. Alternatively, if the inserted sequence fails to establish transcription termination, Cup1 will be synthesized allowing growth. Using this reporter construct they identified Tlc1 fragment with an endpoint at +1218 position was sufficient for facilitating transcription termination [105]. This identified +1218 position is much upstream than the previously predicted polyadenylation sites (+1239-+1252) [91, 105]. Nrd1 and Nab3 binding sites were identified between the mature form end (+1158) and +1218 position of Tlc1 [105, 106]. Preventing the association of Nrd1 and Nab3 to Tlc1, either by disturbing the endogenous Nrd1 and Nab3 protein expression using the corresponding temperature sensitive alleles or by mutating the binding sites of those proteins on Tlc1, led to failed transcription termination in the reporter system [105]. Furthermore, Nrd1 and Nab3 depletion accumulated poly(A+) Tlc1 [105]. With these evidences it was proposed that Tlc1 uses NNS transcription termination as the major pathway, where upon transcription termination

short oligo(A) tails are added using TRAMP complex and subsequently is trimmed to the mature form (+1158) [105]. Poly(A+) transcripts are generated by some read-through of NNS pathway and could be trimmed to the mature form [105].

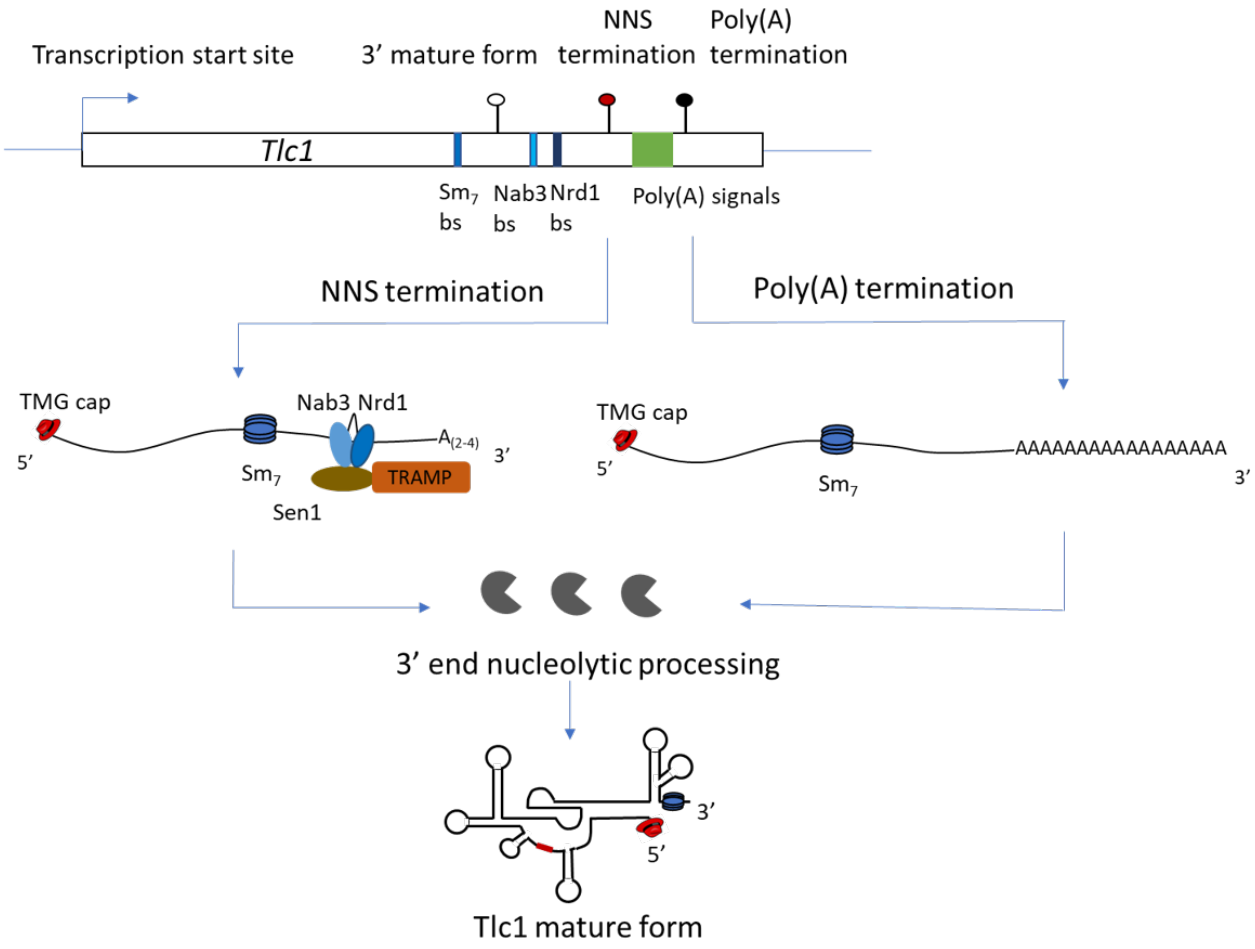

Figure 6: Schematic representation of maturation pathways of Tlc1. Two unique pathways can contribute to mature Tlc1. NNS mediated transcriptional termination acts in concert with TRAMP complex and gives rise Tlc1 precursors with short A-tails. Alternatively, when NNS signals are bypassed by RNA pol II, Tlc1 transcriptional termination is carried out with poly(A) signals, which gives rise to precursors with longer A-tails. Precursors produced via either of the two pathways can undergo nucleolytic processing at the 3' giving rise to the mature Tlc1.

3.5.4. 3' processing of Tlc1

Considering the subset of other RNA species using NNS transcription pathway, we know that these transcripts are subsequently targeted for processing or degradation by exosome [136]. Abolishing the exonuclease activity of exosome (rrp6Δ or dis3 exo- D551N mutant), accumulates poly(A+) Tlc1 [148]. This hinted that exosome could be involved in processing the precursor Tlc1

to the mature form. Exonuclease activity impaired exosome mutants accumulated mature Tlc1 as well [148]. This suggests that the exosome, in addition to 3' processing, is also being involved in the turn-over of the mature form.

Early in 1999, it was shown that Sm_7 is crucial for stabilizing Tlc1. Sm^- mutant, where the complete Sm_7 binding site on Tlc1 was replaced with non-specific sequence, exhibited complete depletion of Tlc1 mature form [86]. Two less severe mutations, Sm2T and Sm4C5C, where 2 uridines were either deleted or substituted with cytosine respectively, exhibited very low levels of poly(A+) Tlc1 [86]. These Tlc1-Sm_7 binding site mutants were introduced into cells with disabled exosome activity [148]. Rrp47 is known to function as a co-factor of Rrp6 and its depletion dramatically accumulated polyA+ and mature form, akin to the exonuclease mutants [148]. In the Sm2T and Sm4C5C mutants, but not in Sm^-, poly(A+) Tlc1 was restored upon rrp47Δ [148]. The restoration of poly(A+) form but not the mature form, further bolstered the precursor-product relationship of poly(A+) and mature form. This experiment conveys that Sm_7 is involved in regulating the 3' processing of Tlc1 by exosome.

In vitro reconstitution of Tlc1 3' trimming with purified exosome complex from *S. pombe* further validated the role of exosome and Sm_7 in the 3' processing of poly(A+) to the mature form [148]. Poly(A+) precursor Tlc1, either bound with functional Sm_7 complex or harboring Sm4C5C mutation, was pulled down using Est2 and subsequently incubated with purified exosome complex. The reconstitution assay demonstrated that the exosome complex trims the precursor Tlc1 to mature form only when Tlc1 is bound by Sm_7, otherwise degrading it [148].

During its biogenesis, the Tlc1 is exported to the cytoplasm after transcription and is re-imported back to the nucleus [87, 90]. When during biogenesis does the 3' processing event happen? This is not clear to us yet as we have experimental evidence for two scenarios: 1) 3' processing happening prior to the nuclear export; 2) 3' processing happening after the nuclear re-import. In the absence of the Tlc1 export factor (Xpo1), there is a stable accumulation of fully processed Tlc1, indicating that the 3' trimming could happen prior to the cytoplasmic export [149]. On the other hand, RNA immunoprecipitation with either Tlc1 nuclear re-import proteins (Mtr10 and Cse1) or with proteins that bind to Tlc1 early during its biogenesis (Cbp20 and Mex67), showed an enrichment for precursor Tlc1 emphasizing that 3' processing could occur after the nuclear re-import [150].

3.5.5. 5’ processing of Tlc1

Active telomerase RNP contains Tlc1 that bears a 2,2,7-trimethyl guanosine (TMG) cap at its 5’ end [86, 146]. This modification on Tlc1 is executed by Tgs1, an S-adenosyl-L-methionine dependent methyltransferase, which is believed to be residing at the nucleolus [92]. During snRNA maturation, the bound Sm_7 complex increases its affinity to Tgs1 [151, 152]. Sm_7 on the Tlc1 could also resemble the same function and thereby aids the hypermethylation of the cap. Depletion of Tgs1 caused a slight nuclear enrichment without affecting the overall Tlc1 abundance, which is consistent with the phenotype observed with snRNAs [87]. Apart from not affecting Tlc1 stability, absence of Tgs1 did not cause any major telomeric defects either [92]. The molecular significance of the TMG capping of Tlc1 is not clear yet and hence, further work is required to understand its role in Tlc1 maturation.

The question regarding the temporal occurrence of 5’ processing during Tlc1 biogenesis naturally arises. This is not clear to us yet. And similar to the timing of 3’ trimming, mixed evidence for 5’ processing too exists in literature. Conditions that caused nuclear accumulation of Tlc1 (est1-3Δ, ku70Δ, disrupting Xpo1 pathway) did not affect the TMG status of Tlc1 molecules, which hinted that the hypermethylation could possibly occur prior to the cytoplasmic export [87]. Alternatively, in the absence of Tlc1 re-import factors (Mtr10 and Cse1), Tlc1 couldn’t be enriched by TMG immunoprecipitation, indicating that TMG capping occurs more likely after the re-import in to the nucleus [150] .

3.5.6. Subcellular trafficking of Tlc1

Tlc1 undergoes nucleo-cytoplasmic shuttling during the telomerase RNP biogenesis [Fig 7]. Tlc1 after being transcribed at the nucleus, is exported to the cytoplasm, and returns to the nucleus to exert its role as telomerase RNP at the telomeres. Additionally, Tlc1 is believed to visit the nucleolus to gain the TMG cap. Let us see in detail the involvement of various factors that orchestrate the subcellular trafficking of Tlc1.

3.5.6.1. Export to the cytoplasm

The very first hint that Tlc1 shuttles between the nucleus and cytoplasm during RNP maturation came from Gallardo’s work in 2008 where he performed fluorescent *in situ* hybridization on native Tlc1. He observed that upon disruption of Est1-3 or Ku70 proteins,

Tlc1 accumulated at the cytoplasm [87]. Interestingly, subsequent disruption of RNA export factor Xpo1(Crm1) led to the nuclear retention of Tlc1 [87]. Maturation steps post transcription of other RNA species, such as the snRNA and mRNA, involves binding of Cap Binding Complex (CBC) onto the m^7G cap. The bound CBC interacts with Mex67/Mtr2 and Xpo1, which in turn facilitates the passage of the RNA molecules through the nuclear pore into the cytoplasm. Tlc1 interaction with Mex67 was confirmed with RNA coimmunoprecipitation (RIP) experiment [149]. And disruption of Mex67 in ku70Δ background led to nuclear accumulation of Tlc1 [149]. Surprisingly. xpo1-1 mex67-5 double mutant, but not the single mutants, exhibited severe telomere shortening [149].

A recent study employing an inducible system to selectively discriminate and visualize newly synthesized Tlc1 molecules, further validated that Tlc1 export was indeed mediated my Xpo1 and Mex67 [90]. However, quite unexpectedly the system revealed that Mex67 is crucial for 3' stabilization of Tlc1 at the nucleus prior to the export [90]. Upon Mex67 disruption, Tlc1 was rapidly degraded via Rrp6-dependent nuclear exosome. This result is in line with what is observed in the case of polyadenylated mRNA in the absence of Mex67 [153]. Rapid depletion of poly(A) bound Nab2 due to the export block, causes the nuclear instability of the mRNA [153]. With our existing knowledge that precursor Tlc1 possesses either a short A-tail or long A-tail (depending on the transcription termination mechanism), it could be that Nab2 binds and protects 3' end of nascent Tlc1 too.

Since Xpo1 cannot directly bind to RNA, Mex67, which is a poly(A) RNA binding protein, could function as an adaptor protein bridging Tlc1 and Xpo1 [90]. Looking at the dramatic effect of Mex67 disruption on Tlc1 stability, Mex67 is considered as an RNA chaperone that is involved in Tlc1 stabilization and nucleo-cytoplasmic shuttling [90]. Despite the clear evidence for cytoplasmic phase of Tlc1, it is not clear yet when and where the different protein components of telomerase associate with Tlc1.

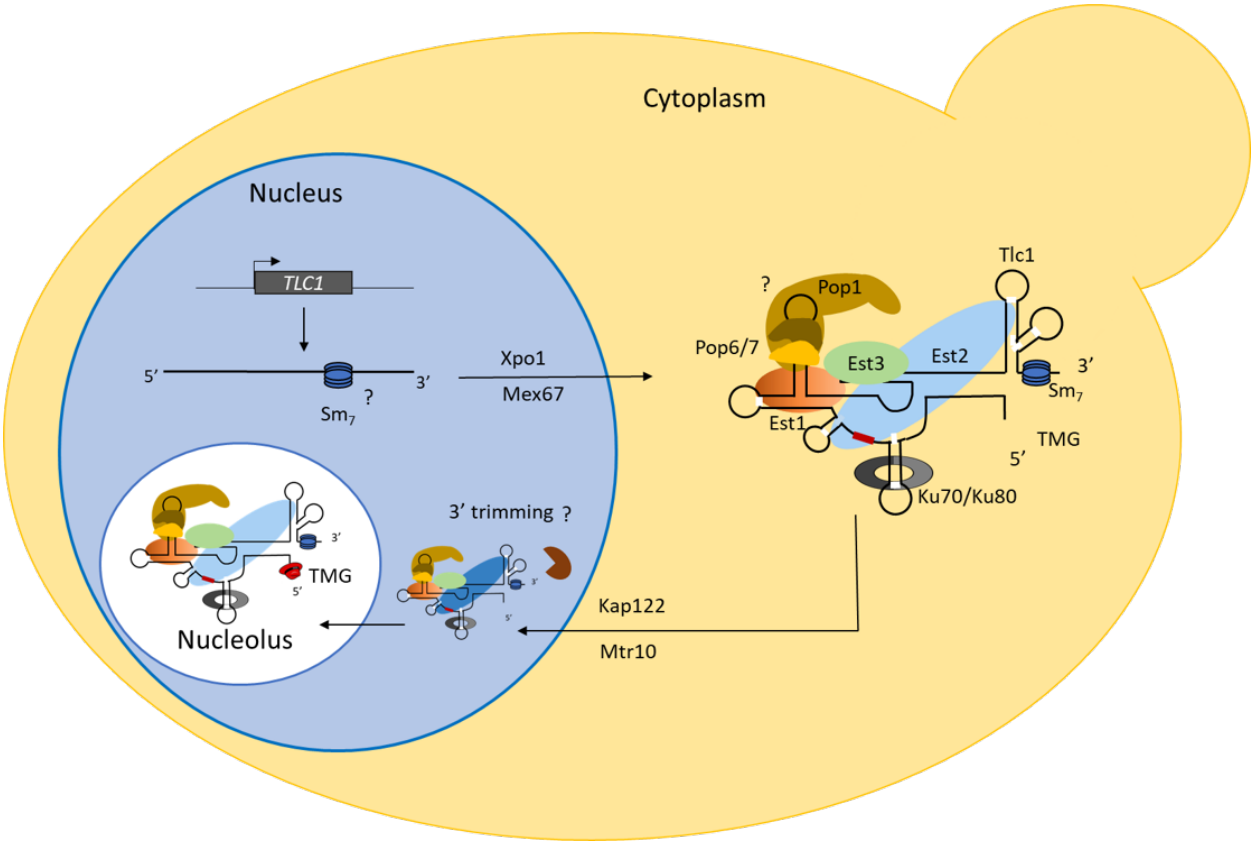

Figure 7: Schematic representation of Tlc1 biogenesis. Tlc1 is initially transcribed in the nucleus as longer precursor. The transcript is exported to the cytoplasm mediated by Xpo1 and Mex67. Tlc1 associates to its protein subunits at the cytoplasm and is re-imported to the nucleus via Kap122 and Mtr10. Tlc1 also shuttles to the nucleolus where it gains the 5' TMG cap. Tlc1 undergoes trimming at its 3' end to give rise to mature form. When the Sm_7 and Pop1/6/7 complex associates to Tlc1 is still unclear. When during biogenesis does 3' processing happen remains elusive too.

3.5.6.2. Import to the nucleus

Since it was obvious that the Tlc1 must return to the nucleus, screening the known potential re-import candidates revealed that *kap122Δ* and *mtr10Δ* mutants significantly reduced the nuclear accumulation of Tlc1 [87]. The inducible system to specifically visualize newly transcribed Tlc1, validated that upon *kap122Δ* there was a delay in the nuclear recruitment of Tlc1 and a drastic reduction in the nuclear fraction of Tlc1 [90]. The delayed re-entry of Tlc1 to the nucleus in the absence of Kap122 suggests that alternative nuclear import pathways can take over the function. The existence of alternative nuclear import pathways for Tlc1 is also confirmed by the observation of only mild defects in telomere maintenance in *kap122Δ* cells [90].

4. Objective of dissertation

In this study, we aim to understand the importance of NNS termination pathway in accounting for the steady state levels of Tlc1-mature form. The approach we took to study the role of NNS termination mechanism was to prevent the recruitment Nrd1 and Nab3 to Tlc1 by mutating their respective binding sites at the genomic locus of *TLC1*. qRT-PCR was performed to monitor the stability of Tlc1 upon NNS disruption. 3' RACE and nanopore sequencing were done to evaluate the effect of defective NNS pathway on 3' processing of Tlc1.

We are interested in understanding the role of 3' end processing mechanisms in accounting for the steady state levels of mature Tlc1. Ribozyme was employed to force terminate Tlc1 at the mature 3' end and thereby skipped the endogenous 3' processing events. Subsequently, we monitored the role of the altered processing kinetics and processing factors on the stability of Tlc1.

.

5. Materials and Methods

5.1. Plasmid construction

All plasmids generated and used in this study are listed in Table 6. Synthetic gene constructs (BLgs1467 and BLgs1470) harboring Tlc1 fragment from +11 to +1155 followed by HDV ribozyme-super-fast or HDV SA1-2 ribozyme-fast sequence [Table 5] cloned in a pEX-A vector was obtained from Integrated DNA Technologies (IDT). The synthetic gene construct BLgs1467 and BLgs1470 digested with NsiI HF and EcoRI HF was subcloned into pRS314-Tlc1 (gift from Kathrine Friedman) digested with the same restriction enzymes to generate pAM1 [TLC1-super-fast Rz, CEN, TRP1] and pAM13 [TLC1-fast Rz, CEN, TRP1] respectively. Site-directed mutagenesis on BLgs1470 either using primer pairs BLoli8511- BLoli8512 or BLoli8465-BLoli8466 or BLoli8467-BLoli8468 was performed with QuikChange II XL Site-Directed Mutagenesis Kit (Agilent Technologies) to generate HDV SA1-2 ribozyme-slow, HDV SA1-2 ribozyme-slower and HDV SA1-2 ribozyme-dead mutants respectively. The mutagenized plasmids digested with NsiI HF and EcoRI HF were subcloned into pRS314-Tlc1 digested with the same restriction enzymes to generate pAM18 [TLC1-slow Rz, CEN, TRP1], pAM16 [TLC1-slower Rz, CEN, TRP1] and pAM17 [TLC1-dead Rz, CEN, TRP1].

pRS314-Tlc1, pAM13, pAM18 and pAM17 digested with BamHI HF and SalI HF were subcloned in to pRS315 digested with the same restriction enzymes to generate pAM20 [TLC1, CEN, LEU2], pAM21 [TLC1-fast Rz, CEN, LEU2], pAM22 [TLC1-slow Rz, CEN, LEU2] and pAM23 [TLC1-dead Rz, CEN, LEU2] respectively.

Overlap extension PCR was done to generate pAM27 [TLC1-slow Rz-PGK1 3'UTR, CEN, TRP1]. Tlc1-slow Rz fragment was amplified by performing a PCR using pAM18 as template with primers BLoli8737-Bloli8738. Genomic DNA prepared from BY4741 was used as template to amplify Pgk1 3'UTR by PCR using primers Bloli8739-Bloli8740. The individual fragments were purified using QIAquick PCR Purification Kit (Qiagen). Overlap PCR reaction containing 0.2 pmol of each fragment, 1x Q5 reaction buffer (NEB), 0.5 mM dNTP mix and 1 unit Q5 High-Fidelity DNA Polymerase (NEB) in a total reaction volume of 50 µL was performed using the following program: 98°C for 30 s, 15 cycles of 98°C for 10 s, 64°C for 30 s, 72°C for 20 s, and final extension at 72°C for 2 min. Following this, 0.5 µM of each Bloli8737 and Bloli8740 was added to the above PCR reaction mix and the same PCR program was run for another 32

cycles. The amplicon was gel purified using QIAquick Gel Extraction Kit (Qiagen) and digested with NsiI HF and EcoR1 HF. The digested amplicon was ligated on to pAM18 backbone resulting from the digestion with same restriction enzymes to generate pAM27.

pAM11[TLC1-sm$^-$, CEN, TRP1], and pAM24[TLC1-sm$^-$-slow Rz, CEN, TRP1], were generated by site-directed mutagenesis using primer pairs BLoli8404-BLoli8405 or BLoli8681-BLoli8682 on either pRS314-Tlc1or pAM18 respectively using QuikChange II XL Site-Directed Mutagenesis Kit (Agilent Technologies).

pAM26 [TLC1-Δ+922-+1126, CEN, LEU2] referred to as mini-Tlc1 in this study was generated by overlap extension PCR. Tlc1-fragment 1 (+412 - +921) was amplified by PCR using primers BLoli8687-BLoli8688 from template DNA pRS314-Tlc1. Tlc1-fragment 2 (+1127 - +1460) was amplified by PCR using primers BLoli8689-BLoli8690 from template DNA pRS314-Tlc1. The two fragments were concatenated by performing overlap extension PCR using primers BLoli8687 and BLoli8690. The concatenated amplicon was digested with NdeI HF and NcoI HF and cloned on to pAM20 backbone resulting from digestion with the same restriction enzymes to generate pAM26.

pAM30[TLC1-kustemΔ+279-+322, CEN, TRP1], and pAM31[TLC1-kustemΔ-slow Rz, CEN, TRP1], were generated by by overlap extension PCR. Tlc1-fragment 1 (+30-+278) was amplified by PCR using primers BLoli8745-BLoli8746 from template DNA pRS314-Tlc1. Tlc1-fragment 2(+323 -+581) was amplified by PCR using primers BLoli8747-BLoli8748 from template DNA pRS314-Tlc1. The two fragments were concatenated by performing overlap extension PCR using primers BLoli8745 and BLoli8748. The concatenated amplicon was digested with BsrGI and NcoI and cloned on to either pRS314-Tlc1backbone or pAM18 backbone resulting from digestion with the same restriction enzymes to generate pAM30 and pAM31 respectively.

5.2. Yeast strains

All yeast strains used in this study are listed in Table 7. All yeast strains that are chromosomally deficient for Tlc1, such as SC164 (tlc1Δ rad52Δ), SC163(tlc1Δ), SCab3(tlc1Δ rrp6 Δ), SCab5(tlc1Δ xrn1Δ), SCab6(tlc1Δ tetOFF:Dis3) and SCab4(tlc1Δ brr1Δ) are maintained with complementing plasmid pRS316-Tlc1[TLC1, CEN, URA3]. These yeast strains were introduced with centromeric plasmid carrying respective Tlc1 mutants/variants by lithium acetate/single-stranded carrier DNA/PEG method of transformation and subsequently selected on appropriate

selective plates. The transformants were subsequently grown on selective plates with 5-Fluroorotic acid (5FOA 1 mg/mL) for 50 generations to kick-out the pRS316-Tlc1 maintenance plasmid.

SCam1 and SCam2 carrying Nrd1 and Nab3 binding site mutations M1 (T+1165C,T+1186G) and M2 (T+1165C,G+1189-TGT) on the genomic locus of *TLC1* was generated by pop-in pop-out method. pAM9[TLC1-NN-M1, URA3] and pAM10[TLC1-NN-M2, URA3] yeast integrating plasmids were introduced with respective mutations using primer pairs Bloli7924-BLoli7925 and Bloli7926-BLoli7927 using pRS305-Tlc1 with QuikChange II XL Site-Directed Mutagenesis Kit (Agilent Technologies). BY4741 was transformed with MfeI digested pAM9 or pAM10 by lithium acetate/single-stranded carrier DNA/PEG method of transformation and selected on SD-Ura drop-out plates. Transformants were subsequently grown for 5 h in 2 mL of YPD at 30°C 300 rpm before being plated on YPD 5FOA (1 mg/mL) plates. Multiple clones were screened by Sanger sequencing to obtain SCam1 and SCam2.

5.3. Acid Phenol RNA extraction

Cells from overnight liquid culture were diluted to OD_{600} of 0.2 in 20 mL of YPD or appropriate selective media and were grown until OD_{600} of 0.8 at 30°C, 300 rpm. The cells were collected by centrifuging at 2500 rcf for 5 min at 4°C and subsequently washed with 20 ml of cold H_2O. Cell pellet was resuspended in 400 µL of AE buffer (50 mM sodium acetate pH 5.3, 10 mM EDTA), to which 40 µL of 10% (v/v) SDS was added and was mixed using vortex. Solid phenol was melted on a hot water bath and equilibrated using equal volume of AE buffer. 400 µL of equilibrated phenol was added to the cell mixture and mixed vigorously using a vortex. The cell mix was then incubated at 65°C for 5 min and was immediately chilled on ice for 5 min. After centrifuging at maximum speed for 5 min at 4°C, the aqueous phase (~ 450 µL) was carefully transferred to a new 1.5 mL tube. 500 µL of phenol/chloroform/isoamyl alcohol (25:24:1) pH 5.2 was added to the separated aqueous phase and incubated for 5 min at room temperature following a vigorous mixing on a vortex. After centrifuging at maximum speed for 5 min at room temperature, the aqueous phase (~ 400 µL) was transferred to a new 1.5 mL tube. RNA was precipitated on ice for 20 min using 40 µL of 3 M sodium acetate (pH 5.3) and 1 mL of ice-cold 100% ethanol. The precipitate was collected by centrifuging at maximum speed for 5 min at 4°C and subsequently washed gently with 1 mL of 80% (v/v) ice-cold ethanol. The RNA pellet was resuspended in 80 µL of H2O containing 40 units of of RNaseOUT (Invitrogen), and DNA

digestion was carried out subsequently using 20 units DNase I (NEB) and 1x DNase I reaction buffer (NEB) at 37°C for 30 min. The RNA was then purified either by another round of phenol/chloroform extraction or using the RNeasy MinElute Cleanup kit (Qiagen).

5.4. Quantitative reverse transcriptase PCR (qRT-PCR)

Reverse-transcription reactions (20 µL) containing 2 µg of total RNA, 1x Vilo reaction mix (Invitrogen), and 1x Superscript III enzyme blend (SuperScript™ VILO cDNA synthesis kit Invitrogen) were incubated at 25°C for 10 min, 42°C for 1 h, and 85°C for 5 min. cDNA enriched for poly(A) transcripts was generated from 2 µg of total RNA by annealing with 0.5 µg oligodT primer and 10 mM dNTP at 65 °C for 5 min, cooled down on ice for 1 min, and transferred to 55 °C for reverse transcription in a total reaction volume of 20 µL containing 1x First Strand buffer, 5 mM DTT, 40 units of of RNaseOUT (Invitrogen), and 200 units Superscript III (Invitrogen) for 60 min. Superscript III was at heat-inactivated at 70 °C for 15 min. Quantitative real-time PCR was performed using 1 µL of cDNA diluted to 1:5 with ddH_2O, 5 µM each of forward and reverse primers specific to the gene of interest and 1x PerfeCTa® SYBR® Green FastMixes ™ with Low-ROX reference dye (VWR). The total reaction volume was made up to 10 µL using ddH_2O. Primers used for qRT-PCR is listed in Table 1. Primer design and validation was evaluated. qRT-PCR was run on ViiA 7 Real-Time PCR System (ThermoFischer Scientific) with the following program: 2 min at 50°C, 10 min at 95°C, 40 cycles of 95°C for 15 s followed by 1 min at 60°C, and 15 sec at 95°C. The run also included a melt curve program as a last step to ensure specific amplification by the primer pairs, which is as follows: 1 min at 60°C and 15 s at 95°C. Each reaction was done in triplicates to account for manual errors, and unadded reverse transcriptase (RT-) template control reactions were set up to ensure there was no genomic DNA contamination. Data analysis was carried out using the ΔΔCt method. Either *ACT1* alone or *ALG9*, *TFC1*, *UBC6* were used as endogenous controls.

5.5. RNA ligase mediated 3' RACE

1 µg of total RNA was treated with 10 units of T4 Polynucleotide kinase (NEB) and PNK buffer (70 mM Tris HCl pH 7.5, 10 mM $MgCl_2$, 1 mM DTT) in a total volume of 20 µL at 37 °C for 5 h. T4 PNK treatment was skipped for 3' RACE experiments done for Tlc1 that are not processed by ribozyme. The T4 PNK treated RNA was subsequently ligated with 3' linker BLoli8291. Ligation reaction contained 10 µL of T4 PNK reaction mix (~500 ng of RNA), 200

units of T4 RNA ligase 2, truncated KQ (NEB), 1x T4 RNA ligase buffer (NEB), 3.5 µM 3' linker BLoli8291 and 8.5 % PEG 8000. The ligation reaction was incubated at 25 °C for 16 h and subsequently RNA was purified using RNA Clean & Concentrator-5 (Zymo Research). 200 ng of purified RNA was annealed with 25 µM RT primer (BLoli 8305) and 10 mM dNTP at 65 °C for 5 min, cooled down on ice for 1 min, and transferred to 55 °C for reverse transcription in a total reaction volume of 20 µL containing 1x First Strand buffer, 5 mM DTT, 40 units of of RNaseOUT (Invitrogen), and 200 units Superscript III (Invitrogen) for 60 min. Superscript III was at heat-inactivated at 70 °C for 15 min. PCR was performed with 2 µL of generated cDNA and 0.5 µM each of BLoli8123 and BLoli8305 in a total reaction volume of 25 µL containing 1x Phusion HF buffer (NEB), 0.2 mM dNTP and 0.5 units Phusion® High-Fidelity DNA Polymerase (NEB) using the following program: 98°C for 60 s, 25 cycles of 98°C for 30 s, 58°C for 30 s, 72°C for 30 s, and final extension at 72°C for 5 min. Amplicons were resolved either on a 1% or 1.5% agarose gel containing 1x SYBR™ Safe (Invitogen) by performing electrophoresis at 80 V for 1 h. The resolved amplicons were excised and purified using QIAquick Gel Extraction Kit (Qiagen). Purified amplicons were cloned on to Zero Blunt™ TOPO™ vector (Invitrogen) by setting up a 6 µL reaction containing 2 µL purified amplicon, 1 µL salt solution (Zero Blunt™ TOPO™ kit, Invitrogen) and 10 ng Zero Blunt™ TOPO™ vector (Invitrogen) and the reaction was incubated for 5 min at room temperature. One Shot™ TOP10 chemically competent cells (Invitrogen) were transformed with 2 µL of the cloning reaction mix and selected on LB plates containing Kanamycin (50 µg/mL). Individual colonies grown in 4 mL LB Kanamycin (50 µg/mL) overnight at 37°C 225 rpm, were used for plasmid extraction employing QIAprep Spin Miniprep Kit (Qiagen). Sanger sequencing using M13 reverse primer was performed with StarSEQ GmnH (U-mix) or Microsynth AG (*E. coli* NightSeq 96-well plate). The sequences were analyzed using Geneious prime software.

For the library preparation of Nanopore sequencing, 13.9 ng or 9.5 ng of 3'RACE amplicons (Tlc1-WT and Tlc1-M1) were repaired to DNA having 5′ phosphorylated and 3′ dA-tailed ends using NEBNext® Ultra™ II End Repair/dA-Tailing Module (NEB) along with the addition of 1 µL of DNA Control Sample (Oxford Nanopore Sequencing kit). The end prep reaction was carried at 20°C for 5 min followed by 65°C for 5 min. Subsequently the amplicon was cleaned up using 2x AMPure XP beads (Beckman Coulter Diagnostics). Adaptor ligation reaction containing 13.39 ng or 11.7 ng of amplicon, 12.5 µL of LNB ligation buffer (Oxford

Nanopore Sequencing kit), 5 µL Quick T4 DNA ligase (NEB) and 2.5 µL of adaptor mix AMX (Oxford Nanopore Sequencing kit) was incubated at room temperature for 15 min. The amplicon was once again cleaned up using 2x AMPure XP beads (Beckman Coulter Diagnostics) and concentration was measured using Qubit™ dsDNA HS kit (Invitrogen). 10 fmol of amplicon was run on MinION Mk1C.

5.6. RNA immunoprecipitation (RIP)

Overnight precultures were diluted to OD_{600} of 0.2 in 150 mL of YPD and were grown until OD_{600} of 0.8 at 30°C, 300 rpm. Cells were pelleted at 4°C by centrifugation (1,731 rcf, 3 min), washed twice with ice-cold PBS, and stored at −80°C until processing. Cell pellets were lysed in FA buffer (50 mM HEPES KOH pH 7.5, 140 mM NaCl, 1 mM EDTA pH 8, 1% Triton X-100, protease inhibitor cocktail) in a lysing Matrix C tube (MP Biomedical) via 2 × 30 s rounds of 6.5 M/s FastPrep (MP Biomedical). Samples were diluted in FA buffer supplemented with 0.1% sodium-deoxycholate (SOD) and soluble fraction of cell extract was collected after centrifugation at 13226 rcf for 7 min at 4°C. Protein concentration was determined by Bradford assay. 2 mg of soluble extracts were incubated overnight at 4°C with 75 µL of pre-washed IgG beads (GE Healthcare) with 5% BSA. 50 µL of extract was separated as an input control. Beads were washed with 1 ml of FA buffer, buffer 500 (50 mM HEPES-KOH pH 7.5, 500 mM NaCl, 1 mM EDTA pH8, 1% Triton X-100, 0.1% SOD), buffer III (10 mM Tris HCl pH 8, 1 mM EDTA pH 8, 150 mM LiCl, 1% NP40, 1% SOD), and TE buffer (100 mM Tris HCl pH 8, 50 mM EDTA pH 8) at 4°C with 5 min incubation times between washes. IP bead slurry and input samples were incubated with 25 % (v/v) stop buffer (100 mM Tris HCl pH 7.5, 200 mM EDTA, 2.5% (w/v) SDS, 10 mg/mL Proteinase K (Sigma) for 15 min at 50°C and 775 rpm and subsequently supernatant was collected by centrifuging at 300 rpm. The beads were rinsed once with each 150 µL TE buffer (10 mM Tris HCl pH 8, 1 mM EDTA) and 150 µL TNE buffer (10 mM Tris HCl pH 7, 200 mM NaCl, 1 mM EDTA), and the rinse was combined with collected supernatant. RNA was extracted using equal volume of phenol/chloroform/isoamyl alcohol (25:24:1) pH 5.2 and subsequent precipitation using 2.5x (v/v) 100% ice-cold ethanol, 0.1x (v/v) 3 M sodium acetate (pH 5.3) and 1 µL glycogen at -20°C overnight. The precipitate was collected by centrifuging at maximum speed for 5 min at 4°C and subsequently washed gently with 1 mL of 70% (v/v) ice-cold ethanol. The RNA pellet was resuspended in 88 µL of H2O containing 40 units of RNaseOUT (Invitrogen), and DNA digestion was carried out subsequently using 4 units TURBO DNase (Invitrogen) and 1x TURBO

DNase reaction buffer (Invitrogen) at 37°C for 30 min. The RNA was then purified either by another round of phenol/chloroform extraction or using the Qiagen RNeasy RNA clean up kit. Reverse-transcription reactions (20 µL) containing 5 µL RNA, 1x Vilo reaction mix (Invitrogen), and 1x Superscript III enzyme blend (SuperScript™ VILO cDNA synthesis kit Invitrogen) was incubated at 25°C for 10 min, 42°C for 1 h, and 85°C for 5 min. Generated cDNA was diluted 1:5 and subjected to qPCR.

5.7. *In vitro* ribozyme kinetics assay

DNA templates for *in vitro* transcription was generated by PCR with 0.5 µM each BLoli8639 and BLoli8640 and 2 ng of either pAM1, pAM13, pAM16, pAM17 or pAM18 in a reaction volume of 50 µL containing 1x Q5 reaction buffer (NEB), 0.5 mM dNTP mix and 1 unit Q5 High-Fidelity DNA Polymerase (NEB) using the following program: 98°C for 60 s, 32 cycles of 98°C for 10 s, 61°C for 30 s, 72°C for 20 s, and final extension at 72°C for 2 min. Four such 50 µL PCR reactions were performed for each DNA template and pooled together. DNA template was purified using QIAquick PCR Purification Kit (Qiagen) and the concentration was measured using Qubit™ BR assay kit (Invitrogen). *In vitro* transcription reaction contained 1 µg DNA template, 10 mM each of ATP, GTP, CTP and UTP, 1x T7 reaction buffer (HiScribe® T7 High Yield RNA Synthesis Kit, NEB) and 2 µL of T7 RNA polymerase mix (HiScribe® T7 High Yield RNA Synthesis Kit, NEB) and incubated for either 2 min or 12 min at 37°C. Template DNA digestion was carried out by mixing the *In vitro* transcription reaction mixture with 80 µL of ddH_2O, 1x DNase I buffer (NEB) and 4 units DNase I (NEB) and incubating at 37°C for 5 min. RNA was purified using RNeasy MinElute Cleanup kit (Qiagen). 65 ng of RNA was resolved on a 10% polyacrylamide gel containing 8 M urea at 15 W for 3 h and subsequently stained using 1x SYBR® Gold (Invitrogen) in 0.5x TBE. The band intensity was measured using Image Lab software 6.0 (Bio-Rad).

Table 1: List of primers used for qPCR

Name (ID)	Sequence		Target
BLoli8016	Fw	GCGGGCGATCAGTAACTGAAC	mature TLC1
BLoli8017	Rv	AGGCATTAGGAGAAGTAGCTGTG	
BLoli8024	Fw	CAGCTACTTCTCCTAATGCCTTC	precursor TLC1
BLoli8025	Rv	ACAGTACGCGCGATTTCTAC	
BLoli8024	Fw	CAGCTACTTCTCCTAATGCCTTC	precursor TLC1-RZ
BLoli8753	Rv	CTCCCTTAGCCATCCGAGTGG	
BLoli8036	Fw	CACGGATAGTGGCTTTGGTGAACAATTAC	ALG9
BLoli8037	Rv	TATGATTATCTGGCAGCAGGAAAGAACTTGGG	
BLoli8038	Fw	GCTGGCACTCATATCTTATCGTTTCACAATGG	TFC1
BLoli8039	Rv	GAACCTGCTGTCAATACCGCCTGGAG	
BLoli8040	Fw	GATACTTGGAATCCTGGCTGGTCTGTCTC	UBC6
BLoli8041	Rv	AAAGGGTCTTCTGTTTCATCACCTGTATTTGC	
BLoli8014	Fw	CCCAGGTATTGCCGAAAGAATGC	Actin
BLoli8015	Rv	TTTGTTGGAAGGTAGTCAAAGAAGCC	

Table 2: List of primers used for 3'RACE

Name (ID)	Sequence		Note
BLoli8291		/5rApp/AGATCGGAAGAGCGGTTCAG/3ddC/	3' Linker
BLoli8305	Rv	GGATCCTGAACCGCT	RT primer
BLoli8123	Fw	TCTTAAGCATCGGTTAGGTT	PCR of 3'RACE
BLoli8305	Rv	GGATCCTGAACCGCT	

Table 3: List of primers use for site directed mutagenesis

Name (ID)	Sequence		Mutant
BLoli8511	Fw	GCATCTCCACCTTCTCGCGGTCCGACC	Tlc1-slow Rz
BLoli8512	Rv	GGTCGGACCGCGAGAAGGTGGAGATGC	
BLoli8465	Fw	CTCCACCTCCTCACGGTCCGACCTG	Tlc1-slower Rz
BLoli8466	Rv	CAGGTCGGACCGTGAGGAGGTGGAG	
BLoli8467	Fw	CGTCCACTCGGATGGATAAGGGAGTTCTTGA	Tlc1-dead Rz
BLoli8468	Rv	TCAAGAACTCCCTTATCCATCCGAGTGGACG	
BLoli8404	Fw	GCCCTTCGATGCATTTAGATATCCAACTTAAACATTTTTTTTCTTGATG	Tlc1-sm$^-$
BLoli8405	Rv	CATCAAGAAAAAAAATGTTTAAGTTGGATATCTAAATGCATCGAAGGGC	
BLoli8681	Fw	CCTTCGATGCATTTAGATATCCAACTTAAACAGGGTCGGCATGGCATC	Tlc1-sm-Slow Rz
BLoli8682	Rv	GATGCCATGCCGACCCTGTTTAAGTTGGAAAGTTGGATATCTAAATGCATCGAAGG	

Bloli7924	Fw	CATTTTTTTTCCTGATGTATATTTTTTGTATTGGAGAAATCGCGCGT	Tlc1-NN-M1
Bloli7925	Rv	ACGCGCGATTTCTCCAATACAAAAAATATACATCAGGAAAAAAAATG	
Bloli7926	Fw	CATTTTTTTTCCTGATGTATATTTTTTGTATTGTATGTAAATCGCGCGT	Tlc1-NN-M2
Bloli7927	Rv	ACGCGCGATTTACATACAATACAAAAAATATACATCAGGAAAAAAAATG	

Table 4: List of primers used for preparing constructs using overlap PCR

Name (ID)	Sequence		Construct
BLoli8737	Fw	CCTAATGCCTTCGATGCATTTA	TLC1-slow Rz-PGK1 3'UTR
BLoli8738	Rv	ATTCAATTCAATTCTCCCTTAGCCATCCGAG	
BLoli8739	Fw	TGGCTAAGGGAGAATTGAATTGAATTGAAATCGATAGATC	
BLoli8740	Rv	ATATCGAATTCGGAAAAAAAAAACTGCATAAAGGC	
BLoli8687	Fw	TCCTCTTCTCGACCTAACC	TLC1-Δ+922-+1126
BLoli8688	Rv	CTAAATGCATCGATAACCGATGCTTAAGAAAGGAC	
BLoli8689	Fw	AAGCATCGGTTATCGATGCATTTAGATAATTTTTGGAAAC	
BLoli8690	Rv	TGATGATGATGTAACAAGCATATGC	
BLoli8745	Fw	CAATGGCTGTTGCGTTTG	TLC1-kustemΔ+279-+322
BLoli8746	Rv	GAATTTACGGTTTGATAAAAAACCACAAATTGCGCAC	
BLoli8747	Fw	TGTGGTTTTTTATCAAACCGTAAATTCTTAAACACTGC	
BLoli8748	Rv	CTGTCACCTTAAACAGTGTCAG	

Table 5: Sequences of Ribozyme used in this study

Ribozyme	Sequence 3'-5'	Mutation
HDV superfast	GGGCGGCATGGTCCCAGCCTCCTCGCTGGCGCCGCCTGGGCAACATGCTTCGGCATG GCGAATGGGACCAAA	
HDV SA1-2 fast	GGGTCGGCATGGCATCTCCACCTCCTCGCGGTCCGACCTGGGCATCCGAAGGAGGAC GTCGTCCACTCGGATGGCTAAGGGAG	
HDV SA1-2-slow	GGGTCGGCATGGCATCTCCACCTTCTCGCGGTCCGACCTGGGCATCCGAAGGAGGAC GTCGTCCACTCGGATGGCTAAGGGAG	C24T
HDV SA1-2 -slower	GGGTCGGCATGGCATCTCCACCTCCTCACGGTCCGACCTGGGCATCCGAAGGAGGAC GTCGTCCACTCGGATGGCTAAGGGAG	G28A
HDV SA1-2-dead	GGGTCGGCATGGCATCTCCACCTCCTCGCGGTCCGACCTGGGCATCCGAAGGAGGAC GTCGTCCACTCGGATGGATAAGGGAG	C76A

Table 6: List of plasmids used in this study

Plasmid name	Vector backbone	Construct	Source
pRS314-Tlc1	pRS314	CEN TRP1 TLC1	gift from Kathrine Friedman
pRS316-Tlc1	pRS316	CEN URA3 TLC1	gift from Kathrine Friedman
pAM1	pRS314	CEN TRP1 TLC1-Superfast Rz	This study
pAM13	pRS314	CEN TRP1 TLC1-fast Rz	This study
pAM16	pRS314	CEN TRP1 TLC1-Slower Rz	This study
pAM17	pRS314	CEN TRP1 TLC1-Slow Rz	This study
pAM18	pRS314	CEN TRP1 TLC1-dead Rz	This study
pAM20	pRS315	CEN LEU2 TLC1	This study
pAM21	pRS315	CEN LEU2 TLC1-fast Rz	This study
pAM22	pRS315	CEN LEU2 TLC1-Slow Rz	This study
pAM23	pRS315	CEN LEU2 TLC1-dead Rz	This study
pAM27	pRS314	CEN TRP1 TLC1-Slow Rz-PGK1 3'UTR	This study
pAM11	pRS314	CEN TRP1 TLC1-sm$^-$	This study
pAM24	pRS314	CEN TRP1 TLC1-sm$^-$-Slow Rz	This study
pAM26	pRS315	CEN LEU2 TLC1-Δ+921-+1126	This study
pAM30	pRS314	CEN TRP1 TLC1-kustemΔ	This study
pAM31	pRS314	CEN TRP1 TLC1-kustemΔ-Slow Rz	This study
pAM9	pRS406	YIp URA3 TLC1-NN-M1	This study
pAM10	pRS406	YIp URA3 TLC1-NN-M2	This study
pBS3269	pFL36	CEN LEU2 lys2Δ:DIS3-TEV-PA	gift from Bertrand Séraphin
pBS3270	pFL36	CEN LEU2 lys2Δ:dis3D551N-TEV-PA	gift from Bertrand Séraphin
pBS3278	pFL36	CEN LEU2 lys2Δ:dis3D171N-TEV-PA	gift from Bertrand Séraphin

Table 7: List of yeast strains used in this study

Name	Genotype	Source
SC163	*tlc1Δ::KanR ade2::hisG his3-11 leu2 trp1 ura3-52 can1::hisG VR::ADE2-TEL + pCEN URA3 TLC1*	gift from Kathrine Friedman
SC164	*tlc1Δ::KanR rad52Δ::LEU2 ade2::hisG his3-11 leu2 trp1 ura3-52 can1::hisG VR::ADE2-TEL + pCEN URA3 TLC1*	gift from Kathrine Friedman
SCam1	*his3Δ1 leu2Δ0 lys2Δ0 ura3Δ0 tlc1Δ::tlc1-NN-M1(T+1165C,T+1186G)*	This study
SCam2	*his3Δ1 leu2Δ0 lys2Δ0 ura3Δ0 tlc1Δ::tlc1-NN-M2(T+1165C,G+1189-TGT)*	This study
SCam3	*his3Δ1 leu2Δ0 lys2Δ0 ura3Δ0 NRD1-TAP::HIS3MX6 tlc1Δ::tlc1-NN-M1(T+1165C,T+1186G)*	This study
SCam4	*his3Δ1 leu2Δ0 lys2Δ0 ura3Δ0 NAB3-TAP::HIS3MX6 tlc1Δ::tlc1-NN-M1(T+1165C,T+1186G)*	This study
SCam5	*his3Δ1 leu2Δ0 lys2Δ0 ura3Δ0 NRD1-TAP::HIS3MX6 tlc1Δ::tlc1-NN-M2(T+1165C,G+1189-TGT)*	This study

SCam6	*his3Δ1 leu2Δ0 lys2Δ0 ura3Δ0 NAB3-TAP::HIS3MX6 tlc1Δ::tlc1-NN-M2(T+1165C,G+1189-TGT)*	This study
SCab3	*tlc1Δ::KanR rrp6Δ::NatMX his3Δ1 leu2Δ0 met15Δ0 ura3Δ0 + pCEN URA3 TLC1*	This study
SCab4	*tlc1Δ::KanR brr1Δ::NatR his3Δ1 leu2Δ0 lys2Δ0 ura3Δ0 trp1 + pCEN URA3 TLC1*	This study
SCab5	*tlc1Δ::KanR xrn1Δ::NatR his3Δ1 leu2Δ0 lys2Δ0 ura3Δ0 + pCEN URA3 TLC1*	This study
SCab6	*NatMX::TetOFF-DIS3 tlc1Δ::KanR ade 2-1 his3-11,15 leu2-3,112 trp1Δ + pCEN URA3 TLC1*	This study
BSY1883	*KanMX6::TetOFF-DIS3 ade 2-1 his3-11,15 leu2-3,112 trp1Δ ura3-1 can1-100*	gift from Bertrand Séraphin

6. Results

6.1. Disruption of Nrd1-Nab3-Sen1 termination pathway of telomerase RNA (Tlc1)

It was previously reported that Tlc1 possess Nrd1 (+1185-+1189) and Nab3 (+1163-+1166) binding sites (bs) at its 3' end which facilitates transcriptional termination [105]. However, the direct implication of the reported Nrd1-Nab3-Sen1 **(**NNS) transcriptional termination for contributing to endogenous Tlc1 mature form (+1157/+1158) has not been studied yet. We wanted to test the contribution of NNS termination pathway in accounting for the steady-state levels of Tlc1 mature form. We took the approach of abolishing the recruitment of Nrd1 and Nab3 proteins to Tlc1 transcript by mutating the reported Nrd1 and Nab3 bs at the genomic locus of *TLC1*. Two combinations of Nrd1 and Nab3 bs mutations were chosen as shown below.

Table 8: Nrd1 and Nab3 binding site mutations on Tlc1. Mutated nucleotides are denoted in red.

	Nab3-bs	**Nrd1-bs**
Tlc1-WT	TCTT	GTAG
Tlc1-M1	TCCT	GGAG
Tlc1-M2	TCCT	GTATGT

The Nrd1 bs mutation on Tlc1-M2 (GTATGT) mimics the major 5' splice site (SS) observed in *S. cerevisiae*. Previously, a former researcher in our group (Dr. Chi Kang Tseng) had looked at the 3' end sequence of precursor Tlc1 and predicted potential 5' SS, branch point and 3' SS. While certain budding yeasts (*Saccharomyces* species) employ specific transcriptional termination mechanism for Tlc1 3' end maturation, few other budding yeasts (*Candida* and *Hansenula* species) have been predicted to employ spliceosomal cleavage to produce TER mature form [73, 105, 113]. Hence, we mutated the Nrd1 bs to mimic the 5'SS, to check if this altered the endogenous processing mechanism of Tlc1 in *S. cerevisiae*.

Tlc1-M1 and Tlc1-M2 were not efficiently enriched by Nrd1 and Nab3 immunoprecipitation [Fig 8]. This ensures the disruption of Nrd1 and Nab3 recruitment and hence the NNS termination pathway of Tlc1.

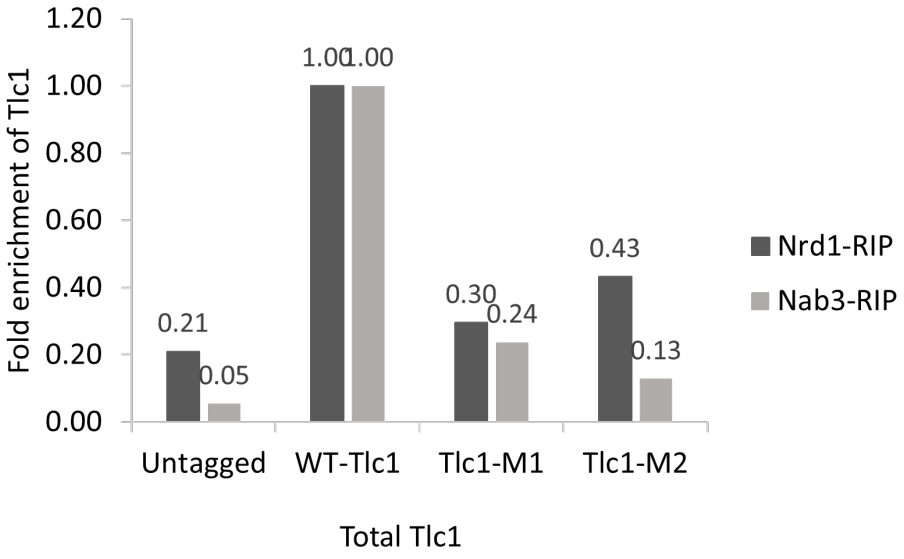

Figure 8 : Disruption of Nrd1 and Nab3 recruitment to Tlc1. Nrd1-TAP-WT-Tlc1, Nrd1-TAP-Tlc1-M1 and Nrd1-TAP-Tlc1-M2 cell lysates were subjected to Nrd1-TAP RIP. Nab3-TAP-WT-Tlc1, Nab3-TAP-Tlc1-M1 and Nab3-TAP-Tlc1-M2 cell lysates were subjected to Nab3-TAP RIP. Enrichment of Tlc1 was determined by performing qRT-PCR with the pulled-down RNA.

6.2. Disruption of Tlc1 NNS signals does not affect synthesis of mature telomerase RNA

Growth of yeast strains carrying the Tlc1-NN-M1 and Tlc1-NN-M2 mutations was monitored up till ~175 generations (7 restreaks) and no aberrant growth phenotype was observed upon disruption of the NNS termination of Tlc1 (data not shown). This observation suggests there are no serious telomeric defects due to the disrupted Tlc1 NNS pathway. In order to directly access the impact of disrupting the NNS signals on steady-state levels of precursor Tlc1 and mature Tlc1, we performed qPCR. Even though there was ~1.7-fold increase in the precursor Tlc1 levels of Tlc1-NN-M1 and Tlc1-NN-M2 mutants, there was no dramatic changes in the total Tlc1 levels of the mutants [Fig 9]. At steady state, in WT cells, 90% of total Tlc1 corresponds to the mature form, and nearly 5~10% of total Tlc1 corresponds to the precursor form [91]. Hence in the absence of any peculiar precursor Tlc1 accumulation, the total Tlc1 measured by qPCR can be extrapolated as the stability of the mature form. Therefore, in the scenario of Tlc1 NNS disruption, the steady-state levels of Tlc1 mature form is not affected. This signifies that the previously reported Nrd1 and Nab3 bs are not essential for stable biogenesis of Tlc1. Additionally, this result hints us that alternate transcriptional termination pathways could compensate for NNS disruption and be accountable for maintenance of steady-state levels of Tlc1.

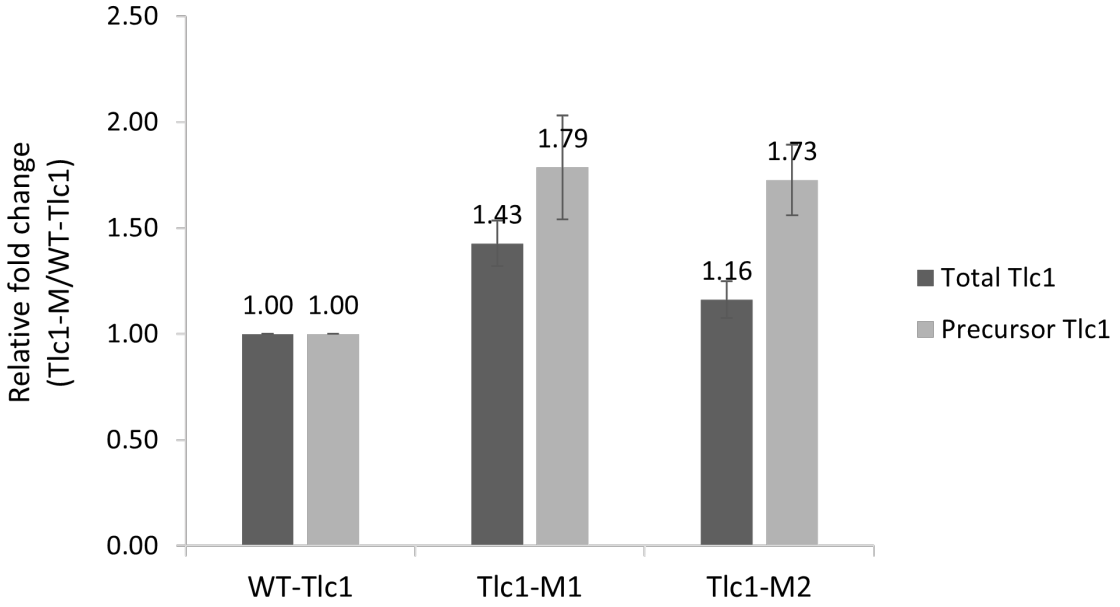

Figure 9: Disruption of Tlc1 NNS signals does not affect the stability of mature Tlc1. qPCR analysis showing the relative fold change of total and precursor Tlc1 in Tlc1-M1 and Tlc1-M2, normalized with Act1. Mean values are calculated from 3 biological replicates and the error bars represent SE.

6.3. Polyadenylated precursor Tlc1 accumulates upon disruption of NNS pathway

Since polyadenylation mediated transcription termination signals are situated downstream the NNS signals on Tlc1, we questioned if the accumulating precursor Tlc1 of Tlc1-NN-M1 and Tlc1-NN-M2 mutants are polyadenylated. To test this, we took the approach of performing qPCR with cDNA that is selectively enriched for poly(A) tailed transcripts using reverse-transcription with oligodT primer. We observed a 2-fold increase of the adenylated total and precursor Tlc1 in Tlc1-NN-M1 and Tlc1-NN-M2 mutants [Fig 10]. Accumulation of polyadenylated Tlc1 molecules upon NNS disruption indicates that the transcriptional termination of Tlc1 is now facilitated via the downstream poly(A) transcription termination signals. This observation signifies that precursor Tlc1 molecules produced via poly(A) transcriptional termination pathway has the potential to contribute to the formation of stable Tlc1-mature form.

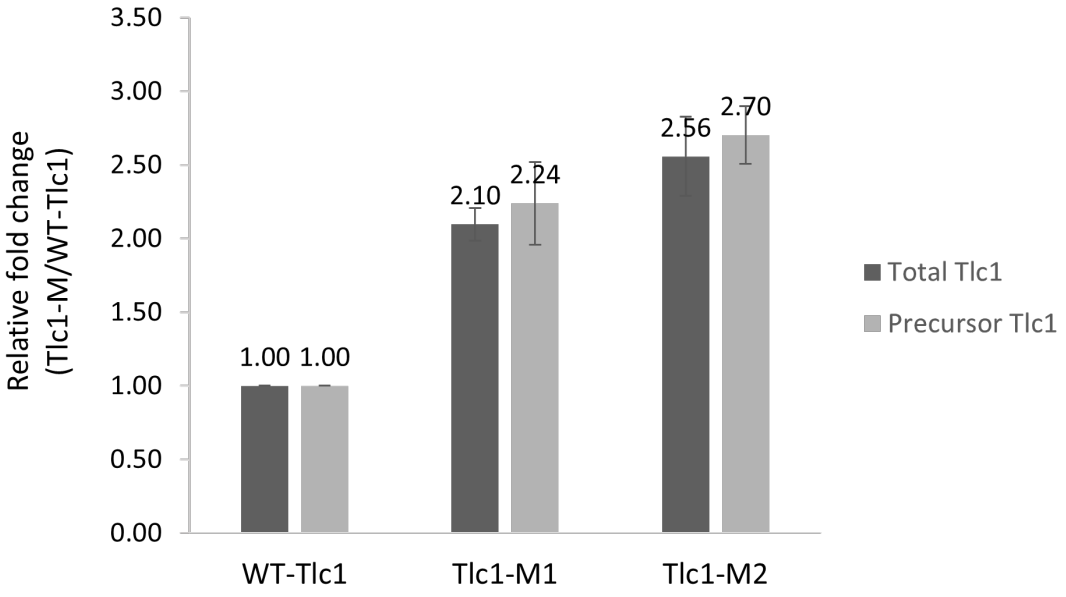

Figure 10: Disruption of NNS signals accumulates polyadenylated precursor Tlc1. Total RNA was prepared from yeast cells harboring mutations M1 or M2 at *TLC1* genomic locus. cDNA was generated using oligo (dT) primer. qPCR analysis showing the relative fold change of total and precursor Tlc1 in Tlc1-M1 and Tlc1-M2, normalized with Act1. Mean values are calculated from 3 biological replicates and the error bars represent SE.

6.4. 3' distribution of precursor and mature Tlc1 upon NNS disruption

With our knowledge that NNS disruption on Tlc1 could still stably accumulate both precursor Tlc1 and mature form, as our next step, we evaluated the direct effect of NNS disruption on the 3' end formation of the precursor and mature Tlc1 by performing 3' RACE assay. Tlc1 mature form of Tlc1-NN-M1 and Tlc1-NN-M2 mutants, majorly terminated at +1157/+1158 position mimicking the 3' end of the mature form of Tlc1-WT [Fig 11]. This bonafides that the alternative transcriptional pathway upon NNS disruption can indeed produce correctly 3'-processed mature Tlc1. The precursor Tlc1 molecules of Tlc1-NN-M1 and Tlc1-NN-M2 terminated majorly at the previously reported poly(A) termination site [Fig 12]. Additionally, we observed that the precursor Tlc1 molecules of Tlc1-NN-M1 and Tlc1-NN-M2 molecules had non-genome encoded A-tails of length between 23~65 nt [Fig 12]. The observation of long A-tails in the precursor Tlc1 of Tlc1-NN-M1 and Tlc1-NN-M2 mutants, can be interpreted to show that the transcriptional termination could be facilitated via poly(A) transcriptional termination signals upon NNS disruption. However, we see the same precursor Tlc1 3' end distribution in Tlc1-WT as observed in the mutants [Fig 12]. In other words, we failed to capture the precursor Tlc1 molecules that terminates via NNS pathway in Tlc1-WT. We had two explanations for missing out NNS

precursor Tlc1 molecules. First being, NNS transcription termination pathway produces precursor Tlc1 molecules that are efficiently and quickly trimmed to the mature form, and hence being missed in our assay. Alternatively, the small sample size of sequences being analyzed could be the reason to miss out the precursor Tlc1 molecules terminating via NNS signals. In order to address the latter issue, we performed Nanopore sequencing.

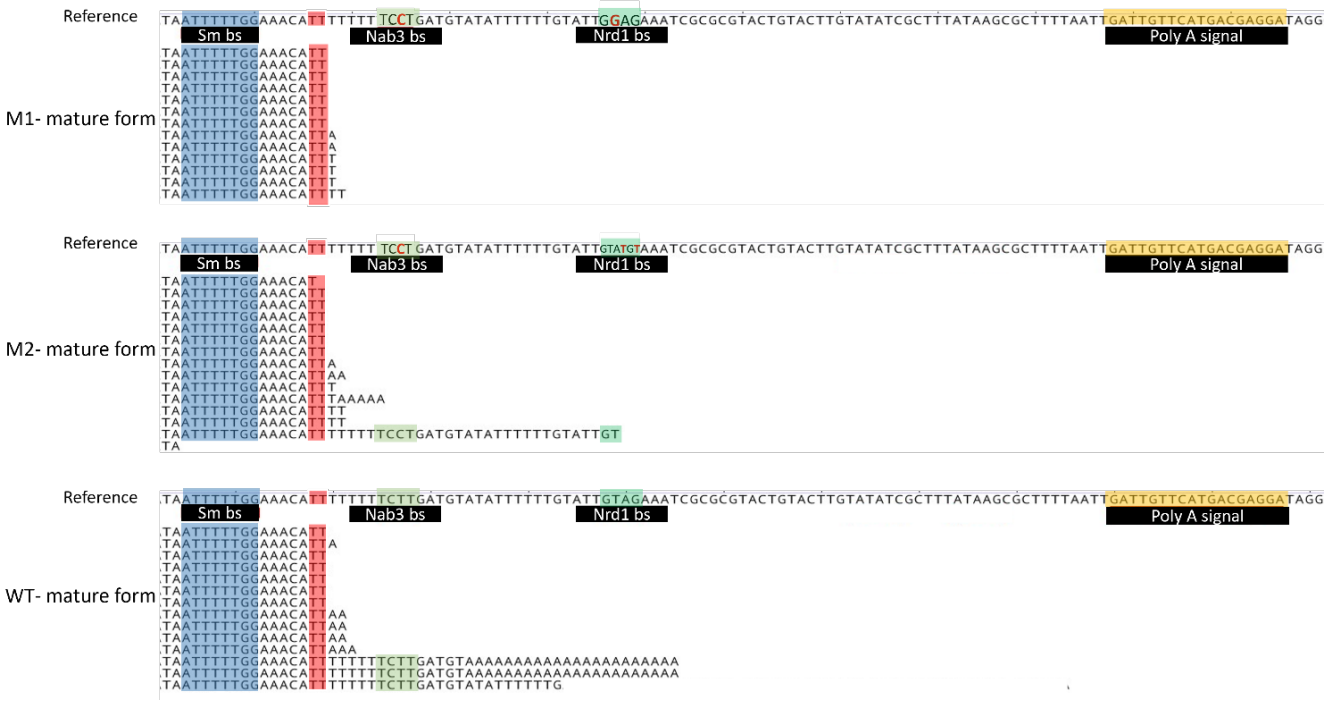

Figure 11: 3'RACE sequences of Tlc1 mature form of Nrd1-Nab3 binding site mutants Tlc1-M1 and Tlc1-M2, and WT-Tlc1.

Nanopore sequencing analysis of precursor Tlc1 revealed that, both Tlc1-WT and Tlc1-M1 samples had 3 populations of precursor Tlc1. One major population terminating between +1242~+1252, and a second set terminating between +1208~+1212, and a third populating terminating between +1170~+1180 [Fig 13]. The first mentioned major population terminating +1242~+1252, had long A-tails (>10 adenosine) and resembles the termination position of poly(A) pathway previously reported in literature [91]. The second mention population terminating +1208~+1212, had relatively less molecules with long A-tails (>10 adenosine) and resembles the termination position of NNS pathway previously reported in literature [105, 106].

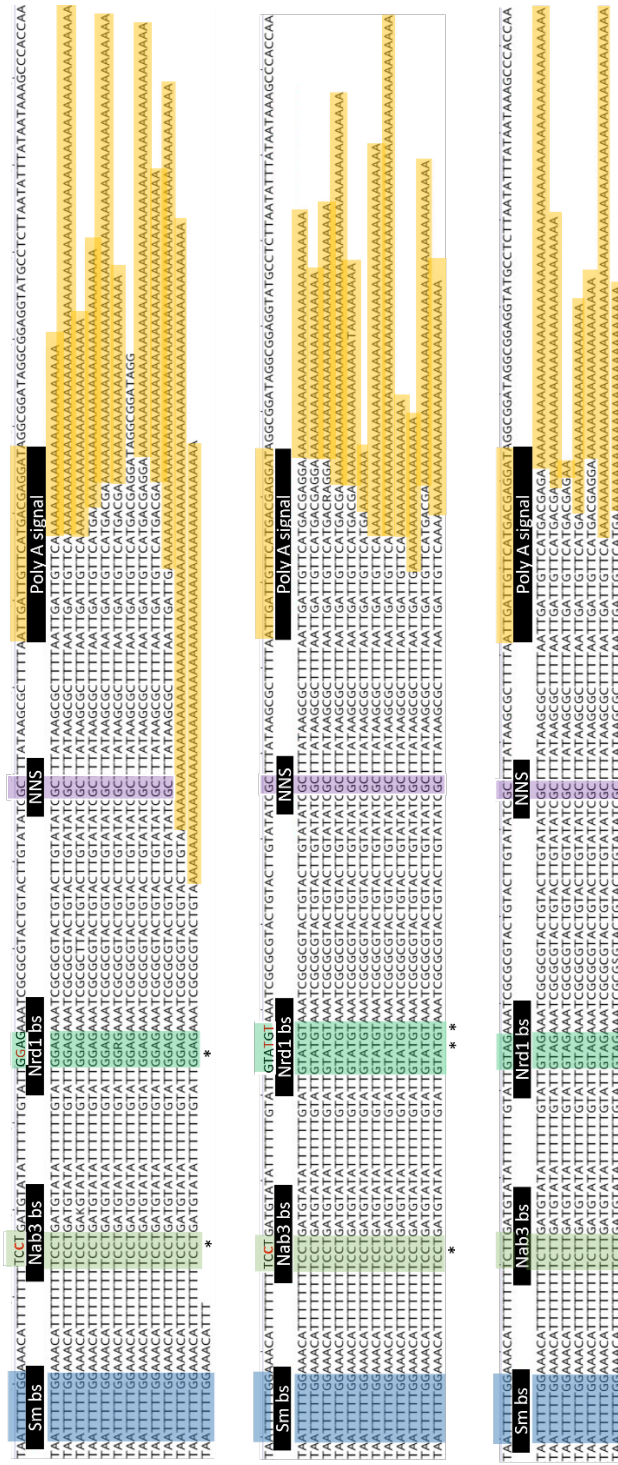

Figure 12: 3'RACE sequences of Tlc1 precursor form of Nrd1-Nab3 binding site mutants Tlc1-M1 and Tlc1-M2, and WT-Tlc1.

When we compare the precursor Tlc1 population terminating at +1208~+1212 of Tlc1-WT and Tlc1-NN-M1, we observed an increase in the fraction of molecules with long A-tails (>10 adenosine). This observation validates our qPCR data, however +1208~+1212 position is much upstream the polyadenylation signals.

Unlike the other two populations, the third set of molecules terminating between +1170~+1180 is surprising and has not been previously reported. We predict that this position on Tlc1 could be occupied by a specific protein(s) during the biogenesis of Tlc1, which halts the 3' processing machinery temporarily. And upon the subsequent falling off of the bound protein(s) from Tlc1, the 3' processing is resumed.

6.5. Tlc1 stability is compromised upon complete loss of endogenous 3' processing signals

We observed that upon Tlc1 NNS disruption, alternative pathway(s) compensates for facilitating 3' end formation of mature Tlc1, without compromising on Tlc1 stability. The converse of our approach, i.e., disruption of alternative polyadenylation transcription termination signals of Tlc1, has been previously reported to not affect the synthesis of mature Tlc1 as well [105]. This hinted us that Tlc1 3' processing mechanism is highly adaptive and flexible. In order to assess the significance of 3' processing mechanism of Tlc1, we deprived Tlc1 of its endogenous 3' processing signals and monitored Tlc1 stability.

An artificial construct that uses ribozyme (Rz) cleavage was leveraged to force terminate Tlc1 at the 3' end of mature form, thereby bypassing its endogenous 3' processing events [Fig 14A]. We engineered a Tlc1-ribozyme construct that expresses Tlc1 under the endogenous promoter and terminates transcription using ribozyme that was inserted immediately downstream of the 3' end of mature form (+1155). Downstream of the ribozyme, the endogenous NNS signals and poly(A) termination signals were retained. When the ribozyme is fully functional, this system directly produces the mature Tlc1. And when the ribozyme is non-functional, processing occurs via Tlc1 endogenous pathway. The ribozyme was inserted at +1155, 3 nt upstream of WT Tlc1 mature 3'-end (+1157/+1158), in order to distinguish the ribozyme processed Tlc1 molecules from those that are processed via Tlc1 endogenous processing signals at the sequence level. No effect on Tlc1 stability due to the removal of terminal 3 nt was validated (data not shown). The Tlc-Rz construct was introduced in yeast cells that were chromosomally deficient for *TLC1* and *RAD52*,

which meant that cells solely rely on the artificial Tlc1 construct for telomere maintenance and survival [Fig 14B].

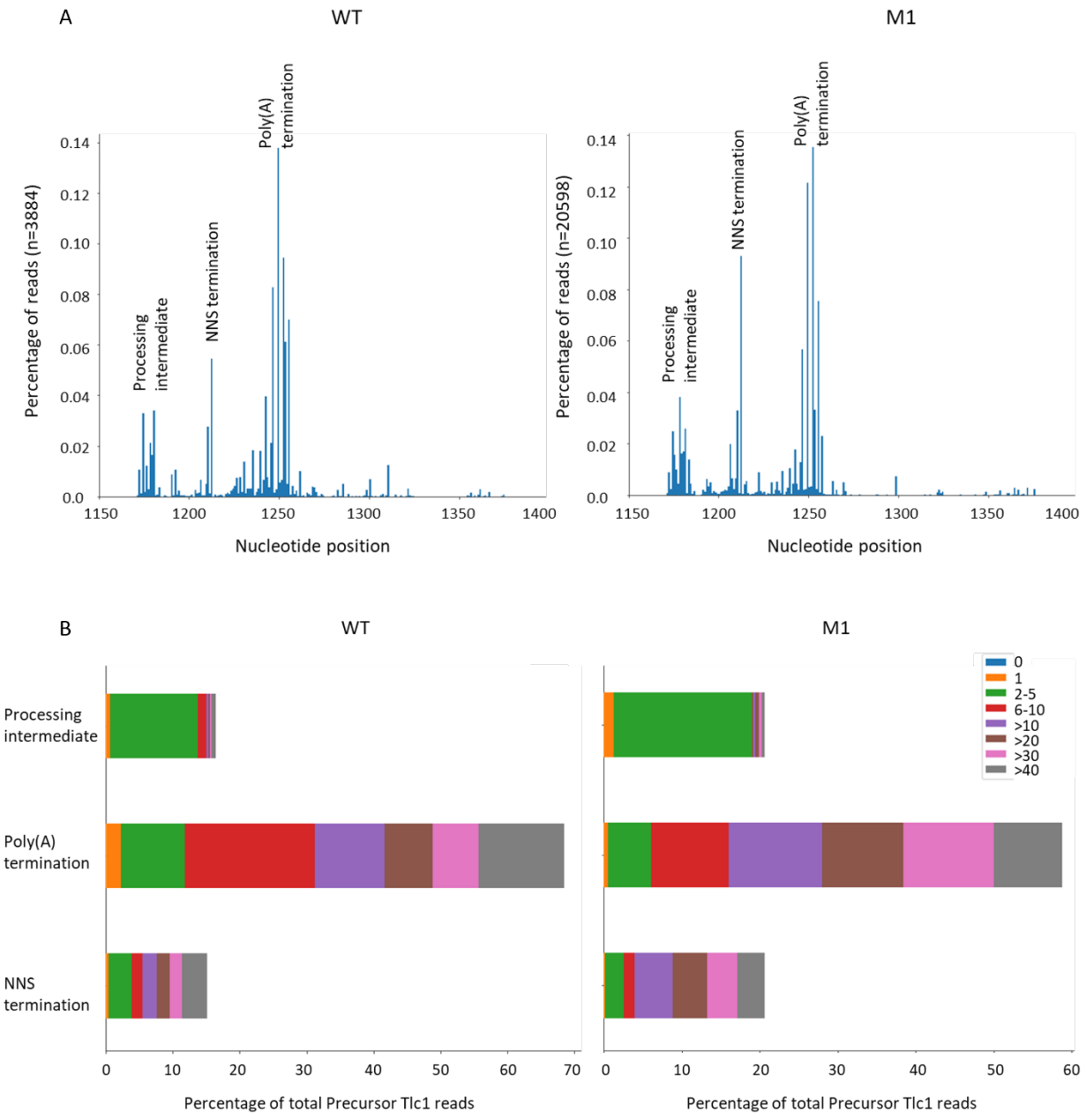

Figure 13: Nanopore sequencing analysis of 3' distribution of Tlc1-M1 and WT-Tlc1. A. Graphs depicting the percentage of reads terminating at specific nucleotide position (Tlc1- mature form (+1156/7) reads are excluded). B. Bar graphs depicting the percentage of precursor Tlc1 reads with different 3' adenylation pattern.

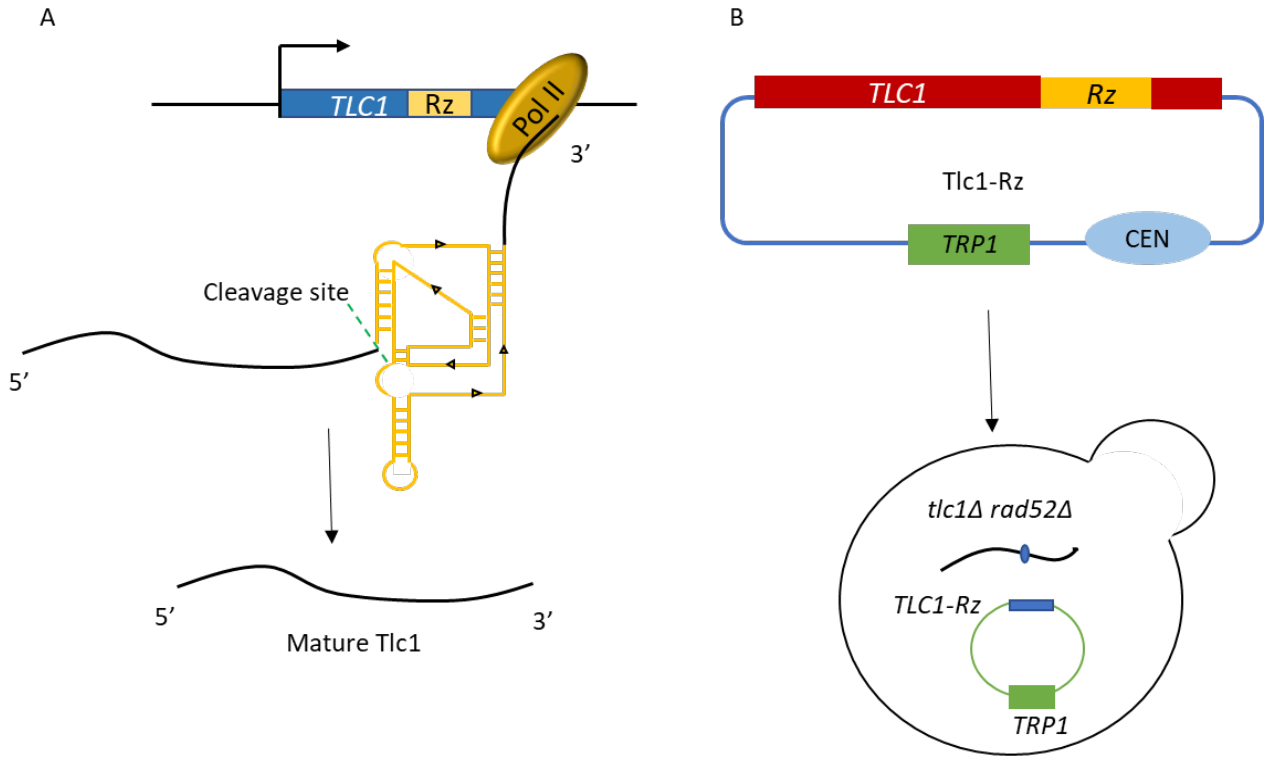

Figure 14: Schematic of the engineered Tlc1-Rz construct. A. The self-cleaving activity of ribozyme is employed to force terminate Tlc1 at the 3' end of mature form (+1155). B. Centromeric Tlc1-ribozyme plasmid is introduced into yeast cells that are chromosomally deficient for *TLC1* and *RAD52*.

We observed that, upon ribozyme processing, total Tlc1 levels were decreased by 4-fold [Fig 15B]. The observed reduction in total Tlc1 is specific to the ribozyme processing, as the total Tlc1 levels were not affected when the ribozyme was non-functional (dead mutant). Additionally, successful ribozyme termination *in vivo* can be inferred from the depleted levels of precursor Tlc1 in functional Rz, and in contrast the precursor Tlc1 levels remain unchanged in the dead ribozyme mutant [Fig 15B].

The instability of Rz processed Tlc1 can either be due to the disruption of signals required for the sequential biogenesis of Tlc1 or due to the accelerated processing kinetics facilitated by Rz. Processing kinetics is crucial for stabilizing telomerase RNA, as we see that perturbation in the telomerase RNA maturation kinetics in humans precipitates disease [154]. On the other hand, temporal regulation of sequential biogenesis of Tlc1 involving subcellular trafficking and processing can be crucial for maintaining Tlc1 stability.

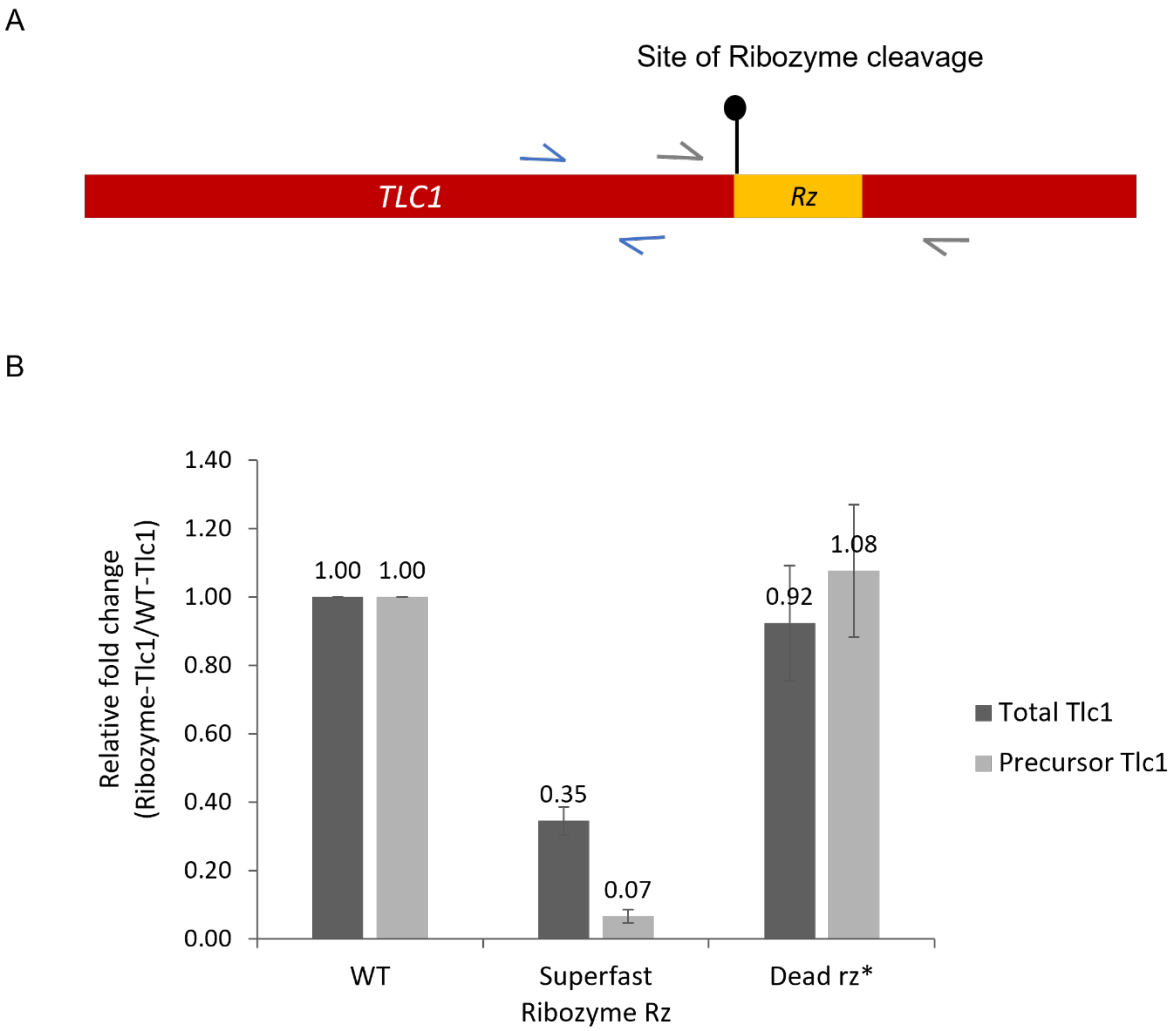

Figure 15: Ribozyme processing causes Tlc1 instability. A. Schematic showing the site of ribozyme cleavage and primers used for qPCR analysis. Blue and grey arrows represent the primer pairs used for measuring total Tlc1 and precursor Tlc1 respectively. B. qPCR analysis showing the relative fold change of total and precursor Tlc1 in superfast Rz and dead rz* system, normalized with Alg9, Tfc1 and Ubc6. Mean values are calculated from 3 biological replicates and the error bars represent SE.

6.6. Instability of ribozyme processed Tlc1 is rescued by lowering the speed of ribozyme cleavage

To test whether the instability of Rz processed Tlc1 is due to the accelerated 3' processing, we employed ribozymes acting at different speeds – superfast, fast, slow, slower and dead. Different speeds of ribozyme cleavage were achieved by point mutations on Rz and the speeds of the Rz mutants were validated by *in vitro* Rz cleavage assay. Immediately, after 2 min of start of the assay, no substrate was detected for superfast Rz and no product was detected for dead Rz [Fig

16]. The rate of product formation by fast and slow Rz validates the gradient of processing speeds of the ribozyme mutants.

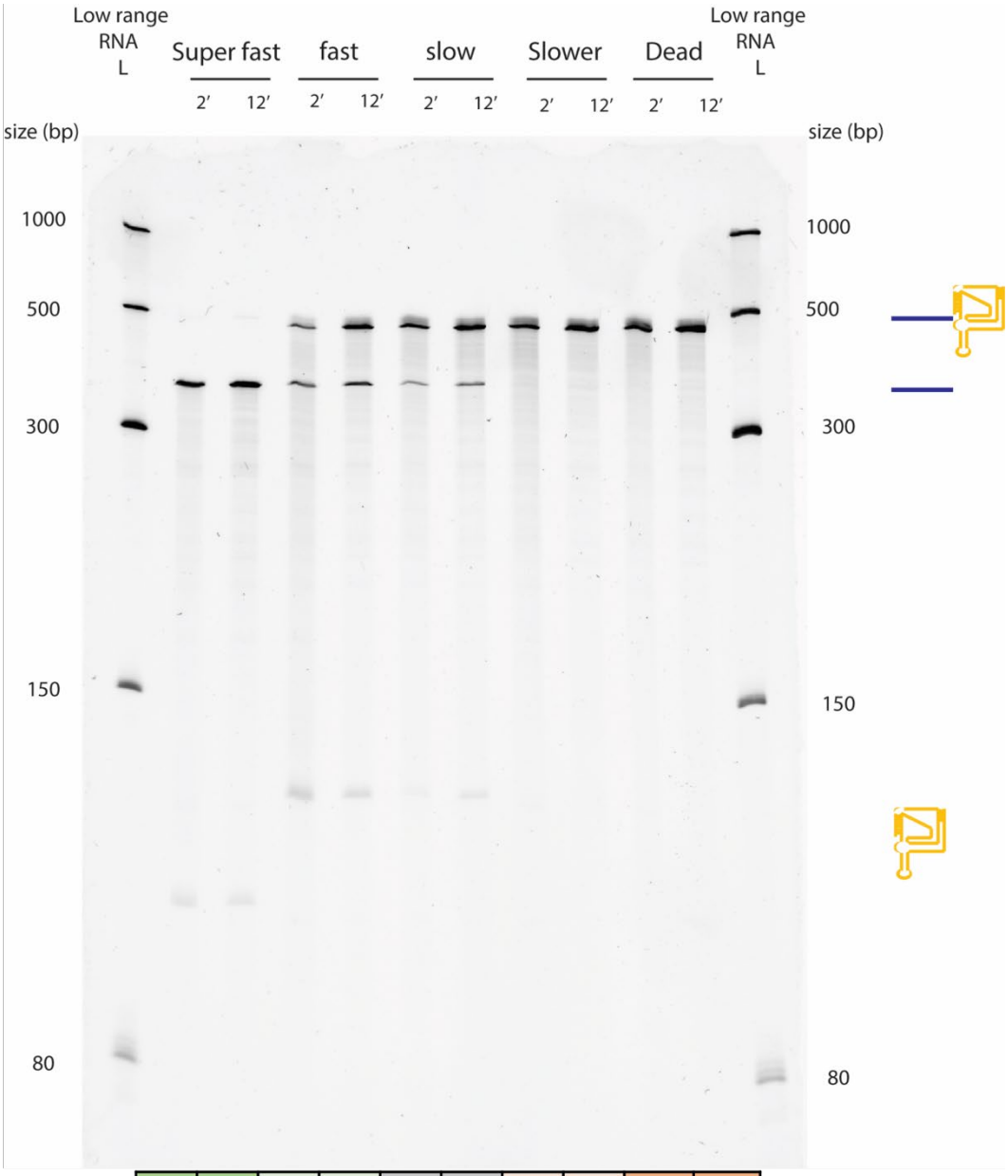

precursor	0.00	0.00	0.18	0.68	0.52	0.78	0.64	0.92	0.70	1.00
product	0.73	1.00	0.28	0.36	0.12	0.20	0.01	0.01	0.01	0.00

Figure 16: *In vitro* analysis of the varying speeds of ribozyme mutants by denaturing PAGE.

Upon introducing these Rz mutants acting at varying speeds *in vivo*, we observed that the slow Rz mutant resets the total Tlc1 levels to that of WT-Tlc1 [Fig 17]. The total Tlc1 levels

decreased with the increasing speeds of Rz. Additionally, the Rz mutants of varying speeds act accordingly *in vivo* which is evident by the gradual decrease in the levels of precursor Tlc1 with the increasing speeds of Rz.

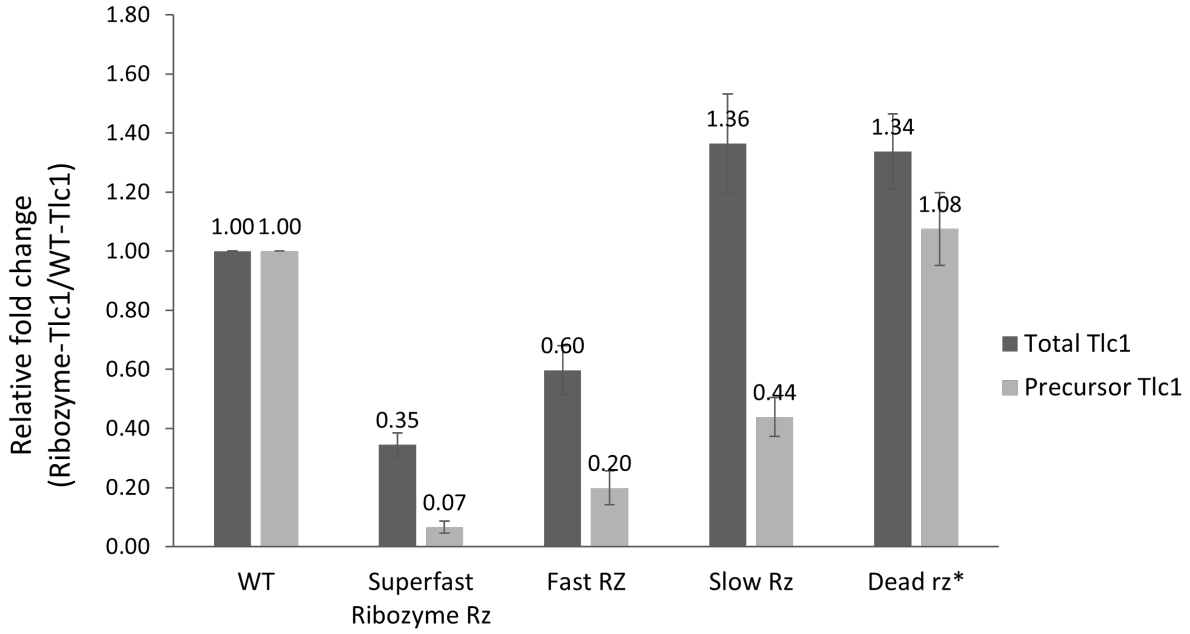

Figure 17: qPCR analysis showing the relative fold change of total and precursor Tlc1 in superfast, fast, slow and dead Rz system, normalized with Alg9, Tfc1 and Ubc6. Mean values are calculated from 3 biological replicates and the error bars represent SE.

The precursor Tlc1 of slow Rz is 2.4-fold lower than that of dead Rz, which signifies that slow Rz is indeed performing its action at a reduced speed [Fig 17]. However, the slow Rz rescues the instability of mature Tlc1 which occurred upon processing by superfast & fast Rz. Thus, lowering the speed of ribozyme cleavage relieves the Tlc1 instability. The regained stability could be due to lowered 3' processing facilitated by slow Rz mutant, where the slower processing is required for necessary Tlc1 stabilizing proteins to bind. Alternatively, as the Rz processing is in competition with the Tlc1 endogenous processing mechanism, the Tlc1 stability rescue can be because the endogenous Tlc1 processing system wins over the slow Rz. The endogenous Tlc1 processing system efficiently competes with the slow Rz, thereby processing more Tlc1 molecules and reestablishing stability.

6.7. Endogenous processing mechanism is crucial for stabilizing Tlc1

As our next step, we performed 3' RACE to look at the 3' ends of Tlc1 molecules processed by fast, slow and dead Rz. 3' RACE experiment enabled us to differentiate Tlc1 molecules that were processed via endogenous mechanism and those that were processed via Rz. Tlc1 transcripts that were processed by endogenous Tlc1 signal, terminated 2~6 nt downstream the Rz cleavage site and possessed a short A-tract [Fig 18]. This A-tract is a hallmark of exosome complex being involved in the endogenous Tlc1 processing. Mainly, this experiment validated the proportion of Tlc1 molecules processed via either of the mechanisms in our fast, slow, and dead Rz constructs. In fast-acting Rz, 9 out of 12 sequences terminated at the Rz cleavage site, ensuring that major processing is via Ribozyme [Fig 18]. In dead Rz mutant, all the sequences except one were processed through Tlc1 endogenous processing mechanism. Whereas, in case of the slow Rz mutant, a minor fraction of the sequences (3/12) was terminated via Ribozyme cleavage and a major fraction of the sequences (9/12) was processed by endogenous processing. This explains that the rescue of Tlc1 stability by slow Rz is indeed due to the takeover by the endogenous Tlc1 processing machinery. The Tlc1 molecules are unstable when processed by Rz, and the endogenous Tlc1 3' processing mechanism is crucial for stabilizing Tlc1.

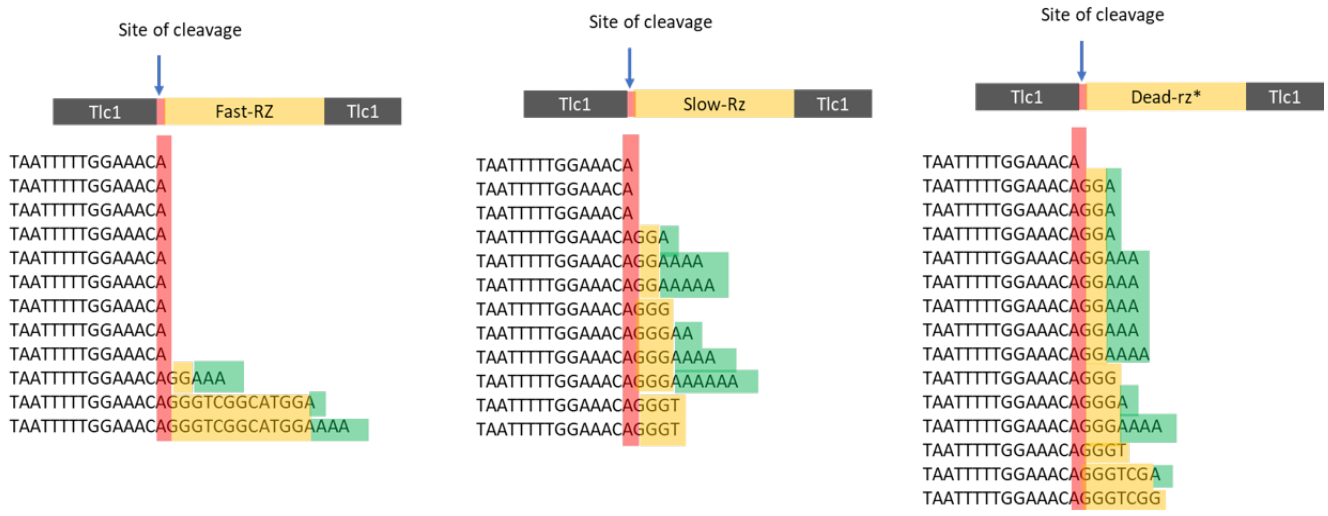

Figure 18: 3'RACE data of Tlc1 molecules processed by fast, slow, dead Rz constructs. The region in red denotes the actual ribozyme cleavage site. The region in yellow denotes the nucleotides retained from the ribozyme sequence. The region in green denotes the short adenosine stretch that is not genome encoded.

6.8. Exosome complex involved in endogenous processing is not responsible for degrading ribozyme processed Tlc1

It has been previously reported that the exosome complex is involved in the 3' processing of Tlc1[148]. Additionally, the presence of short A-tracts at the 3' end of Tlc1 molecules processed by endogenous termination system in our 3' RACE experiment further hinted the involvement of exosome complex [Fig 18]. With this knowledge we hypothesized that 3' exonuclease component of the exosome complex fails to halt and thereby degrades the Rz processed Tlc1, due to the lack of binding of stabilizing proteins e,g. Sm_7. In order to test this hypothesis, we monitored whether the disruption of the 3' exonuclease components of the exosome complex, Rrp6 and Dis3, rescued the stability of Rz processed Tlc1.

rrp6Δ caused a 2-fold increase in the total and precursor WT-Tlc1 [Fig 19], which is slightly higher than what is reported in literature [148].

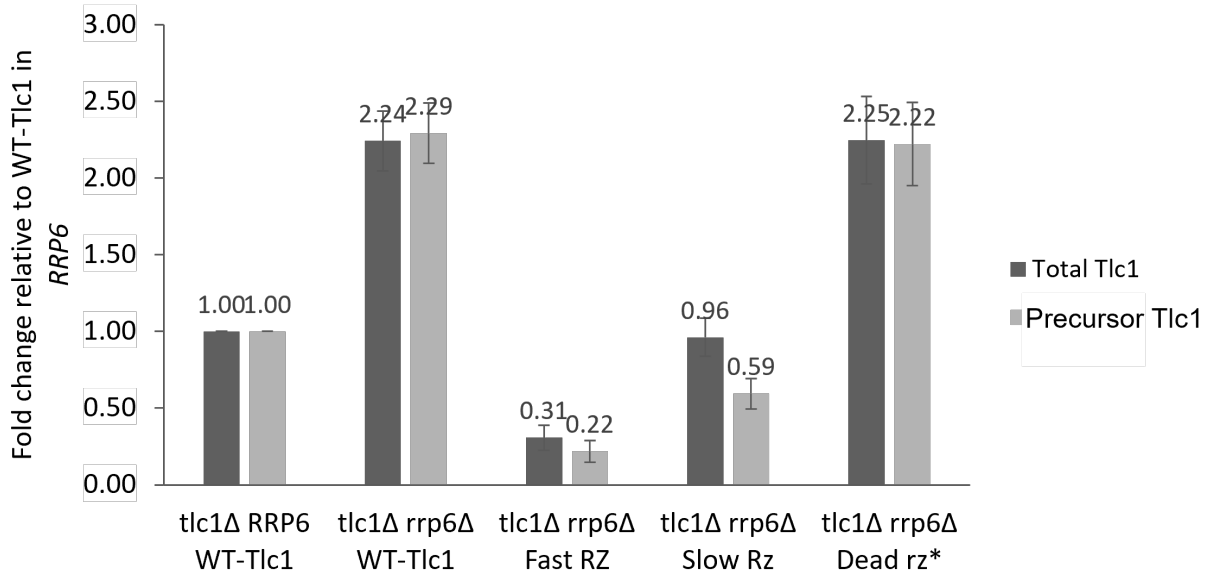

Figure 19: Rrp6 does not degrade Rz processed Tlc1 molecules. qPCR analysis showing the relative fold change of total and precursor Tlc1 in fast, slow, and dead Rz system upon rrp6Δ, normalized with Alg9, Tfc1 and Ubc6. Mean values are calculated from 3 biological replicates and the error bars represent SE.

rrp6Δ did not restore the instability of fast Rz processed Tlc1 [Fig 19]. Hence, Rrp6 is not responsible for degrading the Rz processed Tlc1 transcripts. The slow Rz which previously reestablished the Tlc1 levels to that of WT Tlc1 and dead Rz, upon Rrp6 abolition the total Tlc1 levels were not completely rescued [Fig 19]. With one of the components impaired, the

endogenous processing machinery is handicapped, and hence more transcripts could now be processed by slow Rz, and thereby lowering the stability of Tlc1. This must be tested by performing 3' RACE of slow Rz Tlc1 upon *rrp6Δ* and validate if more fraction of molecules is now processed via Rz.

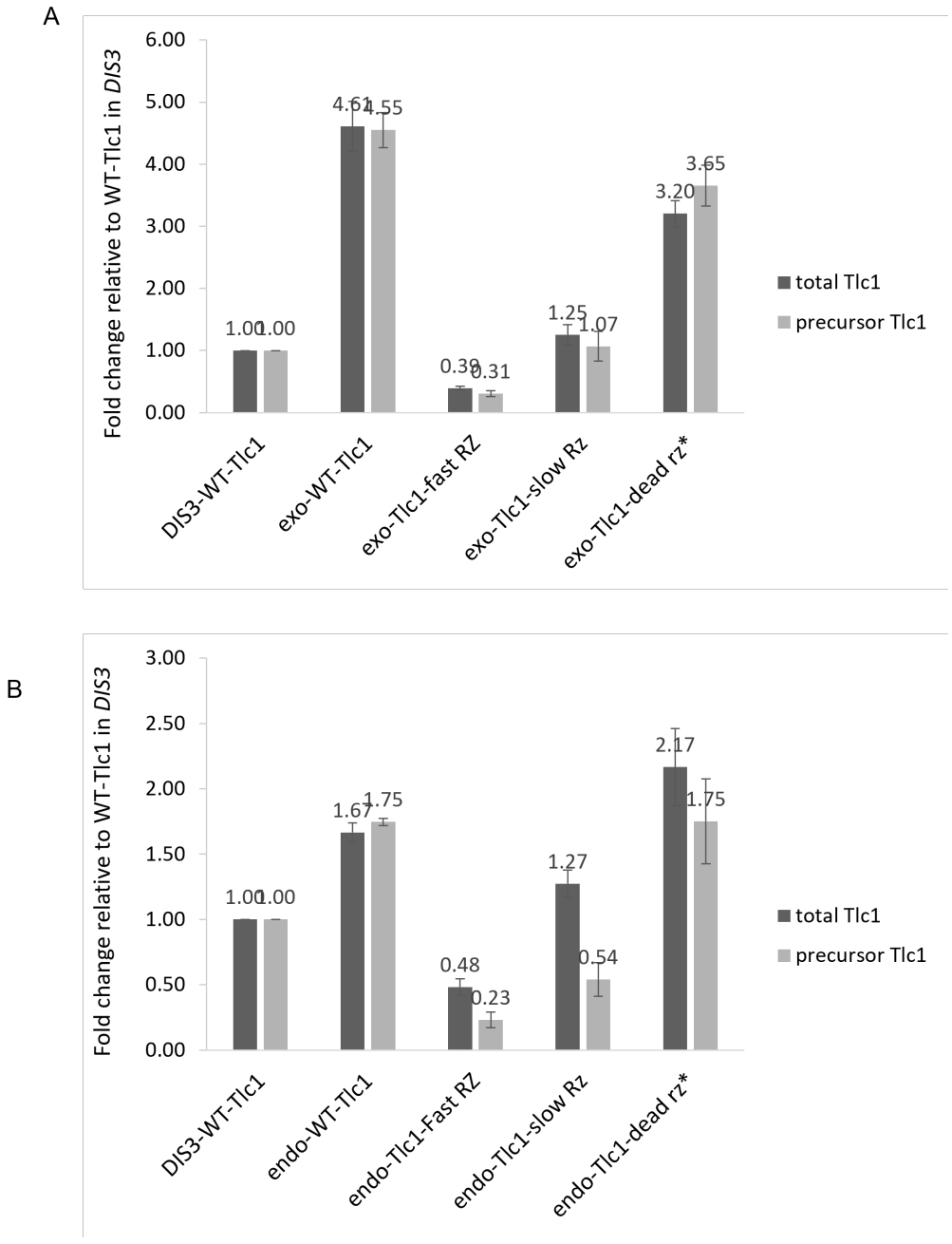

Figure 20: Dis3 does not degrade Rz processed Tlc1 molecules. A. qPCR analysis showing the relative fold change of total and precursor Tlc1 in fast, slow, and dead Rz system upon dis3-exo- (exonuclease activity disrupted) B. dis3-endo- (endonuclease activity disrupted), normalized with Alg9, Tfc1 and Ubc6. Mean values are calculated from 3 biological replicates and the error bars represent SE.

Dis3, another nuclease component of exosome complex, has both 3'-5' exonuclease activity and endonuclease activity. Loss of neither exonuclease activity nor endonuclease activity restores the instability of fast Rz processed Tlc1 [Fig 20A,B]. Hence the exosome complex which plays a role in the 3' processing of Tlc1, is not responsible for degrading the Rz processed Tlc1 molecules.

6.9. 3' processing kinetics is crucial for stabilizing Tlc1

Co-transcriptional cleavage by the fast Rz happens rapidly, which renders the Tlc1 RNA devoid of its endogenous 3' processing signals. To test if this rapid loss of 3' Tlc1 signals is leading to instability. the endogenous Tlc1 signals downstream the slow Rz was replaced with Pgk1 3'UTR [Fig 21]. In such a construct, Tlc1 molecules that skip Rz processing will undergo termination using the Pgk1 3' UTR.

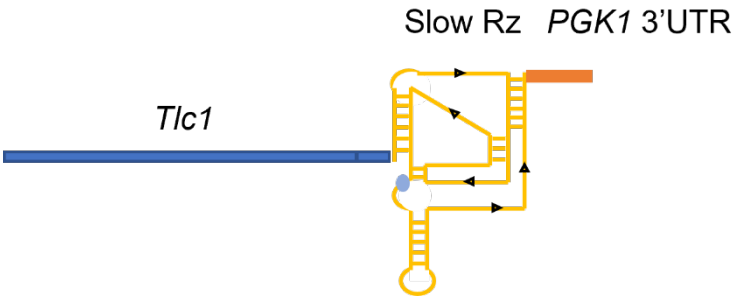

Figure 21: Schematic representation of Slow Rz-Tlc1+ Pgk1 3' UTR construct.

The total Tlc1 molecules from slow Rz + Pgk1 3'UTR construct were stabilized [Fig 22B]. Precursor Tlc1 levels of slow Rz + Pgk1 3'UTR was similar to that of slow Rz + endogenous 3' signal, which informs that the Tlc1 molecules are indeed processed i.e. trimmed at the 3' [Fig 22B]. Performing 3'RACE, educated that Slow Rz + Pgk1 3'UTR molecules were not processed by Rz cleavage, instead were processed using cell's RNA processing machinery (Fig 22C). Slow Rz Tlc1 molecules are stable even when processed by polyadenylation termination signal. Tlc1 appears to be flexible with the 3' processing machinery, however the 3' end processing kinetics is crucial for stabilizing Tlc1.

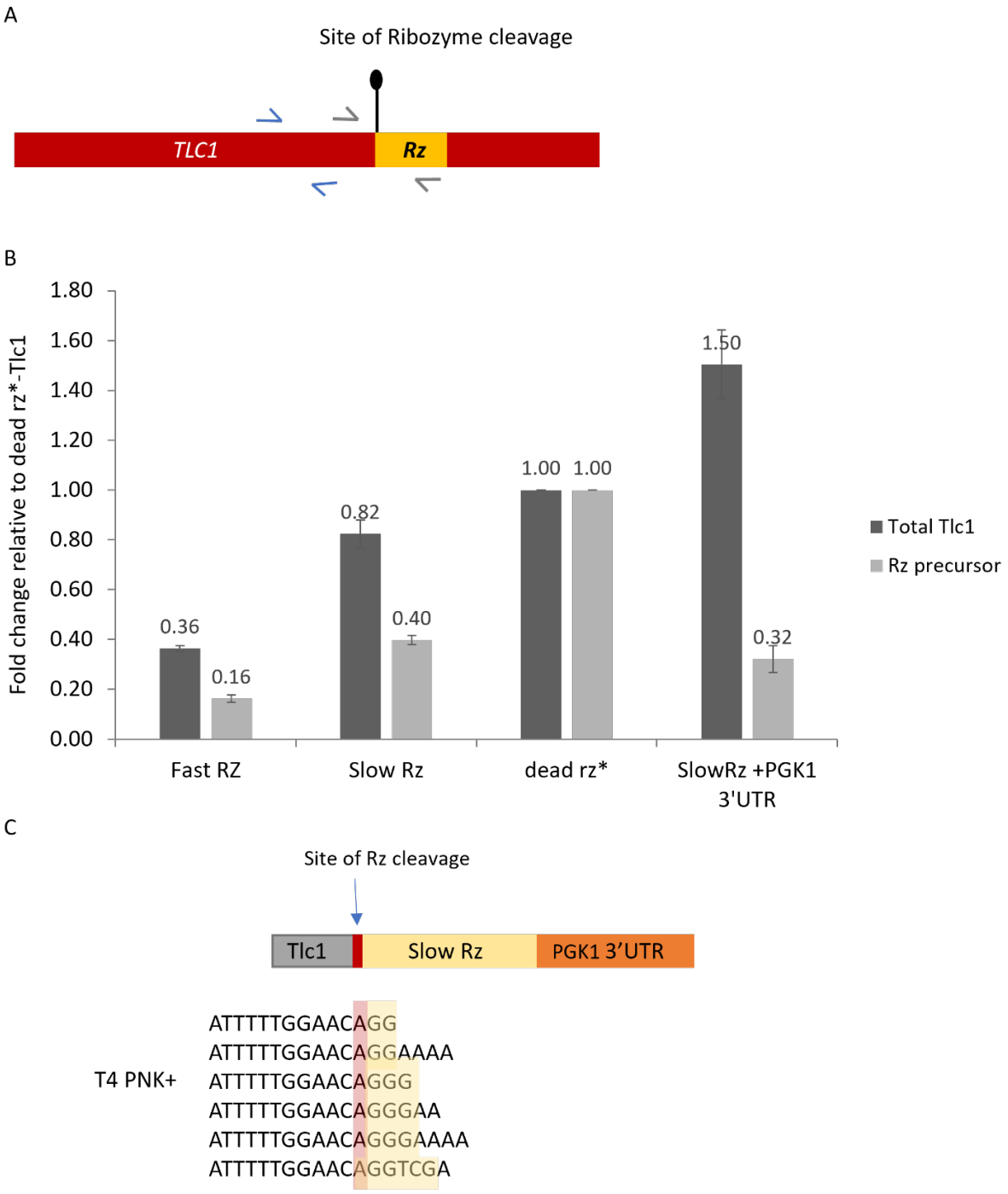

Figure 22*:* Tlc1 can undergo 3' processing using Pgk1 polyadenylation termination signal. A. Schematic showing the site of ribozyme cleavage and primers used for qPCR analysis. Blue and grey arrows represent the primer pairs used for measuring total Tlc1 and precursor Tlc1 respectively. B. qPCR showing the relative fold change of total and precursor Tlc1 in fast, slow, dead Rz and Slow Rz + Pgk1 3' UTR system, normalized with Alg9, Tfc1 and Ubc6. Mean values are calculated from 3 biological replicates and the error bars represent SE. C. 3'RACE data of Tlc1 molecules in Slow Rz + Pgk1 3' UTR. The region in red denotes the actual ribozyme cleavage site. The region in yellow denotes the nucleotides retained from the ribozyme sequence.

6.10. Instability of ribozyme processed Tlc1 is not due to improper ribonucleoprotein assembly

As mentioned earlier, we hypothesized that upon Rz processing, the transcriptional termination happens rapidly allowing no time for necessary stabilizing proteins to bind to Tlc1. Improper ribonucleoprotein assembly might be causing Tlc1 instability upon Rz processing. We checked for two protein complexes, Sm_7 complex and Ku70/80 complex, whether whose lack of binding to Rz processed Tlc1 caused instability.

Sm_7 complex binds to Tlc1 8 nt upstream the 3' end of mature form and is crucial for stabilizing Tlc1 [86]. The Sm_7 biding site on Tlc1 was mutated in the slow Rz-Tlc1 and monitored whether the Slow Rz Tlc1 stability was disturbed, pushing it to behave like the fast Rz Tlc1 molecules [Fig 23A].

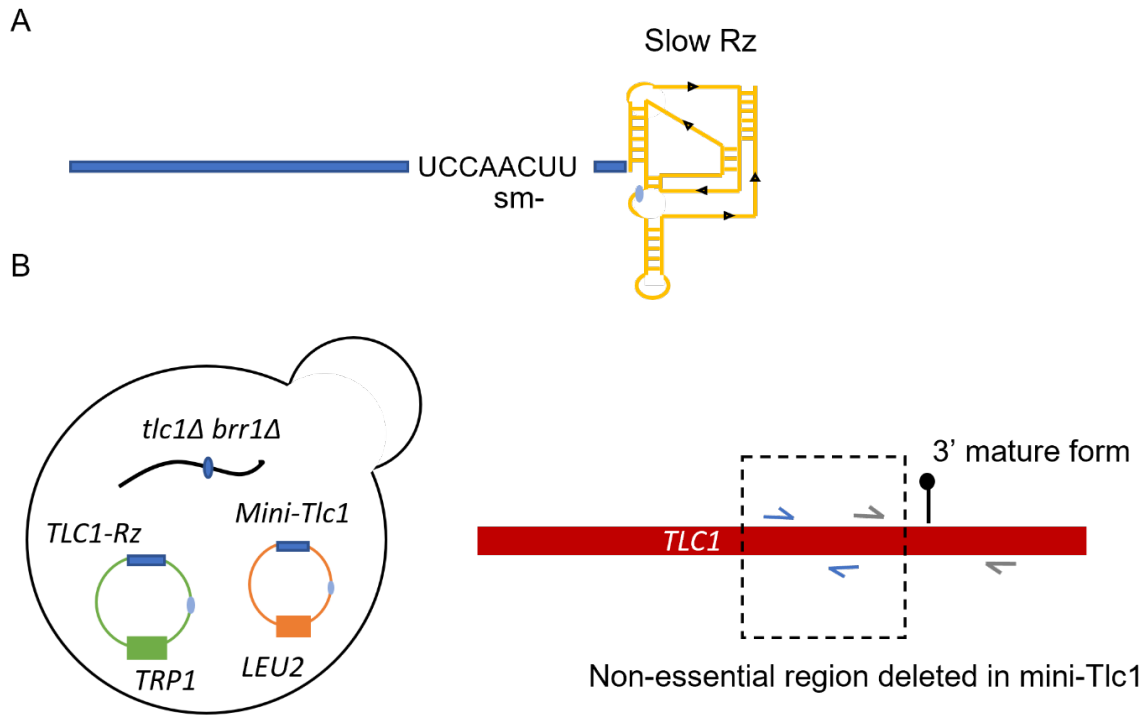

Figure 23: A. Schematic representation of Slow Rz-Tlc1 construct harboring Sm_7 binding site mutation. B. Brr1 aids Sm7 complex loading onto snRNAs and hence brr1Δ slows Sm_7 binding to Tlc1. Mini-Tlc1 generated by deleting a non-essential region, allows normal cell proliferation without interfering with detection of the full length Tlc1 constructs by qRT-PCR.

Brr1 aids Sm_7 complex loading onto snRNA and hence brr1Δ should further aggravate the prevention of Sm_7 binding to Tlc1 in our system [Fig 23B] [155].

To our surprise, the slow Rz-Tlc1 harboring Sm_7- mutation was stabilized [Fig 24]. This observation is puzzling to us and must be further investigated. However, it appears like lack of Sm_7 complex loading is not the reason for rapidly processed Tlc1-Rz instability.

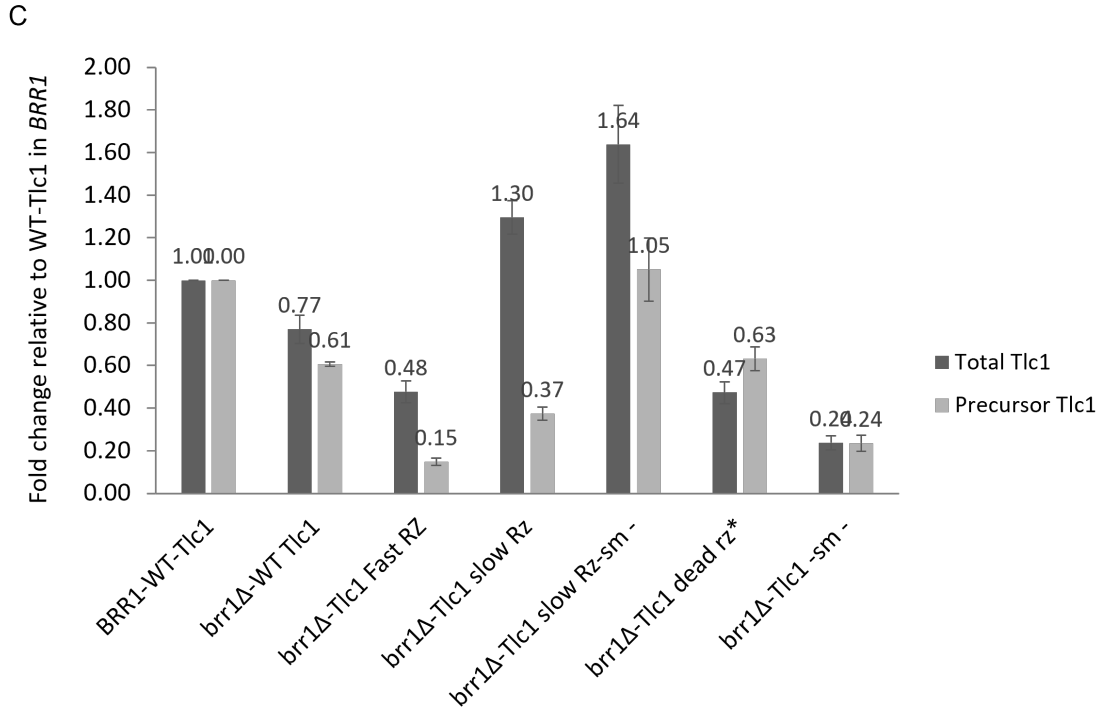

Figure 24: qPCR analysis showing the relative fold change of total and precursor Tlc1 upon sm- binding site mutation on Tlc1-slow Rz and brr1Δ, normalized with Alg9, Tfc1 and Ubc6. Mean values are calculated from 3 biological replicates and the error bars represent SE.

In a similar approach, we deleted the Ku70/80 binding stem in our slow Rz-Tlc1 construct and monitored the stability. kustemΔ affects the stability of Tlc1 [Fig 25]. However, kustemΔ doesn't further aggravate the instability when introduced into the Slow Rz construct i.e., the effect is not synergistic.

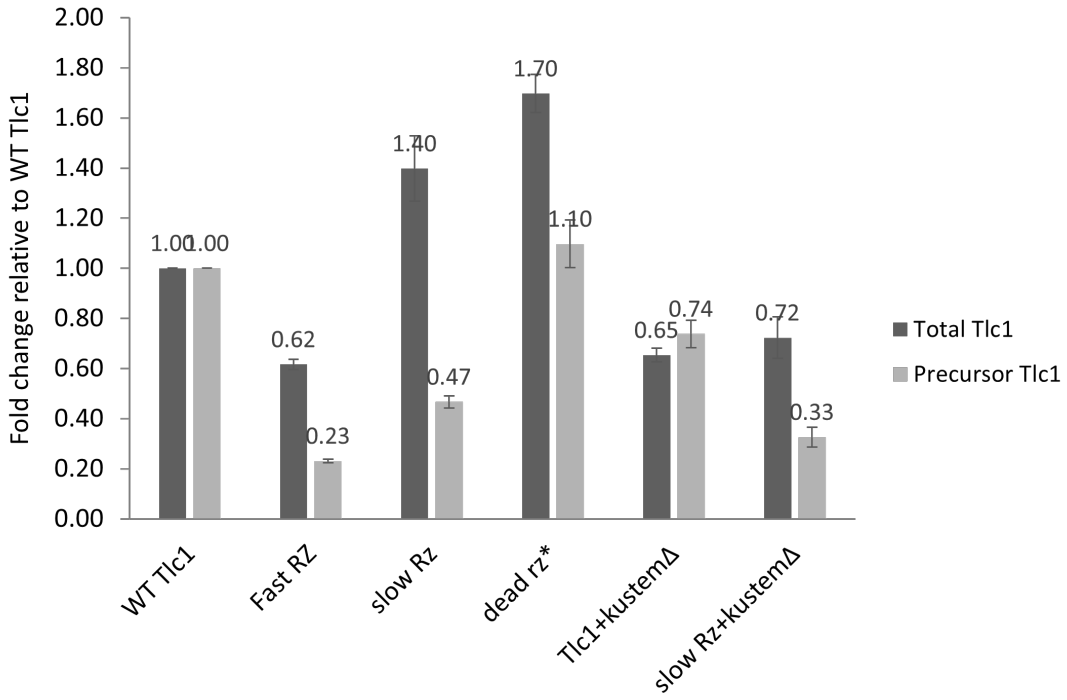

Figure 25: qPCR analysis showing the relative fold change of total and precursor Tlc1 upon kustemΔ on slow Rz Tlc1, normalized with Alg9, Tfc1 and Ubc6. Mean values are calculated from 3 biological replicates and the error bars represent SE.

7. Discussion

The telomerase RNA subunit undergoes a series of maturation steps during telomerase biogenesis in all organisms. Despite the major events such as the 5' capping and 3' processing being conserved, the involved factors and mechanisms appear to be surprisingly diverse. The telomerase RNA (Tlc1) of *S. cerevisiae*, shares certain features of snRNA, such as the possession of TMG cap at the 5' end and the Sm_7 complex at the 3' end [86]. Contrastingly, the Tlc1, due to the occurrence of its poly(A+) form, resembles an mRNA [91]. Not just its striking resemblances to both snRNA and mRNA, but with the knowledge from all the scientific studies aiming to decipher the biogenesis of Tlc1 so far, we are aware that Tlc1 is a unique class of RNA. Since steady state levels of Tlc1 is the rate limiting factor for telomerase activity, the mechanisms underlying the biogenesis of Tlc1 must be clarified. Despite its discovery in 1997, there are many knowledge gaps in the biogenesis of Tlc1 remaining to be filled in. We therefore began investigating the transcriptional termination and 3' processing mechanism of Tlc1.

7.1. Transcriptional termination mechanism of Tlc1

The downstream 3' Tlc1 sequence harbors signals for both NNS transcription termination, as well as polyadenylation mediated transcription termination [91, 105, 106]. The precursor Tlc1 produced via either of the termination pathways varies in their termination position, i.e, the last genome encoded nucleotide position and in their 3' adenylation tail length. The NNS signal precedes the polyadenylation signals on Tlc1 and is predicted to possess a shorter A-tail relative to the poly(A) precursor. Previously it was shown that disturbing the polyadenylation termination, either by depletion of Pap1 or by mutation of the efficiency element on Tlc1, led to the suppression of poly(A+) form and a significant decrease in the mature form [91]. This observation exhibited the precursor-product relationship of the poly(A+) form and the mature form. Moreover, overexpression of Tlc1 using a heterologous promoter increased poly(A+) levels to 100-fold, and whereas only a 10-fold increase in mature form [91]. This indicated that the Tlc1 transcript produced via polyadenylation termination is the initially transcribed form. Contrastingly, mutating the polyadenylation signals on Tlc1 was shown to not affect the quantity and the quality of mature Tlc1, despite the depletion of poly(A+) form [105]. This led to the current tenet in field that NNS termination is the major pathway contributing to the mature Tlc1, and the naturally occurring poly(A+) form is not required for the biogenesis of mature Tlc1 or for contributing to functional telomerase.

We saw two major drawbacks in the current Tlc1 transcriptional termination postulation. Even though mutation of polyadenylation signals depleted the known poly(A+) precursor, a new and a much longer Tlc1 precursor was produced [105]. We cannot eliminate the fact that the new longer transcript could function as the precursor form contributing to the observed unperturbed mature form. Additionally, partial depletion of Nrd1 and Nab3, although led to the increase of the poly(A+) form, did not drastically affect the mature Tlc1 levels [105]. Hence, in this study we tested the importance of NNS pathway in accounting for steady state levels of mature Tlc1.

To understand the significance of NNS pathway in the biogenesis of Tlc1, we mutated the Nrd1 and Nab3 binding sites on Tlc1 and monitored the impact of NNS termination disruption on the stability of Tlc1. We observed that the lack of Nrd1 and Nab3 recruitment to Tlc1, did not affect the steady state levels of mature Tlc1, despite the 1.7-fold increase in the precursor form [Fig 9]. Tlc1 expression analysis performed after enrichment of poly(A) tailed transcripts, led to the observation of 2.2~2.7-fold increase in the precursor Tlc1, indicating that the accumulating precursors are poly(A+) form [Fig 10]. Our 3'RACE experiment further bolstered that disruption of Nrd1 and Nab3 binding to Tlc1 accumulated poly(A+) precursor [Fig 12]. In addition to not having impacted the steady state levels of mature Tlc1, the lack of Nrd1 and Nab3 loading to Tlc1, did not affect the correct 3' trimming of Tlc1 to mature form [Fig 11]. These observations led to our conclusion that NNS transcriptional termination is not essential for Tlc1 biogenesis. And the alternative polyadenylation termination pathway can compensate for the loss of NNS transcriptional termination. Our study unveiled the potential of poly(A+) precursor to contribute to faithfully processed mature form.

Our 3'RACE experiment, however, failed to capture the NNS precursor even in the Wt sample. And so far, the NNS precursor species have not been visualized at the sequence level yet. Hence, nanopore sequencing was performed to visually capture all the existing Tlc1 species that vary in their very 3' end. Surprisingly, we observed three major precursor populations [Fig 13]. One population terminated at +1242~+1252 with long A-tails (>10 adenosines), which corresponds to the known poly(A+) precursor form. A second set of precursor species terminated between +1208~+1212 with short A-tails (<10 adenosines), resembling the NNS precursor form. The third set of Tlc1 molecules terminated at +1170~+1180 with 2~5 terminal adenosines and has not been previously documented in literature. They appear to be a stable intermediate during the

processing from the precursor form to the mature form. The 2~5 nt A-tail serves as a bona fide to the involvement of the TRAMP complex in the 3' processing of Tlc1. We hypothesize that the 3' processing machinery is temporarily impeded at the +1170~+1180 position by an unknown protein bound to Tlc1. Further investigation must be done to unravel the mechanism and the functional significance of +1170~+1180 precursor species.

7.2. Effects of 3' processing on Tlc1 stability

Apart from the existence of two redundant transcriptional termination pathways contributing to the mature Tlc1, the precursor transcript also consists of multiple Nrd1 binding sites and cryptic poly(A) signals [Fig 5]. The presence of multiple dispensable 3' processing signals indicates that the Tlc1 employs a flexible means to achieve the mature form. To better understand the significance of such a lenient 3' processing mechanism, we made use of ribozyme to force transcription termination at the 3' end of mature form. Such a forceful termination enabled us to deprive Tlc1 of its endogenous 3' processing mechanism(s).

Ribozyme processing caused instability of mature Tlc1 [Fig 15B]. Additionally, we employed ribozymes acting at different speeds-superfast, fast, slow and dead, thereby creating a gradient of competition, in terms of kinetics, with the endogenous processing system of Tlc1. The stability of mature form decreased with the increasing speed of ribozyme cleavage [Fig 17]. The observation of the instability of Rz processed Tlc1 and the subsequent rescue of its stability by lowering the ribozyme cleavage speed, can be interpreted with two explanations. The instability can be due to the accelerated processing kinetics mediated by the ribozyme. Hence, the endogenous 3' processing kinetics of Tlc1 can be crucial for stabilizing the mature form. It is important to note that perturbation in maturation kinetics of human telomerase RNA triggers diseases such as dyskeratosis congenita and pulmonary fibrosis [154]. Alternatively, Tlc1 instability arising from Rz processing can be due to the deprivation of endogenous 3' processing signals. When the Rz processing gives rise to the mature form by skipping the sequential biogenesis of Tlc1, the stability of mature form is compromised.

Additionally, our 3'RACE data revealed that the rescue of Tlc1 stability by slow Rz is due to the increase in the fraction of Tlc1 molecules processed by the endogenous processing machinery [Fig 18]. This confirms that the Tlc1 endogenous 3' processing mechanism plays an important role in giving rise to stable mature Tlc1.

The NNS complex acts in concert with the TRAMP complex and the exosome complex [108]. The exosome complex is involved in the 3' processing of Tlc1 [148]. We hypothesized that during the 3' processing event, the exosome complex degrades the Rz processed Tlc1 due to the lack of binding of stabilizing proteins, e.g., Sm_7. However, disruption of nuclease activity of exosome did not restore the stability of Rz processed Tlc1, thereby disregarding our hypothesis [Fig 19, 20].

Disrupted ribonucleoprotein assembly onto Rz processed Tlc1 does not appear to be the reason for the observed instability [Fig 24, 25]. Additionally, Tlc1 was able to use the Pgk1 polyadenylation termination signal and produce stable mature form, provided that the ribozyme cleavage did not take place [Fig 22B,C]. These observations further endorse the importance of processing kinetics in stabilizing Tlc1.

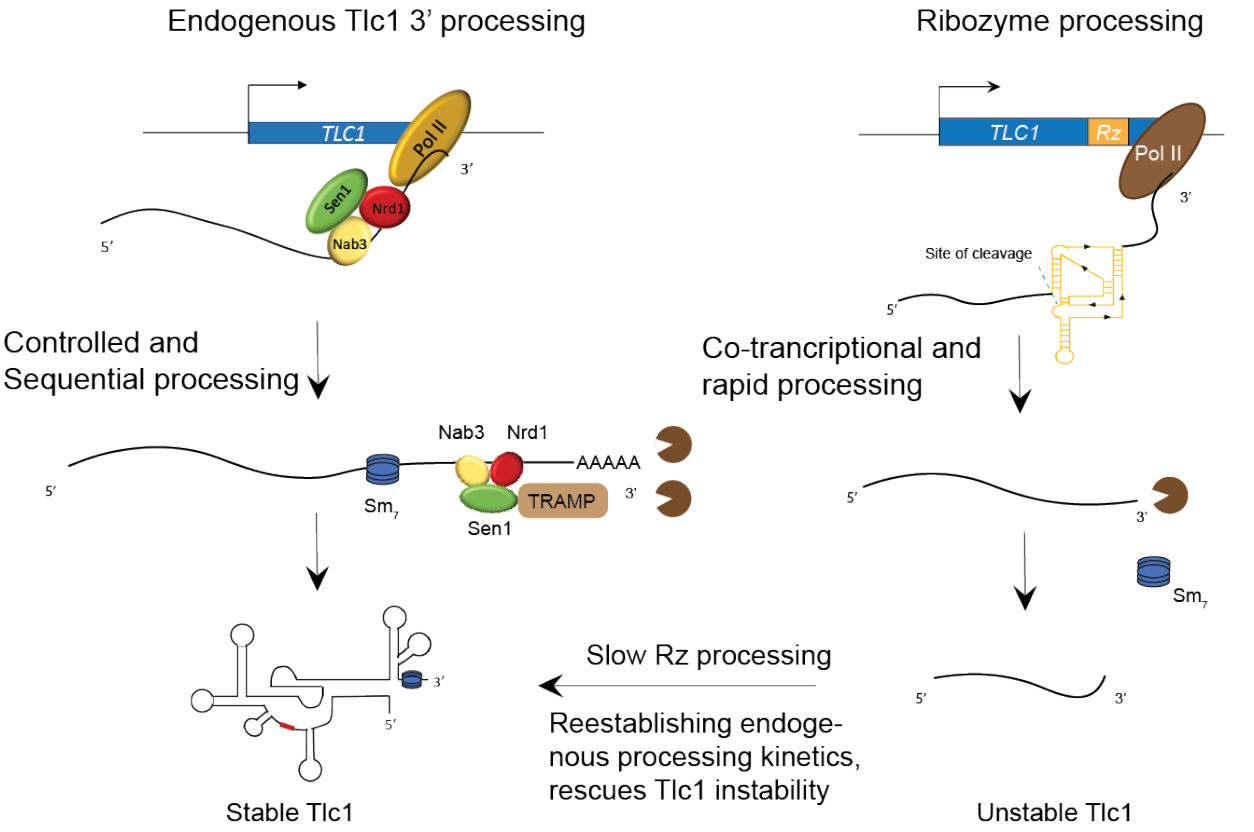

Figure 26: Speculative model describing the instability of ribozyme processed Tlc1. Endogenous 3' processing of Tlc1 happens in a sequential and regulated manner. Necessary proteins bind to Tlc1 conferring stability to the RNA. However, the ribozyme processing takes place co-transcriptionally and releases the mature form rapidly. Such an accelerated processing leaves the Tlc1 unstable. A slow ribozyme mutant loses its competition with the endogenous processing system and thereby re-establishes the processing kinetics and rescues Tlc1 stability.

Our speculative model predicts that ribozyme processing disturbs Tlc1 stability due to the accelerated processing, which in turn can prevent the loading of stabilizing proteins. The slow ribozyme mutant, owing to its incapacity, enables the endogenous 3' processing mechanism to take-over and thereby re-establish the processing kinetics that stabilize Tlc1 [Fig 26].

8. Conclusion and future perspectives

The RNA component of telomerase in *S. cerevisiae* (known as Tlc1) is initially transcribed as a longer form and then trimmed at its 3' end to become the functional version found in active telomerase. Tlc1 possesses two distinct signals for transcriptional termination: one involving Nrd1-Nab3-Sen1 (NNS) and the other involving polyadenylation. The significance of these two termination pathways and the process by which the mature and functional Tlc1 is generated through 3' processing have not been well understood.

Disruption of NNS signal did not affect the steady state levels of mature Tlc1. Furthermore, hampered NNS termination pathway accumulated poly(A) precursor. Even in the absence of recruitment of Nrd1 and Nab3, the poly(A) precursor is correctly trimmed at the 3' end, contributing to the mature form (+1156/1157). Therefore, NNS termination pathway is not essential for generating stable mature Tlc1. In our attempt to capture the 3' distribution of Tlc1 precursors, we identified a third stable intermediate form (+1170~+1180), apart from the previously known NNS and poly(A) precursor forms. Our hypothesis suggests that an unidentified protein attached to Tlc1 might temporarily hinder the 3' processing machinery around the +1170~+1180 position. To fully understand the process and the functional importance of the precursor species at +1170~+1180, further investigation is required.

Bypassing the Tlc1's endogenous 3' processing signals by employing ribozyme to generate the mature form, caused severe instability of mature Tlc1. The observed instability was rescued upon lowering the speed of ribozyme activity. This instability could be due to the accelerated processing kinetics facilitated by the ribozyme. The natural 3' processing kinetics of Tlc1 might play a key role in stabilizing the mature form. Alternatively, Tlc1's instability resulting from ribozyme processing could stem from the lack of native 3' processing signals. When ribozyme processing creates the mature form by skipping the usual step-by-step development of Tlc1, the stability of the mature form becomes compromised. Our speculative model proposes that ribozyme processing disrupts Tlc1 stability due to the accelerated processing, which consequently hinders the binding of stabilizing proteins. The slower ribozyme mutant, due to its limited functionality, allows the native 3' processing mechanism to take over, thus reestablishing the processing kinetics that ensure the stability of Tlc1.

Additional research is needed to identify the protein(s) responsible for stabilizing Tlc1 during the 3’ processing phase. Moreover, certain events of Tlc1 maturation could be essential for its stability. A swift loss of native 3’ processing signals could impact the nucleo-cytoplasmic shuttling of Tlc1, potentially leading to instability. Our Tlc1-Rz system could serve as a tool to elucidate the specific event(s) in Tlc1's biogenesis that play a pivotal role in ensuring the RNA stability.

9. References

1. Bendich, A.J. and K. Drlica, *Prokaryotic and eukaryotic chromosomes: what's the difference?* Bioessays, 2000. **22**(5): p. 481-6.
2. Ishikawa, F. and T. Naito, *Why do we have linear chromosomes? A matter of Adam and Eve.* Mutat Res, 1999. **434**(2): p. 99-107.
3. Dani, G.M. and V.A. Zakian, *Mitotic and meiotic stability of linear plasmids in yeast.* Proc Natl Acad Sci U S A, 1983. **80**(11): p. 3406-10.
4. Williams, G.C., *Sex and evolution.* Monogr Popul Biol, 1975(8): p. 3-200.
5. de Lange, T., *Shelterin: the protein complex that shapes and safeguards human telomeres.* Genes Dev, 2005. **19**(18): p. 2100-10.
6. McClintock, B. and H.E. Hill, *The Cytological Identification of the Chromosome Associated with the R-G Linkage Group in ZEA MAYS.* Genetics, 1931. **16**(2): p. 175-90.
7. Muller, H.J., *The remaking of chromosomes.* Collecting Net, 1938(13): p. 181-198.
8. Kornberg, A., *The synthesis of DNA.* Sci Am, 1968. **219**(4): p. 64-78.
9. Meselson, M. and F.W. Stahl, *The Replication of DNA in Escherichia Coli.* Proc Natl Acad Sci U S A, 1958. **44**(7): p. 671-82.
10. Okazaki, R., et al., *Mechanism of DNA chain growth. I. Possible discontinuity and unusual secondary structure of newly synthesized chains.* Proc Natl Acad Sci U S A, 1968. **59**(2): p. 598-605.
11. Watson, J.D., *Origin of concatemeric T7 DNA.* Nat New Biol, 1972. **239**(94): p. 197-201.
12. Blackburn, E.H. and J.G. Gall, *A tandemly repeated sequence at the termini of the extrachromosomal ribosomal RNA genes in Tetrahymena.* J Mol Biol, 1978. **120**(1): p. 33-53.
13. Blackburn, E.H., et al., *DNA termini in ciliate macronuclei.* Cold Spring Harb Symp Quant Biol, 1983. **47 Pt 2**: p. 1195-207.
14. Orr-Weaver, T.L., J.W. Szostak, and R.J. Rothstein, *Yeast transformation: a model system for the study of recombination.* Proc Natl Acad Sci U S A, 1981. **78**(10): p. 6354-8.
15. Szostak, J.W. and E.H. Blackburn, *Cloning yeast telomeres on linear plasmid vectors.* Cell, 1982. **29**(1): p. 245-55.
16. Wellinger, R.J. and D. Sen, *The DNA structures at the ends of eukaryotic chromosomes.* Eur J Cancer, 1997. **33**(5): p. 735-49.
17. Klobutcher, L.A., et al., *All gene-sized DNA molecules in four species of hypotrichs have the same terminal sequence and an unusual 3' terminus.* Proc Natl Acad Sci U S A, 1981. **78**(5): p. 3015-9.
18. Kipling, D. and H.J. Cooke, *Hypervariable ultra-long telomeres in mice.* Nature, 1990. **347**(6291): p. 400-2.
19. Makarov, V.L., Y. Hirose, and J.P. Langmore, *Long G tails at both ends of human chromosomes suggest a C strand degradation mechanism for telomere shortening.* Cell, 1997. **88**(5): p. 657-66.
20. Wright, W.E., et al., *Normal human chromosomes have long G-rich telomeric overhangs at one end.* Genes Dev, 1997. **11**(21): p. 2801-9.
21. Levis, R.W., et al., *Transposons in place of telomeric repeats at a Drosophila telomere.* Cell, 1993. **75**(6): p. 1083-93.
22. Gottschling, D.E., et al., *Position effect at S. cerevisiae telomeres: reversible repression of Pol II transcription.* Cell, 1990. **63**(4): p. 751-62.
23. Conrad, M.N., et al., *RAP1 protein interacts with yeast telomeres in vivo: overproduction alters telomere structure and decreases chromosome stability.* Cell, 1990. **63**(4): p. 739-50.
24. Nugent, C.I., et al., *Cdc13p: a single-strand telomeric DNA-binding protein with a dual role in yeast telomere maintenance.* Science, 1996. **274**(5285): p. 249-52.
25. Hayflick, L. and P.S. Moorhead, *The serial cultivation of human diploid cell strains.* Exp Cell Res, 1961. **25**: p. 585-621.

26. Hayflick, L., *The Limited in Vitro Lifetime of Human Diploid Cell Strains.* Exp Cell Res, 1965. **37**: p. 614-36.
27. Olovnikov, A.M., *A theory of marginotomy. The incomplete copying of template margin in enzymic synthesis of polynucleotides and biological significance of the phenomenon.* J Theor Biol, 1973. **41**(1): p. 181-90.
28. Greider, C.W. and E.H. Blackburn, *Identification of a specific telomere terminal transferase activity in Tetrahymena extracts.* Cell, 1985. **43**(2 Pt 1): p. 405-13.
29. Greider, C.W. and E.H. Blackburn, *The telomere terminal transferase of Tetrahymena is a ribonucleoprotein enzyme with two kinds of primer specificity.* Cell, 1987. **51**(6): p. 887-98.
30. Greider, C.W. and E.H. Blackburn, *A telomeric sequence in the RNA of Tetrahymena telomerase required for telomere repeat synthesis.* Nature, 1989. **337**(6205): p. 331-7.
31. Yu, G.L., et al., *In vivo alteration of telomere sequences and senescence caused by mutated Tetrahymena telomerase RNAs.* Nature, 1990. **344**(6262): p. 126-32.
32. Lundblad, V. and J.W. Szostak, *A mutant with a defect in telomere elongation leads to senescence in yeast.* Cell, 1989. **57**(4): p. 633-43.
33. Singer, M.S. and D.E. Gottschling, *TLC1: template RNA component of Saccharomyces cerevisiae telomerase.* Science, 1994. **266**(5184): p. 404-9.
34. Cohn, M. and E.H. Blackburn, *Telomerase in yeast.* Science, 1995. **269**(5222): p. 396-400.
35. Lingner, J., et al., *Three Ever Shorter Telomere (EST) genes are dispensable for in vitro yeast telomerase activity.* Proc Natl Acad Sci U S A, 1997. **94**(21): p. 11190-5.
36. Nugent, C.I. and V. Lundblad, *The telomerase reverse transcriptase: components and regulation.* Genes Dev, 1998. **12**(8): p. 1073-85.
37. Lingner, J., et al., *Reverse transcriptase motifs in the catalytic subunit of telomerase.* Science, 1997. **276**(5312): p. 561-7.
38. Lundblad, V. and E.H. Blackburn, *An alternative pathway for yeast telomere maintenance rescues est1- senescence.* Cell, 1993. **73**(2): p. 347-60.
39. Adzuma, K., T. Ogawa, and H. Ogawa, *Primary structure of the RAD52 gene in Saccharomyces cerevisiae.* Mol Cell Biol, 1984. **4**(12): p. 2735-44.
40. Shinohara, A. and T. Ogawa, *Stimulation by Rad52 of yeast Rad51-mediated recombination.* Nature, 1998. **391**(6665): p. 404-7.
41. Sandell, L.L. and V.A. Zakian, *Loss of a yeast telomere: arrest, recovery, and chromosome loss.* Cell, 1993. **75**(4): p. 729-39.
42. Abdallah, P., et al., *A two-step model for senescence triggered by a single critically short telomere.* Nat Cell Biol, 2009. **11**(8): p. 988-93.
43. Khadaroo, B., et al., *The DNA damage response at eroded telomeres and tethering to the nuclear pore complex.* Nat Cell Biol, 2009. **11**(8): p. 980-7.
44. Hackett, J.A., D.M. Feldser, and C.W. Greider, *Telomere dysfunction increases mutation rate and genomic instability.* Cell, 2001. **106**(3): p. 275-86.
45. Hackett, J.A. and C.W. Greider, *End resection initiates genomic instability in the absence of telomerase.* Mol Cell Biol, 2003. **23**(23): p. 8450-61.
46. Teng, S.C. and V.A. Zakian, *Telomere-telomere recombination is an efficient bypass pathway for telomere maintenance in Saccharomyces cerevisiae.* Mol Cell Biol, 1999. **19**(12): p. 8083-93.
47. Lydeard, J.R., et al., *Break-induced replication and telomerase-independent telomere maintenance require Pol32.* Nature, 2007. **448**(7155): p. 820-3.
48. Teng, S.C., et al., *Telomerase-independent lengthening of yeast telomeres occurs by an abrupt Rad50p-dependent, Rif-inhibited recombinational process.* Mol Cell, 2000. **6**(4): p. 947-52.
49. Chan, C.S. and B.K. Tye, *A family of Saccharomyces cerevisiae repetitive autonomously replicating sequences that have very similar genomic environments.* J Mol Biol, 1983. **168**(3): p. 505-23.

50. Horowitz, H., P. Thorburn, and J.E. Haber, *Rearrangements of highly polymorphic regions near telomeres of Saccharomyces cerevisiae.* Mol Cell Biol, 1984. **4**(11): p. 2509-17.
51. Zakian, V.A., H.M. Blanton, and L. Wetzel, *Distribution of telomere-associated sequences in yeast.* Basic Life Sci, 1986. **40**: p. 493-8.
52. Larrivee, M. and R.J. Wellinger, *Telomerase- and capping-independent yeast survivors with alternate telomere states.* Nat Cell Biol, 2006. **8**(7): p. 741-7.
53. Lin, C.Y., et al., *Extrachromosomal telomeric circles contribute to Rad52-, Rad50-, and polymerase delta-mediated telomere-telomere recombination in Saccharomyces cerevisiae.* Eukaryot Cell, 2005. **4**(2): p. 327-36.
54. Virta-Pearlman, V., D.K. Morris, and V. Lundblad, *Est1 has the properties of a single-stranded telomere end-binding protein.* Genes Dev, 1996. **10**(24): p. 3094-104.
55. Seto, A.G., et al., *A bulged stem tethers Est1p to telomerase RNA in budding yeast.* Genes Dev, 2002. **16**(21): p. 2800-12.
56. Lin, J.J. and V.A. Zakian, *An in vitro assay for Saccharomyces telomerase requires EST1.* Cell, 1995. **81**(7): p. 1127-35.
57. Steiner, B.R., K. Hidaka, and B. Futcher, *Association of the Est1 protein with telomerase activity in yeast.* Proc Natl Acad Sci U S A, 1996. **93**(7): p. 2817-21.
58. Chan, A., J.B. Boule, and V.A. Zakian, *Two pathways recruit telomerase to Saccharomyces cerevisiae telomeres.* PLoS Genet, 2008. **4**(10): p. e1000236.
59. Evans, S.K. and V. Lundblad, *Est1 and Cdc13 as comediators of telomerase access.* Science, 1999. **286**(5437): p. 117-20.
60. Taggart, A.K., S.C. Teng, and V.A. Zakian, *Est1p as a cell cycle-regulated activator of telomere-bound telomerase.* Science, 2002. **297**(5583): p. 1023-6.
61. Taggart, A.K. and V.A. Zakian, *Telomerase: what are the Est proteins doing?* Curr Opin Cell Biol, 2003. **15**(3): p. 275-80.
62. Friedman, K.L. and T.R. Cech, *Essential functions of amino-terminal domains in the yeast telomerase catalytic subunit revealed by selection for viable mutants.* Genes Dev, 1999. **13**(21): p. 2863-74.
63. Livengood, A.J., A.J. Zaug, and T.R. Cech, *Essential regions of Saccharomyces cerevisiae telomerase RNA: separate elements for Est1p and Est2p interaction.* Mol Cell Biol, 2002. **22**(7): p. 2366-74.
64. Morris, D.K. and V. Lundblad, *Programmed translational frameshifting in a gene required for yeast telomere replication.* Curr Biol, 1997. **7**(12): p. 969-76.
65. Lendvay, T.S., et al., *Senescence mutants of Saccharomyces cerevisiae with a defect in telomere replication identify three additional EST genes.* Genetics, 1996. **144**(4): p. 1399-412.
66. Hughes, T.R., et al., *Identification of the single-strand telomeric DNA binding domain of the Saccharomyces cerevisiae Cdc13 protein.* Proc Natl Acad Sci U S A, 2000. **97**(12): p. 6457-62.
67. Friedman, K.L., et al., *N-terminal domain of yeast telomerase reverse transcriptase: recruitment of Est3p to the telomerase complex.* Mol Biol Cell, 2003. **14**(1): p. 1-13.
68. Osterhage, J.L., J.M. Talley, and K.L. Friedman, *Proteasome-dependent degradation of Est1p regulates the cell cycle-restricted assembly of telomerase in Saccharomyces cerevisiae.* Nat Struct Mol Biol, 2006. **13**(8): p. 720-8.
69. Talley, J.M., et al., *Stimulation of yeast telomerase activity by the ever shorter telomere 3 (Est3) subunit is dependent on direct interaction with the catalytic protein Est2.* J Biol Chem, 2011. **286**(30): p. 26431-9.
70. Tuzon, C.T., et al., *The Saccharomyces cerevisiae telomerase subunit Est3 binds telomeres in a cell cycle- and Est1-dependent manner and interacts directly with Est1 in vitro.* PLoS Genet, 2011. **7**(5): p. e1002060.

71. Esakova, O. and A.S. Krasilnikov, *Of proteins and RNA: the RNase P/MRP family.* RNA, 2010. **16**(9): p. 1725-47.
72. Lemieux, B., et al., *Active Yeast Telomerase Shares Subunits with Ribonucleoproteins RNase P and RNase MRP.* Cell, 2016. **165**(5): p. 1171-1181.
73. Gunisova, S., et al., *Identification and comparative analysis of telomerase RNAs from Candida species reveal conservation of functional elements.* RNA, 2009. **15**(4): p. 546-59.
74. Garcia, P.D., et al., *Stability and nuclear localization of yeast telomerase depend on protein components of RNase P/MRP.* Nat Commun, 2020. **11**(1): p. 2173.
75. Laterreur, N., et al., *A new telomerase RNA element that is critical for telomere elongation.* Nucleic Acids Res, 2013. **41**(16): p. 7713-24.
76. Feldmann, H. and E.L. Winnacker, *A putative homologue of the human autoantigen Ku from Saccharomyces cerevisiae.* J Biol Chem, 1993. **268**(17): p. 12895-900.
77. Boulton, S.J. and S.P. Jackson, *Identification of a Saccharomyces cerevisiae Ku80 homologue: roles in DNA double strand break rejoining and in telomeric maintenance.* Nucleic Acids Res, 1996. **24**(23): p. 4639-48.
78. Gravel, S., et al., *Yeast Ku as a regulator of chromosomal DNA end structure.* Science, 1998. **280**(5364): p. 741-4.
79. Martin, S.G., et al., *Relocalization of telomeric Ku and SIR proteins in response to DNA strand breaks in yeast.* Cell, 1999. **97**(5): p. 621-33.
80. Fisher, T.S. and V.A. Zakian, *Ku: a multifunctional protein involved in telomere maintenance.* DNA Repair (Amst), 2005. **4**(11): p. 1215-26.
81. Stellwagen, A.E., et al., *Ku interacts with telomerase RNA to promote telomere addition at native and broken chromosome ends.* Genes Dev, 2003. **17**(19): p. 2384-95.
82. Peterson, S.E., et al., *The function of a stem-loop in telomerase RNA is linked to the DNA repair protein Ku.* Nat Genet, 2001. **27**(1): p. 64-7.
83. Pfingsten, J.S., et al., *Mutually exclusive binding of telomerase RNA and DNA by Ku alters telomerase recruitment model.* Cell, 2012. **148**(5): p. 922-32.
84. Fisher, T.S., A.K. Taggart, and V.A. Zakian, *Cell cycle-dependent regulation of yeast telomerase by Ku.* Nat Struct Mol Biol, 2004. **11**(12): p. 1198-205.
85. Gallardo, F., et al., *Live cell imaging of telomerase RNA dynamics reveals cell cycle-dependent clustering of telomerase at elongating telomeres.* Mol Cell, 2011. **44**(5): p. 819-27.
86. Seto, A.G., et al., *Saccharomyces cerevisiae telomerase is an Sm small nuclear ribonucleoprotein particle.* Nature, 1999. **401**(6749): p. 177-80.
87. Gallardo, F., et al., *TLC1 RNA nucleo-cytoplasmic trafficking links telomerase biogenesis to its recruitment to telomeres.* EMBO J, 2008. **27**(5): p. 748-57.
88. Teixeira, M.T., et al., *Intracellular trafficking of yeast telomerase components.* EMBO Rep, 2002. **3**(7): p. 652-9.
89. Ferrezuelo, F., et al., *Biogenesis of yeast telomerase depends on the importin mtr10.* Mol Cell Biol, 2002. **22**(17): p. 6046-55.
90. Vasianovich, Y., E. Bajon, and R.J. Wellinger, *Telomerase biogenesis requires a novel Mex67 function and a cytoplasmic association with the Sm(7) complex.* Elife, 2020. **9**.
91. Chapon, C., T.R. Cech, and A.J. Zaug, *Polyadenylation of telomerase RNA in budding yeast.* RNA, 1997. **3**(11): p. 1337-51.
92. Franke, J., J. Gehlen, and A.E. Ehrenhofer-Murray, *Hypermethylation of yeast telomerase RNA by the snRNA and snoRNA methyltransferase Tgs1.* J Cell Sci, 2008. **121**(Pt 21): p. 3553-60.
93. Mozdy, A.D. and T.R. Cech, *Low abundance of telomerase in yeast: implications for telomerase haploinsufficiency.* RNA, 2006. **12**(9): p. 1721-37.

94. Dionne, I., et al., *Cell cycle-dependent transcription factors control the expression of yeast telomerase RNA.* RNA, 2013. **19**(7): p. 992-1002.
95. Larose, S., et al., *RNase III-dependent regulation of yeast telomerase.* J Biol Chem, 2007. **282**(7): p. 4373-4381.
96. Feng, J., et al., *The RNA component of human telomerase.* Science, 1995. **269**(5228): p. 1236-41.
97. Zappulla, D.C., K. Goodrich, and T.R. Cech, *A miniature yeast telomerase RNA functions in vivo and reconstitutes activity in vitro.* Nat Struct Mol Biol, 2005. **12**(12): p. 1072-7.
98. Zappulla, D.C. and T.R. Cech, *RNA as a flexible scaffold for proteins: yeast telomerase and beyond.* Cold Spring Harb Symp Quant Biol, 2006. **71**: p. 217-24.
99. Zappulla, D.C., *Yeast Telomerase RNA Flexibly Scaffolds Protein Subunits: Results and Repercussions.* Molecules, 2020. **25**(12).
100. Hass, E.P. and D.C. Zappulla, *Repositioning the Sm-Binding Site in Saccharomyces cerevisiae Telomerase RNA Reveals RNP Organizational Flexibility and Sm-Directed 3'-End Formation.* Noncoding RNA, 2020. **6**(1).
101. Podlevsky, J.D., et al., *The telomerase database.* Nucleic Acids Res, 2008. **36**(Database issue): p. D339-43.
102. Chen, J.L. and C.W. Greider, *An emerging consensus for telomerase RNA structure.* Proc Natl Acad Sci U S A, 2004. **101**(41): p. 14683-4.
103. O'Connor, C.M., C.K. Lai, and K. Collins, *Correction: Two purified domains of telomerase reverse transcriptase reconstitute sequence-specific interactions with RNA.* J Biol Chem, 2019. **294**(22): p. 8713.
104. Witkin, K.L. and K. Collins, *Holoenzyme proteins required for the physiological assembly and activity of telomerase.* Genes Dev, 2004. **18**(10): p. 1107-18.
105. Noel, J.F., et al., *Budding yeast telomerase RNA transcription termination is dictated by the Nrd1/Nab3 non-coding RNA termination pathway.* Nucleic Acids Res, 2012. **40**(12): p. 5625-36.
106. Jamonnak, N., et al., *Yeast Nrd1, Nab3, and Sen1 transcriptome-wide binding maps suggest multiple roles in post-transcriptional RNA processing.* RNA, 2011. **17**(11): p. 2011-25.
107. Grzechnik, P. and J. Kufel, *Polyadenylation linked to transcription termination directs the processing of snoRNA precursors in yeast.* Mol Cell, 2008. **32**(2): p. 247-58.
108. Vasiljeva, L. and S. Buratowski, *Nrd1 interacts with the nuclear exosome for 3' processing of RNA polymerase II transcripts.* Mol Cell, 2006. **21**(2): p. 239-48.
109. Leonardi, J., et al., *TER1, the RNA subunit of fission yeast telomerase.* Nat Struct Mol Biol, 2008. **15**(1): p. 26-33.
110. Box, J.A., et al., *Spliceosomal cleavage generates the 3' end of telomerase RNA.* Nature, 2008. **456**(7224): p. 910-4.
111. Tang, W., et al., *Telomerase RNA biogenesis involves sequential binding by Sm and Lsm complexes.* Nature, 2012. **484**(7393): p. 260-4.
112. Qi, X., et al., *Prevalent and distinct spliceosomal 3'-end processing mechanisms for fungal telomerase RNA.* Nat Commun, 2015. **6**: p. 6105.
113. Smekalova, E.M., et al., *Specific features of telomerase RNA from Hansenula polymorpha.* Rna, 2013. **19**(11): p. 1563-1574.
114. Kannan, R., et al., *Intronic sequence elements impede exon ligation and trigger a discard pathway that yields functional telomerase RNA in fission yeast.* Genes & Development, 2013. **27**(6): p. 627-638.
115. Kannan, R., et al., *Diverse mechanisms for spliceosome-mediated 3' end processing of telomerase RNA.* Nat Commun, 2015. **6**: p. 6104.

116. Mayas, R.M., et al., *Spliceosome discards intermediates via the DEAH box ATPase Prp43p.* Proceedings of the National Academy of Sciences of the United States of America, 2010. **107**(22): p. 10020-10025.
117. Mayas, R.M., H. Maita, and J.P. Staley, *Exon ligation is proofread by the DExD/H-box ATPase Prp22p.* Nature Structural & Molecular Biology, 2006. **13**(6): p. 482-490.
118. Nguyen, D., et al., *A Polyadenylation-Dependent 3' End Maturation Pathway Is Required for the Synthesis of the Human Telomerase RNA.* Cell Rep, 2015. **13**(10): p. 2244-57.
119. Tseng, C.K., et al., *Human Telomerase RNA Processing and Quality Control.* Cell Rep, 2015. **13**(10): p. 2232-43.
120. Egan, E.D. and K. Collins, *Specificity and stoichiometry of subunit interactions in the human telomerase holoenzyme assembled in vivo.* Mol Cell Biol, 2010. **30**(11): p. 2775-86.
121. Fu, D. and K. Collins, *Purification of human telomerase complexes identifies factors involved in telomerase biogenesis and telomere length regulation.* Mol Cell, 2007. **28**(5): p. 773-85.
122. Rubtsova, M.P., et al., *Integrator is a key component of human telomerase RNA biogenesis.* Sci Rep, 2019. **9**(1): p. 1701.
123. Porrua, O. and D. Libri, *Transcription termination and the control of the transcriptome: why, where and how to stop.* Nature Reviews Molecular Cell Biology, 2015. **16**(3): p. 190-202.
124. Arndt, K.M. and D. Reines, *Termination of Transcription of Short Noncoding RNAs by RNA Polymerase II.* Annual Review of Biochemistry, Vol 84, 2015. **84**: p. 381-404.
125. Mischo, H.E. and N.J. Proudfoot, *Disengaging polymerase: Terminating RNA polymerase II transcription in budding yeast.* Biochimica Et Biophysica Acta-Gene Regulatory Mechanisms, 2013. **1829**(1): p. 174-185.
126. Kuehner, J.N., E.L. Pearson, and C. Moore, *Unravelling the means to an end: RNA polymerase II transcription termination.* Nature Reviews Molecular Cell Biology, 2011. **12**(5): p. 283-294.
127. Kuehner, J.N., E.L. Pearson, and C. Moore, *Unravelling the means to an end: RNA polymerase II transcription termination.* Nat Rev Mol Cell Biol, 2011. **12**(5): p. 283-94.
128. Carroll, K.L., et al., *Interaction of yeast RNA-binding proteins Nrd1 and Nab3 with RNA polymerase II terminator elements.* Rna, 2007. **13**(3): p. 361-373.
129. Carroll, K.L., et al., *Identification of cis elements directing termination of yeast nonpolyadenylated snoRNA transcripts.* Molecular and Cellular Biology, 2004. **24**(14): p. 6241-6252.
130. Vasiljeva, L., et al., *The Nrd1-Nab3-Sen1 termination complex interacts with the Ser5-phosphorylated RNA polymerase II C-terminal domain.* Nature Structural & Molecular Biology, 2008. **15**(8): p. 795-804.
131. Porrua, O. and D. Libri, *A bacterial-like mechanism for transcription termination by the Sen1p helicase in budding yeast.* Nature Structural & Molecular Biology, 2013. **20**(7): p. 884-+.
132. Han, Z., et al., *Termination of non-coding transcription in yeast relies on both an RNA Pol II CTD interaction domain and a CTD-mimicking region in Sen1.* Embo Journal, 2020. **39**(7).
133. Tudek, A., et al., *Molecular Basis for Coordinating Transcription Termination with Noncoding RNA Degradation.* Molecular Cell, 2014. **55**(3): p. 467-481.
134. Jia, H.J., et al., *RNA unwinding by the Trf4/Air2/Mtr4 polyadenylation (TRAMP) complex.* Proceedings of the National Academy of Sciences of the United States of America, 2012. **109**(19): p. 7292-7297.
135. Jia, H.J., et al., *The RNA Helicase Mtr4p Modulates Polyadenylation in the TRAMP Complex.* Cell, 2011. **145**(6): p. 890-901.
136. Houseley, J., J. LaCava, and D. Tollervey, *RNA-quality control by the exosome.* Nature Reviews Molecular Cell Biology, 2006. **7**(7): p. 529-539.

137. Schaeffer, D., et al., *The exosome contains domains with specific endoribonuclease, exoribonuclease and cytoplasmic mRNA decay activities.* Nature Structural & Molecular Biology, 2009. **16**(1): p. 56-62.
138. Dziembowski, A., et al., *A single subunit, Dis3, is essentially responsible for yeast exosome core activity.* Nature Structural & Molecular Biology, 2007. **14**(1): p. 15-22.
139. Callahan, K.P. and J.S. Butler, *Evidence for core exosome independent function of the nuclear exoribonuclease Rrp6p.* Nucleic Acids Research, 2008. **36**(21): p. 6645-6655.
140. Synowsky, S.A., et al., *Comparative Multiplexed Mass Spectrometric Analyses of Endogenously Expressed Yeast Nuclear and Cytoplasmic Exosomes.* Journal of Molecular Biology, 2009. **385**(4): p. 1300-1313.
141. Harlen, K.M. and L.S. Churchman, *The code and beyond: transcription regulation by the RNA polymerase II carboxy-terminal domain.* Nature Reviews Molecular Cell Biology, 2017. **18**(4): p. 263-273.
142. Lunde, B.M., et al., *Cooperative interaction of transcription termination factors with the RNA polymerase II C-terminal domain.* Nature Structural & Molecular Biology, 2010. **17**(10): p. 1195-+.
143. Rondon, A.G., H.E. Mischo, and N.J. Proudfoot, *Terminating transcription in yeast: whether to be a 'nerd' or a 'rat'.* Nature Structural & Molecular Biology, 2008. **15**(8): p. 775-776.
144. Viphakone, N., F. Voisinet-Hakil, and L. Minvielle-Sebastia, *Molecular dissection of mRNA poly(A) tail length control in yeast.* Nucleic Acids Research, 2008. **36**(7): p. 2418-2433.
145. Tudek, A., et al., *Global view on the metabolism of RNA poly(A) tails in yeast Saccharomyces cerevisiae.* Nature Communications, 2021. **12**(1).
146. Bosoy, D., et al., *Conserved N-terminal motifs of telomerase reverse transcriptase required for ribonucleoprotein assembly in vivo.* J Biol Chem, 2003. **278**(6): p. 3882-90.
147. Guo, Z.J. and F. Sherman, *3'-end-forming signals of yeast mRNA.* Trends in Biochemical Sciences, 1996. **21**(12): p. 477-481.
148. Coy, S., et al., *The Sm Complex Is Required for the Processing of Non-Coding RNAs by the Exosome.* Plos One, 2013. **8**(6).
149. Wu, H., D. Becker, and H. Krebber, *Telomerase RNA TLC1 shuttling to the cytoplasm requires mRNA export factors and is important for telomere maintenance.* Cell Rep, 2014. **8**(6): p. 1630-1638.
150. Hirsch, A.G., et al., *Unraveling the stepwise maturation of the yeast telomerase including a Cse1 and Mtr10 mediated quality control checkpoint.* Scientific Reports, 2021. **11**(1).
151. Plessel, G., U. Fischer, and R. Luhrmann, *M(3)G Cap Hypermethylation of U1 Small Nuclear Ribonucleoprotein (Snrnp) in-Vitro - Evidence That the U1 Small Nuclear Rna-(Guanosine-N2)-Methyltransferase Is a Non-Snrnp Cytoplasmic Protein That Requires a Binding-Site on the Sm Core Domain.* Molecular and Cellular Biology, 1994. **14**(6): p. 4160-4172.
152. Mouaikel, J., et al., *Hypermethylation of the cap structure of both yeast snRNAs and snoRNAs requires a conserved methyltransferase that is localized to the nucleolus.* Molecular Cell, 2002. **9**(4): p. 891-901.
153. Tudek, A., et al., *A Nuclear Export Block Triggers the Decay of Newly Synthesized Polyadenylated RNA.* Cell Rep, 2018. **24**(9): p. 2457-2467 e7.
154. Roake, C.M., et al., *Disruption of Telomerase RNA Maturation Kinetics Precipitates Disease.* Molecular Cell, 2019. **74**(4): p. 688-+.
155. Noble, S.M. and C. Guthrie, *Transcriptional pulse-chase analysis reveals a role for a novel snRNP-associated protein in the manufacture of spliceosomal snRNPs.* EMBO J, 1996. **15**(16): p. 4368-79.

Acknowledgements

I owe my sincere gratitude to my mentor for his guidance and support. I am thankful to him for believing in me and giving me an opportunity to work under his guidance. I thank him for inspiring me to do good quality science. The feedback from my mentor has helped me identify my strengths and weaknesses and has greatly contributed to my professional development. I thank him for providing a supportive and discrimination free working atmosphere.

I would like to thank my thesis advisory committee members for their valuable input that greatly aided in shaping my PhD project.

I would like to thank all the lab members for the wonderful working environment, and for all the helpful scientific & non-scientific discussions. Lab members gave me the sense of belongingness in a foreign land where I'm far away from my family.

I'm thankful to be a part of the International PhD program which provided a wonderful environment enabling healthy scientific support and knowledge exchange. The program also provided opportunities to hone many soft skills which has greatly contributed to my professional development and growth. A very huge thanks to the coordinators**,** for the immense support during my PhD journey.

I would like to thank all my friends who have been my support system during my PhD. Thank you for encouraging me and supporting me during difficult times. A special mention to a person with whom I started this PhD journey, my PhD companion. He subdued difficult situations and brought color and fun to my PhD life.

I'm indebted to my parents for all the sacrifices they made to provide me with good education and for being supportive to follow my dreams. Thank you for the unconditional love and support. I thank my brother for the moral support.

Declaration

Herewith I, Abinaya Manivannan, declare that the work presented in this thesis is my very own. I confirm that any information or data that have been derived from other sources are referred to and correctly cited in the thesis.